LAWRENCE
LIVERMORE
NATIONAL
LABORATORY

LLNL-TR-771451

# PROBABILISTIC SEISMIC HAZARD ASSESSMENT FOR GEORGIA

T. Onur, R. Gok, T. Godoladze, I. Gunia, G. Boichenko, A. Buzaladze, N. Tumanova, M. Dzmanashvili, L. Sukhishvili, Z. Javakishvili, E. Cowgill, I. Bondar, G. Yetirmishli

April 8, 2019

**Disclaimer**

This document was prepared as an account of work sponsored by an agency of the United States government. Neither the United States government nor Lawrence Livermore National Security, LLC, nor any of their employees makes any warranty, expressed or implied, or assumes any legal liability or responsibility for the accuracy, completeness, or usefulness of any information, apparatus, product, or process disclosed, or represents that its use would not infringe privately owned rights. Reference herein to any specific commercial product, process, or service by trade name, trademark, manufacturer, or otherwise does not necessarily constitute or imply its endorsement, recommendation, or favoring by the United States government or Lawrence Livermore National Security, LLC. The views and opinions of authors expressed herein do not necessarily state or reflect those of the United States government or Lawrence Livermore National Security, LLC, and shall not be used for advertising or product endorsement purposes.

This work performed under the auspices of the U.S. Department of Energy by Lawrence Livermore National Laboratory under Contract DE-AC52-07NA27344.

# PROBABILISTIC SEISMIC HAZARD ASSESSMENT FOR GEORGIA

TUNA ONUR[1], RENGIN GOK[2], TEA GODOLADZE[3], IRAKLI GUNIA[3], GIORGI BOICHENKO[3], ALBERT BUZALADZE[3], NINO TUMANOVA[3], MANANA DZMANASHVILI[3], LASHA SUKHISHVILI[3], ZURAB JAVAKASHVILI[3], ERIC COWGILL[4], ISTVAN BONDAR[5], AND GURBAN YETIRMISHLI[6]

[1] Onur Seemann Consulting, Inc. Victoria, BC, Canada
[2] Lawrence Livermore National Laboratory, Livermore, CA, USA
[3] Institute of Earth Sciences, Ilia State University, Tbilisi, Georgia
[4] University of California, Davis, CA, USA
[5] Research Centre for Astronomy and Earth Sciences of HAS, Budapest, Hungary
[6] Republic Seismic Survey Center of ANAS, Baku, Azerbaijan

## INTRODUCTION

Probabilistic Seismic Hazard Assessments (PSHA) form the basis for most contemporary seismic provisions in building codes around the world. The current building code of Georgia (2009) is not fully compatible with seismic hazard and design concepts of modern codes. The Ministry of Economy and Sustainable Development of Georgia is currently undertaking an update to the building code to align it with EuroCode. In conjunction with EuroCode, a National Annex specific to Georgia is needed, including seismic hazard values for the territory of Georgia. A comprehensive earthquake catalogue is fundamental to a robust PSHA in the region. The Caucasus has had an uneven seismic recording and reporting history both temporally and spatially. Therefore, there has been a strong regional effort to bring together data from all the countries in the Caucasus, to digitize and standardize paper-based data from the Soviet era, and to re-examine magnitude and location calculations. The earthquake catalogue resulting from this effort forms the basis for a reliable seismic hazard assessment.

Recognizing these needs, the U.S. Department of Energy through Lawrence Livermore National Laboratory (LLNL) initiated a project in 2015 to engage and train local scientists in the Caucasus to install new equipment, to enhance the quality of seismic monitoring and reporting, and to improve and harmonize the regional earthquake catalogue. In 2016, the project scope was expanded to include the modernization of seismic hazard assessments. To this end, a series of workshops were held in Georgia, the first one of which presented an overview of PSHA and its components to various participants from the universities and other research organizations in the region. This kick-off workshop was followed by numerous hands-on training workshops in 2017 and 2018, covering all aspects of PSHA. In addition to their training goals, the workshops brought together existing and new information relevant to PSHA studies in the region, providing a platform for local scientists/engineers and experts from other parts of the world to interact, co-operate and discuss various pieces of the PSHA input.

This report outlines the aspects of the earthquake catalogue development and PSHA project that were specifically undertaken to form the basis for the building code update in Georgia. Georgia straddles the Greater Caucasus and Lesser Caucasus Fold and Thrust belts, where the

convergent tectonic setting generates significant earthquake activity. To the east of the country, evidence indicates the possibility of a remnant subducting slab that causes earthquakes deeper than 40km (Mellors et al, 2012; Cowgill et al., 2016). This study systematically compiles and improves all available data on local seismicity, active faults, and ground motion attenuation characteristics of the region; and builds a framework to enable a contemporary PSHA to be carried out with the engagement of local scientists. To this end, six regional workshops were organized in total (Figure 1) over a three-year period of time, with participation from the United States, Canada and Hungary as well as countries in the Caucasus: Georgia, Armenia, Azerbaijan and Turkey. The workshops served multiple purposes such as training, data collection, interactions between local earth scientists and engineers, and brainstorming and knowledge exchange among local and international experts.

*Figure 1. One of the six workshops held in Georgia for the project.*

Global hazard maps are necessarily generalized and use existing earthquake catalogues (e.g. GSHAP: Giardini et el., 1999; GEM-EMME: Sesetyan et al., 2018). The PSHA framework developed specifically for Georgia as part of this project was designed to help develop a new earthquake catalogue and generate hazard information in a form that is useful for development of the new building code for Georgia.

## SEISMIC SOURCE CHARACTERIZATION

The PSHA framework used in this project has two main components: 1) seismic source characterization, and 2) ground motion characterization. Seismic source characterization requires compilation of all available information regarding the tectonic setting of the region, active faults and a comprehensive earthquake catalogue in terms of moment magnitude, Mw.

### ACTIVE TECTONICS IN GEORGIA

The Greater and Lesser Caucasus fold and thrust zones are part of the larger Alpine Himalayan continental collision zone, the world's largest active convergent deformation zone that stretches from Western Europe to Eastern China. In this system, Georgia lies within the convergent boundary between the Arabian and Eurasian plates (Figure 2), where the relative motion is taken up mainly by the fold and thrust belts within the Greater and Lesser Caucasus (Jackson, 1992; Reilinger et al., 2004; Forte et al, 2014). The Arabia-Eurasia collision is in its early stages of development, and as such provides earth scientists with the opportunity to understand the dynamics and evolution of young continent-continent collisions and mountain orogeny (Cowgill et al., 2016).

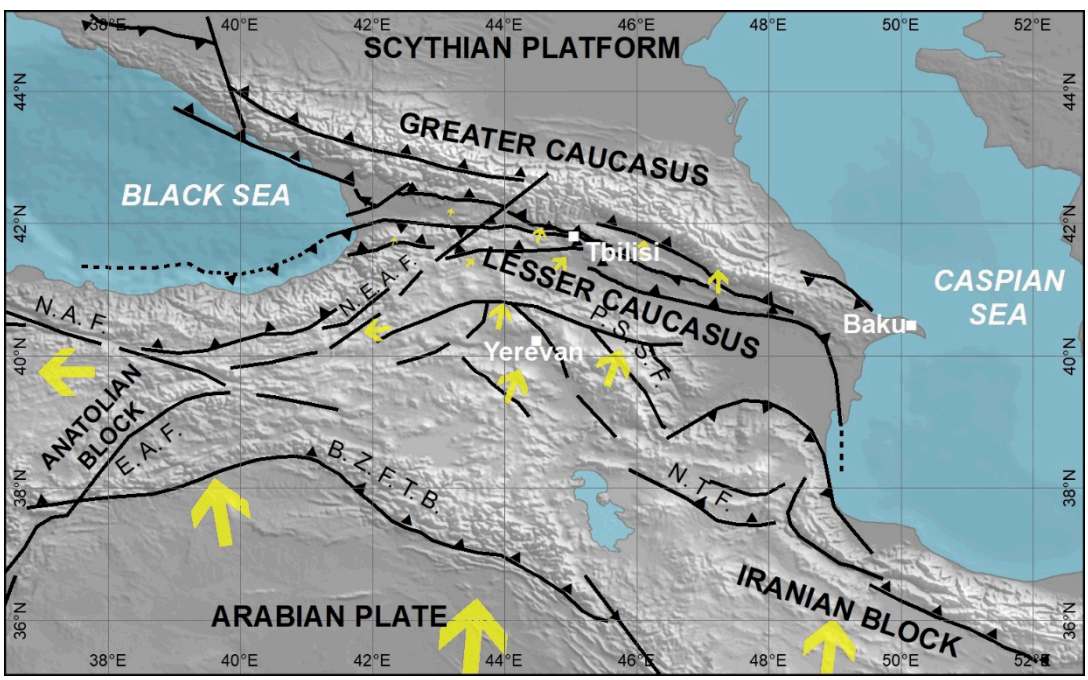


*Figure 2. Tectonic Setting of the Caucasus Region. N.A.F.: North Anatolian Fault, E.A.F.: East Anatolian Fault, N.E.A.F.: Northeast Anatolian Fault, B.Z.F.T.B.: Bitlis-Zagros Fold and Thrust Belt, N.T.F.: North Tebriz Fault, P.S.S.F.: Pambak-Sevan-Sunik Fault. Fastest velocity vector is the northward movement of Arabian Plate at 25 mm/yr.*

The continental convergence and active crustal shortening that is still going on between Arabian and Eurasian plates is evidenced by GPS measurements and high seismic activity observed in the region (Reilinger et al. 2006, Kadirov et al. 2015, Sokhadze et al. 2018). There is also a northward subduction process, thought to be active along the Eastern Caucasus and Central Caspian (Cowgill et al., 2016). Several active faults are capable of generating large magnitude earthquakes in the region (Mellors et al. 2012), though reliable recurrence information is generally not available. The convergence rate increases systematically from ~4 mm/yr in the west, near the Black Sea coast, to ~14 mm/yr in the east, along the Caspian Sea coast (Reilinger et al., 2004). In general, the Greater Caucasus accommodates more of this relative plate motion than the Lesser Caucasus (Forte et al., 2014; Kadirov et al., 2012), although locally in the Tbilisi region shortening appears to be localized within the Lesser Caucasus (Sokhadze et al., 2018).

The tectonic boundary between the Arabian and Eurasian plates is a complex zone of compressional tectonics that gives rise to dominantly thrust and reverse faulting (Figure 3) within the two fold and thrusts belt systems, the Greater Caucasus in the north and Lesser Caucasus to the south; and normal faulting along with other types of faulting in the foreland basins, which are relatively less folded (Gamkrelidze 1986; Nikishin et al. 2001; Stampfli et al. 2001; Hafkenscheid et al. 2006; Kazmin & Tikhonova 2006; Nemčok et al., 2013; Alania et al., 2017).

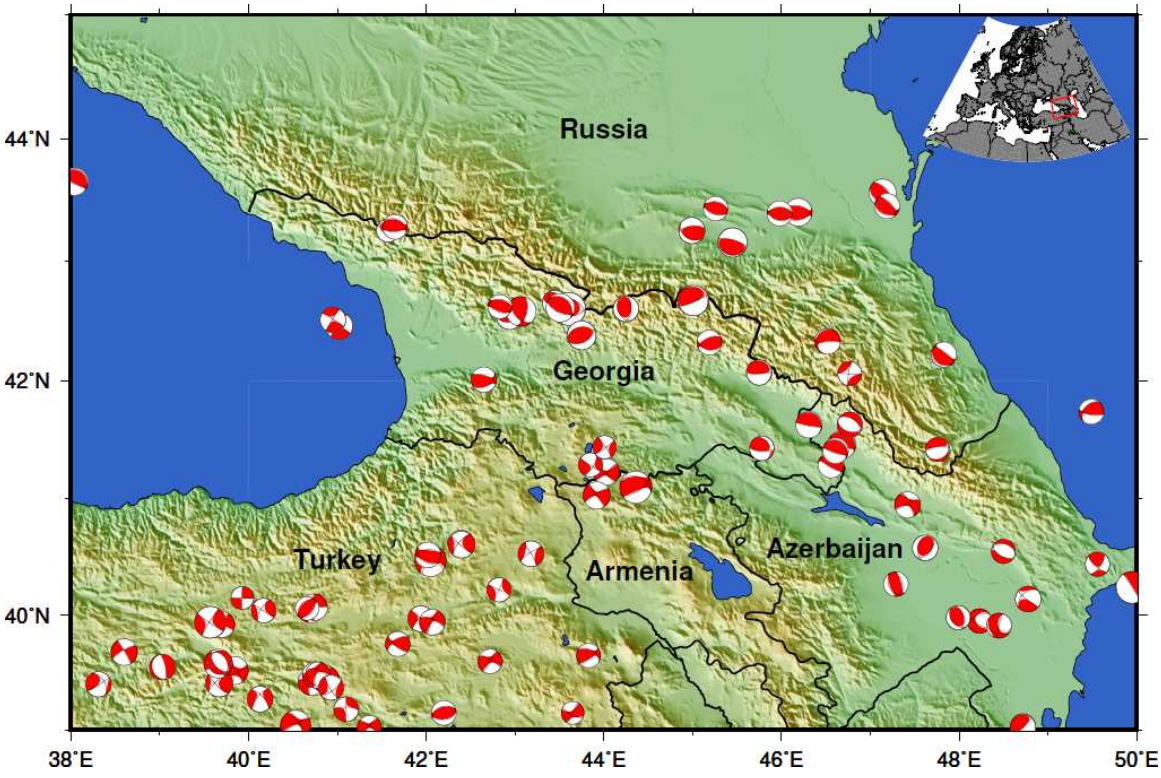


*Figure 3. Focal Mechanisms (GCMT) of Major Earthquakes in Georgia and Surrounding Regions*

A major, south-directed regional-scale thrust system defines the boundary between the intermontane foreland basin and the Greater Caucasus to the north along the entire length of the orogen between Black Sea and Caspian Sea (Figure 2). A similar, major north-directed thrust system defines the boundary between the foreland basins and the Lesser Caucasus to the south

between the Black Sea and the capital of Georgia, Tbilisi (Philip et al. 1989; Forte et al. 2014; Cowgill et al. 2016; Banks et al., 1997).

Despite the fact that the region represents significant earthquake risk, hosts various active fault systems, and has been the subject of geological investigations for more than a century, most studies in the region do not provide the sort of detailed information required to include these faults in a PSHA. To explicitly include an active fault in a PSHA, the information required includes location, type of faulting, seismogenic depth, full geometry (e.g. variation of the dip angle down to the seismogenic depth), length and segmentation, and rate of occurrence of earthquakes on the fault (from instrumental era seismic activity, paleoseismology, geologic slip rates, geodetic slip rates, etc.). Many of these parameters are highly uncertain and quantification of this uncertainty is also desirable where possible.

The first tectonic zonation map in Georgia depicted the major regional fold and fault systems (Gamkrelidze, 1957); subsequent studies have further investigated the regional structure (e.g. Nalivkin, 1973; Dotduyev, 1986; Philip et al., 1989; Banks et al. 1997; Caputo et al. 2000; Adamia and Gujabidze, 2004; Allen et al., 2004; Mosar et al. 2010; Sosson et al. 2010; Adamia et al., 2011; Gamkrelidze et al., 2013; Forte et al. 2014). However, detailed studies of active faults are lacking in the region, with a notable dearth of neotectonic investigations of active faults and folds, paleoseismic dating of major events on active fault systems; or determination of Late Quaternary rates of fault slip or fold growth. With a few exceptions (e.g. Caputo et al., 2000), tectonic units are not parameterized, making it challenging to include active faults explicitly as fault sources in PSHA. Field studies are currently insufficient to document many of the structures and to support detailed delineation of observed structures. As such, advancing understanding of seismic hazard in the Caucasus region requires extensive new geologic, neotectonic, paleoseismic, and geodetic investigations, along with analysis of existing instrumental and historical seismicity, geologic, and topographic data to identify and characterize potential seismic sources.

In this project, we use geologic and geodetic data from existing studies (e.g. CAUSIN compilation, as described in Martin, 2007; Caputo et al, 2000; Cowgill et al., 2016; Adamia and Gujabidze, 2004; etc.), together with inferences drawn from the general structure and mechanical behavior of fold and thrust systems to generate a new active fault model to calculate seismic hazard for Georgia. This information along with data from ongoing unpublished studies in the region was analysed and discussed in various workshops as part of our project with participants from Georgia, Armenia, Azerbaijan, Turkey, the US, and Canada. As a result, while we acknowledge that this compilation incomplete and needs further research and refinement, we use the best available information in the model we generated as a result of this project. For those active faults for which there is insufficient information, we characterize seismic activity using area sources. For those faults for which there is information but disagreement among researchers as to how to interpret the information, we use logic trees to quantify the uncertainty.

To the extent possible, we cross-checked information from various lines of evidence to make sure they were consistent and reflected appropriately in our best estimates and uncertainty bounds. For example, to interpret the geometry of faults and folds, we compared their representations across different sources (e.g. publications listed above, 1:200,000-scale and 1:50,000-scale Soviet-era geologic maps of the region such as Nalivkin (1976), and preliminary results from ongoing unpublished studies).

Most fault slip rates in the region are derived from GPS studies (e.g. Reilinger et al., 2004; Sokhadze et al., 2018; Kadirov et al., 2012). We analysed existing geodetic data to assess slip rates on the faults, assuming that earthquakes release only 20% of the accumulated stresses in region (Jackson, 1992), as evidenced by available geologic slip rates, and instrumental/historical seismic activity rates (unfortunately, paleoseismological studies are sparse in the region). As the next section describes, we used a careful examination of the instrumental earthquake catalogue to confirm delineation of some of the active fault structures and their seismogenic depth, in cases where other information was lacking.

We used the available GPS data throughout the collision zone in the Caucasus region and enhanced the existing GPS network and data by means of installing new permanent stations and performing trans-section GPS surveys from the western part of the Caucasus to the very eastern edge of the main Caucasus thrust (Figure 4). This effort utilized and built upon a new GPS velocity field (1994-2018) including all GPS sites of the Caucasus countries (Armenia, Azerbaijan, Georgia), and was further constrained by geodetic observations available in Turkey, the northern part of the Arabian Plate, the northern Caucasus in Russia, and Iran. Our study provides new constraints on 1) convergence across the Greater Caucasus (spatial distribution of active faults and their associated slip rates and locking depths) from the Black Sea to the Caspian Sea, and 2) faulting and block rotation in the Lesser Caucasus.

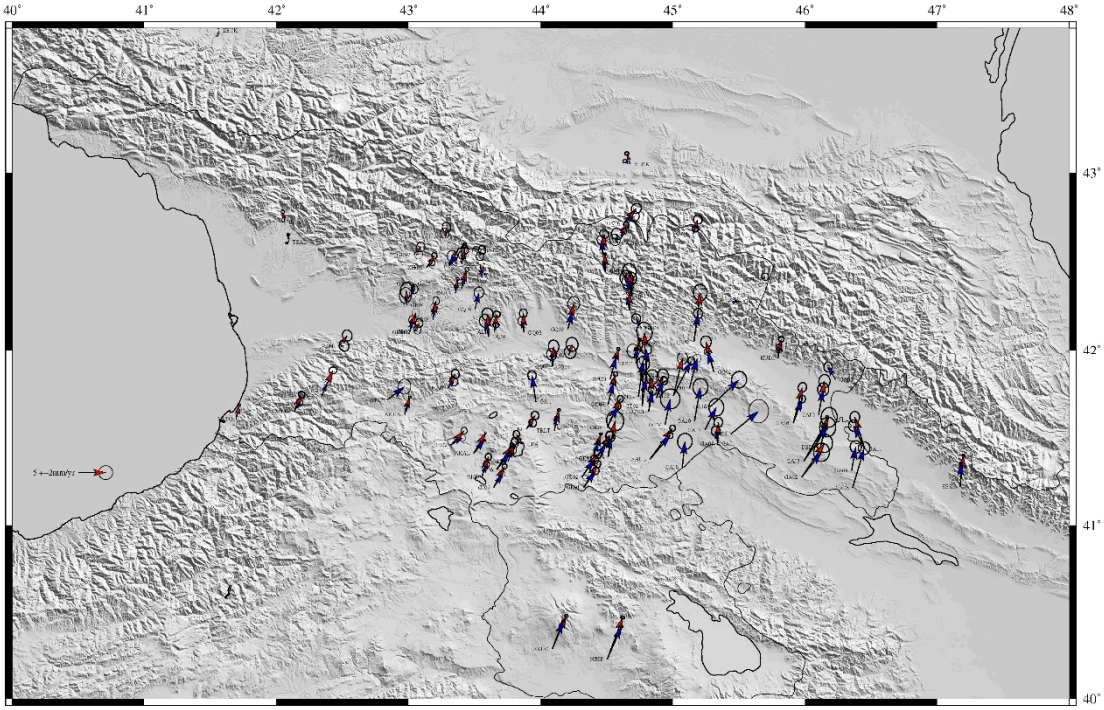


*Figure 4. GPS vectors in and around Georgia (after Akhalaia, in preparation). Legend arrow length indicates a movement of 5±2 mm/year.*

While there are numerous known and possible active faults in the Caucasus, as noted above, often key information about these faults is missing, particularly full geometry and slip rates. The

active faults specifically chosen for the PSHA study are described below and presented in Figure 5 and Table 1. The characteristic magnitude is assigned based on the length of the fault and the potential for the fault (or fault segment) to rupture with neighbouring faults (or fault segments). Various strike, dip and slip combinations are used in a logic tree to characterize earthquake occurrence on the faults. Geodetic slip rates were adjusted based on evidence from geology and seismology as well as earthquake rates for the area sources that underlie the faults, to avoid double counting.

**Frontal Thrust of Caucasus:** The frontal branch of the Main Caucasus Thrust is a well-studied system of faults (e.g. Adamia and Gujabidze, 2004; Caputo et al., 2000; Gamkrelidze, et al., 2013; Mosar et al., 2010). Activity of this system is mainly derived from seismic and geodetic data. We segment this fault system based on the variation of activity rates from west to east (Western, Central and Eastern; as shown in Figure 5).

**Southern Thrust of Kura Fold and Thrust Belt:** This thrust fault lies within the Kura Fold and Thrust Belt (Adamia and Gujabidze, 2004; Alania et al., 2017; Forte et al., 2010; Caputo et al., 2000; Gamkrelidze et al., 2013). Activity of this fault is mainly derived from seismicity and geodetic data.

**Kura Thrust:** This fault is the frontal thrust system bounding the southern margin of the Kura Fold and Thrust Belt (Adamia and Gujabidze, 2004; Caputo et al., 2000; Gamkrelidze et al., 2013; Philip et al., 1989; Forte et al., 2010; Forte et al., 2013). This fault and others within the fold-thrust belt, including the Southern Thrust are inferred to connect at depth with a major, north-dipping basal thrust that roots in the Greater Caucasus and is a main source of earthquakes in eastern Georgia and Azerbaijan.

**Borjomi-Kazbegi Fault System (Tskhinvali-Kazbegi Fault, Eastern Dzirula Fault, Borjomi Fault):** Although this fault system is shown on overview maps in numerous publications, the evidence for the fault is disputed (e.g. Caputo et al., 2000; Koçyigit, et al., 2001; Philip et al., 1989). We include this structure based on a zone of seismic activity in this area, and separate the fault system to three segments based on changes in activity rates: Tskhinvali-Kazbegi Fault, Eastern Dzirula Fault, and Borjomi Fault.

**Tsaishi Fault:** This fault is one of the separated branches of the Caucasus fold and thrust system. We use published activity rates for this fault system, confirmed against seismic data (Caputo et al., 2000; Tibaldi et al., 2017).

**Poti-Abedathi Fault:** This fault forms the eastern portion of the Tsaishi uplift (Adamia and Gujabidze, 2004; Caputo et al., 2000; Gamkrelidze, 2013; Tibaldi et al., 2017). Activity of this fault is mainly derived from seismic and geodetic data.

**Pambak-Sevan-Sunik Fault System:** This is a well-studied fault system in the Lesser Caucasus and East Anatolian Plateau. We use published activity rates to characterize this fault (e.g. Philip et al., 2001; Karakhanyan et al., 2004).

**North Adjara-Trialeti Fault:** This fault is in the northern part of the Lesser Caucasus. Activity and structure of this fault system are published by various researchers (e.g. Adamia and Gujabidze, 2004; Banks et al., 1997; Caputo et al., 2000; Gamkrelidze et al., 2013). We separate

this fault system into three segments, i.e. Eastern, Central and Western segments, based on structural changes in the fault system and the variation in seismic activity rates.

**South Adjara-Trialeti Fault:** This fault represents the back-thrust of the Adjara-Trialeti fold and thrust belt (Adamia and Gujabidze, 2004; Banks et al., 1997; Caputo et al., 2000; Gamkrelidze et al., 2013). Based on structural and seismic parameters, we segment this fault into Western and Eastern segments.

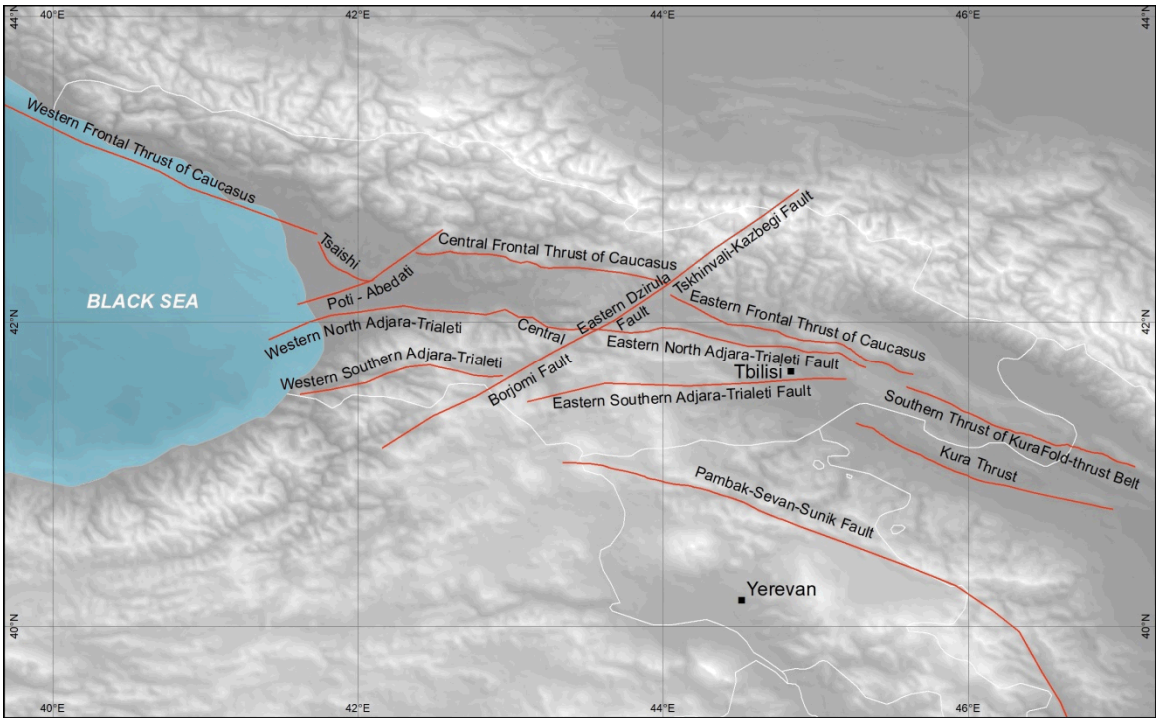


*Figure 5. Fault Sources Explicitly Considered in the Hazard Assessment*

*Table 1. Parameters for Faults Included in the Hazard Assessment*

| FAULT ID. | FAULT NAME | MECHANISM | $M_{CHAR}$ | SLIP RATE (CM/YR) |
|---|---|---|---|---|
| EFTC | Eastern Frontal Thrust of Caucasus | Thrust | 7.5 | 1.0 |
| WFTC | Western Frontal Thrust of Caucasus | Thrust | 7.6 | 0.3 |
| CFTC | Central Frontal Thrust of Caucasus | Reverse | 7.5 | 0.7 |
| KTF | Kura Thrust | Thrust | 7.5 | 1.4 |
| TSF | Tsaishi Fault | Thrust | 7.2 | 0.4 |
| PAF | Poti-Abedathi Fault | SS-RL | 7.3 | 0.5 |
| BF | Borjomi Fault | SS-LL | 7.5 | 0.4 |
| PSS | Pambak-Sevan-Sunik Fault System | SS-RL | 7.8 | 1.3 |
| STK | Southern Thrust of Kura fold-thrust belt | Thrust | 7.5 | 1.4 |
| ENAT | Eastern North Adjara-Trialeti Fault | Thrust | 7.5 | 1.3 |

| | | | | |
|---|---|---|---|---|
| WNAT | Western North Adjara-Trialeti Fault | Thrust | 7.4 | 0.7 |
| CNAT | Central North Adjara-Trialeti Fault | Reverse | 7.3 | 0.9 |
| TKF | Tskhinvali-Kazbegi Fault | SS-LL | 7.3 | 0.8 |
| EDF | Eastern Dzirula Fault | SS-LL | 7.2 | 0.6 |
| WSAT | Western Southern Adjara-Trialeti | Thrust | 7.3 | 0.7 |
| ESAT | Eastern Southern Adjara-Trialeti | Thrust | 7.4 | 1.3 |

## EARTHQUAKE CATALOGUE

While active faults with available slip rate information were included in the hazard model to the extent possible, a comprehensive earthquake catalogue remains a fundamental input into the PSHA in the Caucasus due to lack of good quality information on many of the active fault systems.

Global earthquake catalogues are generally sparse in terms of local earthquakes in this region, particularly in early monitoring period. For example, the ISC catalogue has 30 earthquakes above Mw 5.0 for our study region (36.5°N-45.5°N, 37°E-55°E) between the years 1900 and 1954 (inclusive). In contrast, our compilation includes 378 earthquakes over the same magnitude range and time period.

The most recent regional effort for cataloguing earthquakes in terms of Mw in this area is the Earthquake Model of the Middle East (EMME) project under the auspices of Global Earthquake Model (GEM) (Zare et al., 2014). Although the EMME catalogue is rich in terms of earthquakes in the southwestern portion of our study area (i.e. areas in Eastern Turkey), it is relatively sparse in the Georgian territory.

While the global and regional catalogues are lacking data, in actual fact the region has a rich monitoring history, with much of the data sitting in Soviet-era archives, most of which are paper based and not appearing in any global or regional earthquake catalogues. Consequently, compilation of a comprehensive earthquake catalogue for Georgia was undertaken as part of this project, including digitization of the paper based data, relocation of earthquakes using this newly added dataset, and harmonization of magnitude scales.

### *DATA COMPILATION*

The Caucasus has a documented history of cataloguing earthquakes stretching back to the beginning of the Christian era. Most of the largest historical earthquakes prior to the 19th century are assumed to have occurred on active faults of the Greater Caucasus, but size and location of those events have high uncertainties and hence they cannot be directly assigned to one or another active tectonic structure in the area. Instrumental seismic observation in the Caucasus began in 1899, when the first seismograph was installed in Tbilisi, Georgia. During the Soviet era number of stations increased in the region, providing better network coverage and valuable data set for seismic research. Data from many thousands of earthquakes recorded by this regional network was stored on paper in seismic bulletins. In this project, we pulled together all available paper bulletins from Georgia and neighbouring countries. This allowed significant improvements

in location accuracy for earthquakes in this region. It also paved the way for future collaboration and data exchange among the countries in the Caucasus.

To compile a common regional catalogue of the Caucasus, various catalogues of historical and instrumental seismicity of the region were examined, including:

- ISC catalogue
- Corrected Catalogue of the Caucasus, compiled by the Institute of Earth Sciences (IES), Ilia State University (unpublished),
- Earthquake catalogues provided by the Caucasus project participants: Georgia, Armenia, Azerbaijan, and Turkey
- Paper-based Soviet era bulletins that were digitized for this project
- Catalogues of strong earthquakes in the Soviet era (e.g. Kondorskaya and Shebalin, 1977)
- Earthquake catalogues of Northern Eurasia (Balassanyan et al., 1998)
- The Special Catalogue of Earthquakes for GSHAP Test Area Caucasus (SCETAC), compiled in the frame of the Global Seismic Hazard Assessment Program (GSHAP), for the period of 2000 BC-1993.

Most catalogues for this region consists of both historical and instrumental eras. The documented historical earthquake catalogue stretches back to the ancient period. The source parameters for these historical earthquakes are generally estimated by analyses of the reported intensity data, from contemporary description of damage and other impacts caused by earthquakes. For the older events, the errors, in both location and date/time are likely to be substantial. In particular, the location is often biased by where population centres were located, which is where most of the observed effects of the earthquake would have been reported. The accuracy of parameters of nineteenth century and early instrumental period is relatively better. The quality of the data from early instrumental era (until 1930) is similar to the 19th century. Source parameters of earthquakes at this time were still mainly estimated on the basis of intensity data due to sparse instrumentation.

### *EARTHQUAKE RELOCATIONS*

First arrival and amplitude data for about 15,000 earthquakes were digitized from the Soviet era paper bulletins. Participant countries (Georgia, Armenia, Azerbaijan and Turkey) provided these data for all events with magnitude (in any magnitude scale) greater than 3.7 (from both analogue and digital seismic networks). All data was stored in a web database, open to all project participants, developed particularly for this project by the Georgian project team. After being digitized, 15,000 events that correspond to 118 years of observation in the Caucasus were relocated using procedures detailed below, significantly improving earthquake locations.

In the Soviet era, seismologists located earthquakes using the circle method. Consequently, earthquake location uncertainty was high. Soviet earthquake location routine used the so-called fixed depth approach, assuming seismogenic depth in the region being 10 to 25 km. Therefore accuracy of depth determinations was also low.

When relocating events in this project, it became apparent that many events were completely missing from existing digital catalogues or missing their first arrival data. Therefore, it was necessary to relocate all the events with the combined dataset (local and global) in order to have a reliable assessment of seismic hazard. Within the scope of this project, most of the paper bulletins with earthquake primary data and bulletin data were digitized for all earthquakes larger than magnitude 3.7. Because magnitude scales were non-unique, 3.7 was taken as the threshold magnitude regardless of the magnitude scale used among the Soviet or international magnitudes scales. Since primary data was digitized from the first primary data source, i.e. paper handwritten bulletins, the copies often had mistakes due to difficulties in deciphering the handwritten notes. These problems were resolved, to the extent possible, by cross-checks against data from other sources.

We first relocated merged events with HypoInverse using a 1-D reference model (Godoladze et al., in preparation). For earthquakes greater than ML4.5, we used events with minimum five P-arrivals and maximum 180 degrees of azimuthal gap. Additional depth phases were incorporated from ISC bulletin and these events were relocated using the ILOC location algorithm, which is based on the ISC location algorithm (Bondár and Storchak, 2011; Bondár et al., 2018) and accounts for correlated travel-time prediction errors and attempts for depth resolution. In addition, events with minimum station distance > 100km and azimuthal gap > 180 were double checked against global catalogues, if these events were included in the global catalogues.

### *EARTHQUAKE MAGNITUDES*

The preferred magnitude scale for the earthquake catalogue compiled for this project is moment magnitude, Mw. For sparse local and regional seismic networks, a stable Mw is important for establishing good quality seismicity catalogues and estimating recurrence of earthquakes for seismic source zones. The Gutenberg-Richter b-value can vary significantly, biasing the recurrence rates higher or lower, if the magnitude conversions from small events of traditional magnitudes (ML, mb and Ms) are not regionally and accurately derived. If the moment magnitude (Mw) value is greater than 5.0, it is usually well-determined by global moment tensor solution centers (e.g. GCMT, ETHZ). However, reliable moment magnitude estimates for small/moderate size events (5.0>Mw>3.5) can be difficult to obtain due to the uneven distribution of stations, the complex tectonic structure, and effects of strong structural variations that are not necessarily well-captured with a simple 1-D velocity and attenuation structure.

We find that the coda envelope amplitude measurements are not very sensitive to 3-D path heterogeneity at lower frequencies and source radiation patterns, provided that ample duration is available for the amplitude measurements (Mayeda and Walter, 1996; Mayeda et al., 2003; Gök et al., 2016). Direct wave amplitude measurements are affected by source radiation pattern,

directivity and heterogeneities along the path, which causes large amplitude variability whereas coda-derived magnitudes provide great stability due to their averaging nature.

Hence we use coda calibration technique to directly obtain Mw from the source spectra that were obtained at 14 narrow frequency-band envelopes (0.02Hz – 8Hz) using the Java-based Coda Calibration Tool (CCT), recently developed at LLNL and available online at: https://github.com/LLNL/coda-calibration-tool. We empirically derived coda envelope shape (each region has unique decay parameters) and path (attenuation and geometrical spreading) correction parameters. We then used those parameters to measure coda amplitudes at 100 sec measure time after the start time of the envelope. We analyzed more than 400 regional waveforms (200km < epicentral distance < 1,600km) recorded by the Global Seismic Network (GSN) and regional networks of Azerbaijan and Georgia.

Examples of amplitudes are presented from the Azerbaijan network data. Figure 6a shows before and after the path correction at 0.7Hz to 1.0Hz band coda amplitudes of BRD and HYR, and 4.0 Hz to 6.0 Hz coda amplitudes of IML and BLQ stations of Azerbaijan. Final source spectra are robust up to high frequencies (Figure 6b shows an example spectrum). This indicates that the 1-D path correction and coda envelope models can adequately estimate reliable Mw's down to Mw3.0.

After directly obtaining Mw for as many events as possible, there still remained many events in the catalogue for which a conversion was needed from other magnitude scales such as ML, mb, Ms or the Soviet-era scales such as K class, MLH and MPV. Majority of these events had K class available along with other magnitudes. Fortunately, a few stations from the former Soviet Union were co-located with modern broad-band sensors. This provided an opportunity to directly compare moment magnitudes (Mw) with Soviet type magnitudes (especially K class, since it was available for majority of the events in the catalogue), and derive region-specific relationships between them, as described in the next section.

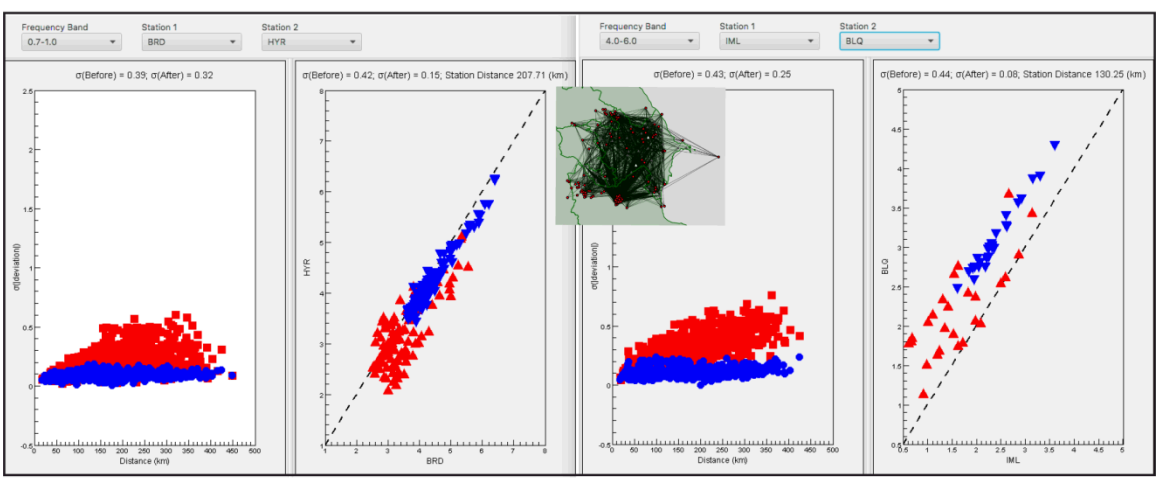


*Figure 6a. Path correction at 0.7 to 1.0 Hz and 4.0 to 6.0 Hz. Red indicates before, and blue after the correction. Left panel shows the improvement at each station pair, right panel is the improvement at specific station pair (the offset from dotted line is the site term). Path map shows 0.7_1.0 Hz coda envelopes used in calibration.*

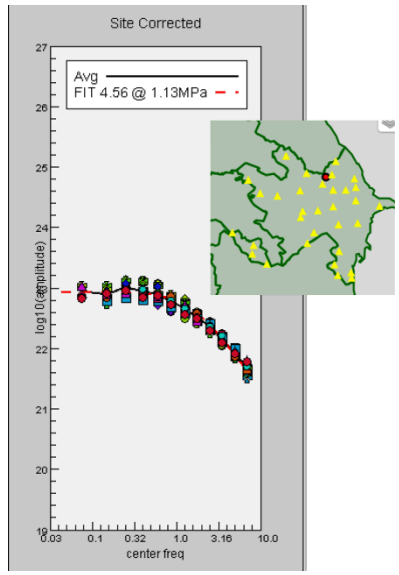


*Figure 6b. Final source spectra of an event that occurred in Greater Caucasus and recorded by nearly 32 stations (Mw=4.56). Note the similarity of source spectra at each station over the wide range of frequencies. In the right panel, yellow triangles are stations, solid red circle is the location of the earthquake shown on the left.*

## *PSHA-READY CATALOGUE*

Further details on the catalogue compilation can be found in Godoladze et al. (in preparation). The resulting catalogue encompasses the region between 37°E-55°E longitudes and 36.5°N-45.5°N latitudes, and includes nearly 47,000 earthquakes of Mw1.5 and above, about 4,000 of which are Mw4.0 and greater. The geographic extent of the catalogue's coverage is intended to include sources of seismicity beyond Georgia's borders, but may be damaging inside the territory of Georgia.

The catalogue was harmonized to Mw by obtaining as many directly calculated Mw's as possible and converting from other magnitude scales where necessary. The hierarchy of preferred magnitudes varied, depending on the time interval, reflecting changes in the instrumentation history. We used three different time intervals: 1900-1954, 1955-2003, and 2004-2017. In the Soviet-era, K class was the dominant magnitude scale used. Taking advantage of the co-located Soviet era and digital instruments (Azerbaijan National Network of the Republican Seismic Survey Center), we computed K class and Mw for 85 earthquakes of Mw between 3.6 and 6.5 to derive a direct relationship between Mw and K class (Figure 7; Equation 1). Orthogonal regression was used to derive this relationship.

Other magnitude conversions, though used less prominently, were developed as needed using orthogonal regression between each magnitude scale and Mw from a combination of coda calibration technique based Mw calculated as part of this project and the existing Mw from global compilations such as GCMT and ISC.

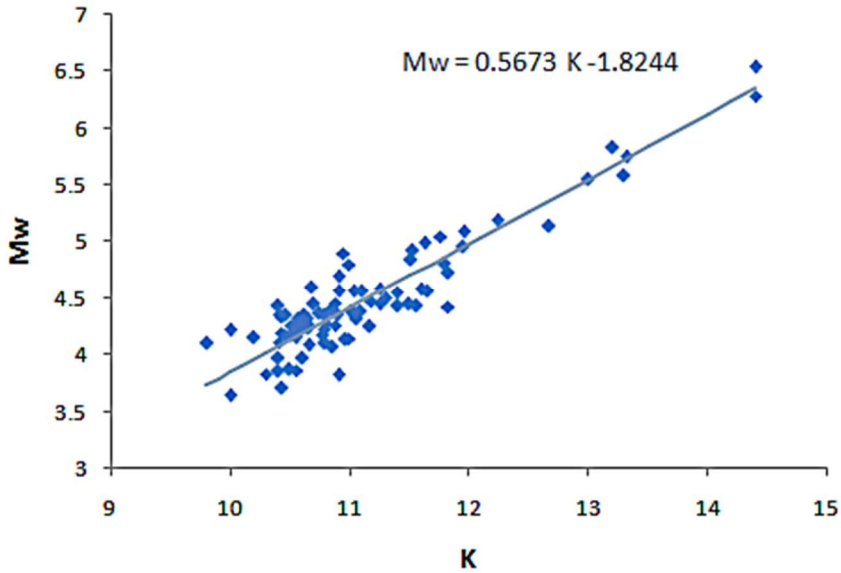


*Figure 7. Orthogonal Regression between K Class and Mw*

$$Mw = 0.5673\,K - 1.8244 \qquad \text{[Equation 1]}$$

Completeness of the earthquake catalogue was investigated for individual magnitude and year bands. Cumulative earthquake rates were plotted iteratively for various year bands to find the corner magnitude, and number of earthquakes was plotted by year for each 0.1 magnitude unit (Figure 8) to refine each corner magnitude.

The resulting completeness intervals for the entire catalogue are as follows: Mw5.1 and above are complete since 1900, Mw4.4 and above since 1955, Mw4.0 and above since 1965, Mw3.7 and above since 1981, Mw3.5 and above since 2004, and Mw2.5 and above since 2009 (Figure 8; bottom panel). There is a significant geographic variation in completeness of the earthquake catalogue across the Caucasus. Therefore, it should be noted that these completeness intervals are specifically derived for calculating seismic hazard in Georgia, and may not be appropriate for neighbouring countries. In particular, the strong monitoring history in Georgia provides a significantly more complete catalogue for earlier years of monitoring compared to many other regions in the world.

After the completeness intervals are applied, the complete catalogue (bottom panel in Figure 8 and Figure 9) includes about 16,000 events of Mw2.5 and larger, and about 3,600 events of Mw4.0 and larger between the years 1900 and 2017 inclusive.

While majority of the earthquakes in the west have a depth of between 0 and 35km, there is a significant number of earthquakes with depths larger than 40km to the east (Figure 9). This indicates the possibility of remnant or incipient subduction in eastern Caucasus (e.g. Mellors et al., 2012), which is currently the subject of further investigations.

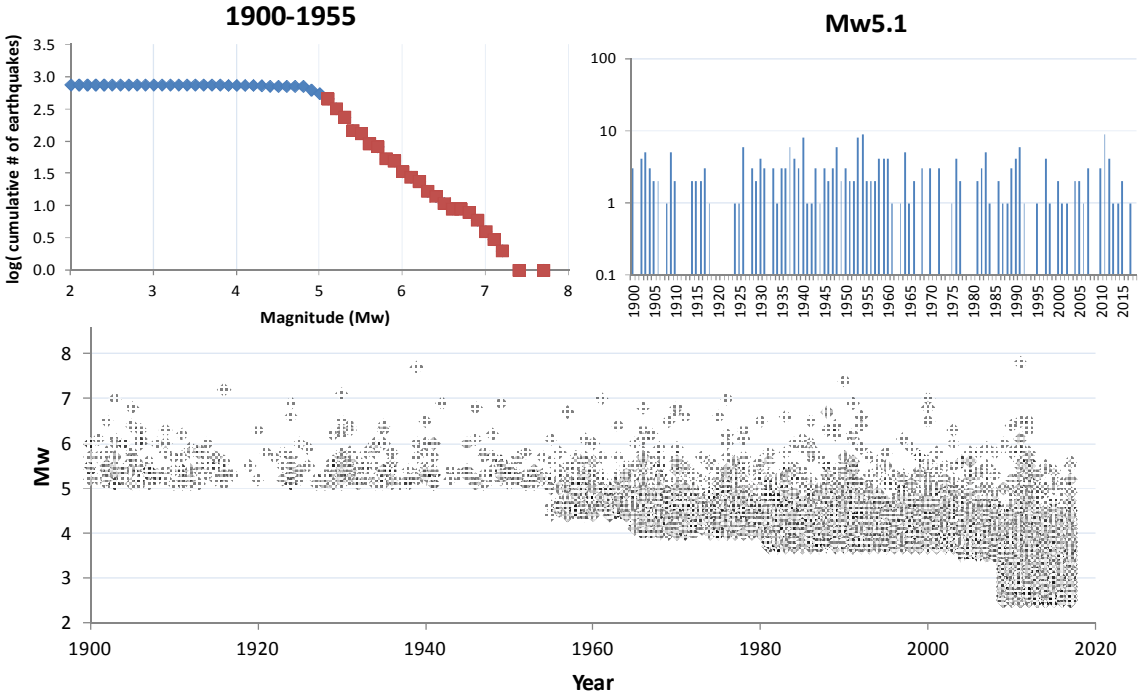


*Figure 8. Upper left panel: An example cumulative rate plot to determine the corner magnitude of completeness. These were prepared iteratively for various year bands to determine completeness intervals. Upper right panel: An example plot of number of earthquakes by year. These were prepared for each 0.1 magnitude unit to check stability of the corner magnitudes. Lower panel: Final catalogue, after completeness intervals are applied.*

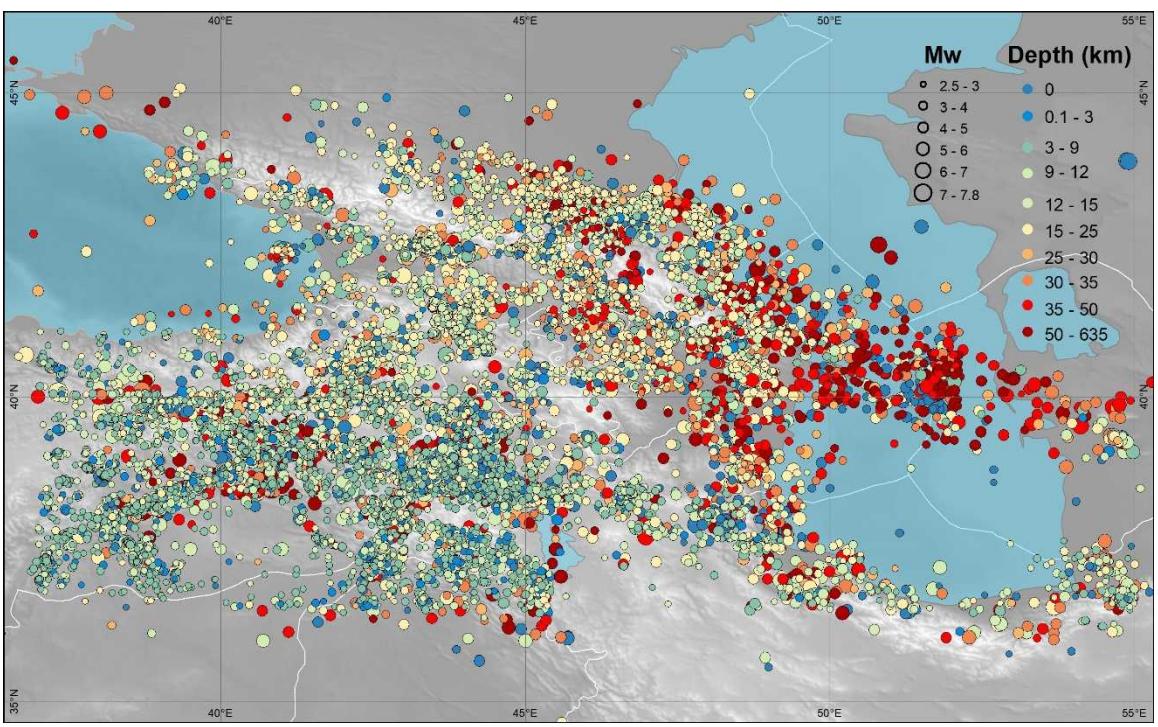


*Figure 9. Complete Catalogue of Instrumental Seismicity for Georgia in terms of Mw and Depth.*

The earthquake catalogue was declustered using various algorithms (Gardner and Knopoff, 1974; Reasenberg, 1985; Uhrhammer, 1986, etc.) and recurrence parameters were calculated based on the various versions of the declustered catalogue. Some algorithms (e.g. Gardner and Knopoff, 1974; Uhrhammer, 1986) declustered the catalogue to the point where the robustness of the statistics on the recurrence parameters was compromised. Such algorithms were taken out of consideration. The remaining algorithms were tested to see their impact on the recurrence relations, and the impact was not significant. Hence, given the disagreements in the scientific and engineering community regarding the use of catalogue declustering in PSHA, our preference was not to decluster the catalogue.

## SEISMIC SOURCE ZONES

Area sources are used to characterize the distributed shallow crustal seismicity that could not be associated with active faults used in the PSHA. Seismicity rates are assumed to be uniform inside each source zone. When delineating the source zones, tectonics of the region as well as the seismicity patterns were taken into account. Two alternate sets of area sources are used in order to represent the uncertainty in the source zone boundaries (Figures 10a and 10b). In addition to the shallow crustal seismicity, one area source is used to represent the deeper seismicity (>40km) in the eastern Caucasus.

Five source zones are located along the main axis of the Greater Caucasus. Delineation of the sources reflects abrupt structural changes along the southern margin of Greater Caucasus, as well as changes in earthquake activity rates. Two different interpretations of the segmentation are shown in Figures 10a and 10b.

On the northern margin of the Greater Caucasus, where the range transitions to the Scythian Platform, area sources are used to represent potential seismic sources in the Kuban and Terek foreland basins, Stravropol High between the basins, and the Dagestan fold and thrust belt. The northern edges of these sources are positioned based on the cut-off distance beyond which the impact on hazard in Georgia is negligible. Delineation of the east-west boundaries is varied between the two alternative source zone models to reflect the increase in seismic activity rates while acknowledging the physical structural boundaries such as the Dagestan fold and thrust belt. To the south of the Greater Caucasus are source zones that span from the Rioni Basin in the west to the Kartli and Kura Basins in the east.

Further south, the Lesser Caucasus structures and the intense seismicity in the Javakheti highland are also characterized with two alternative area source representations. The level of detail in the delineation of the zones generally gets lower for zones that are relatively distant from Georgian territory since they do not have a significant contribution to hazard in Georgia.

Maximum magnitudes were assigned to each source zone based on various considerations such as maximum historical earthquake inside the zone as a lower bound, and geometry of known faults within each zone as a physical basis for potential for large earthquakes. For the the multiple segments within the Greater Caucasus, the lengths of the segments were used as a guiding consideration as well. The geometry and length of the faults were taken into account using Wells and Coppersmith (1994) relations between rupture length/area and magnitude. Generally, no zone was assigned a maximum magnitude lower than Mw7.2.

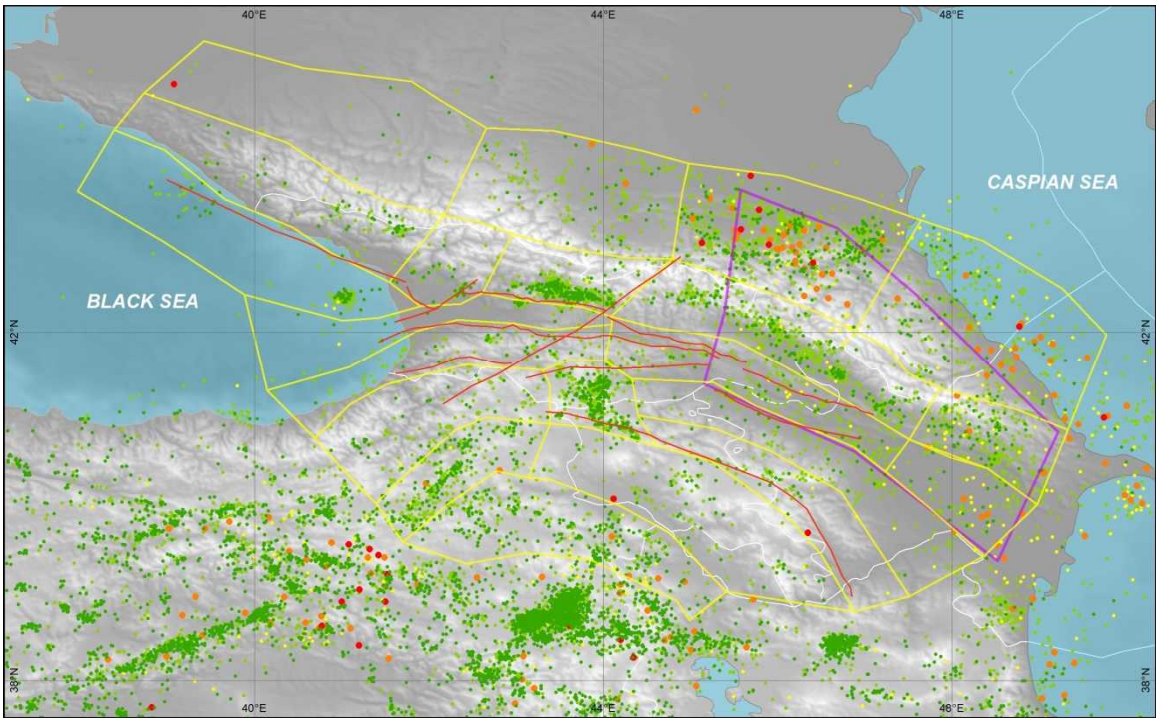


*Figure 10a. Delineation of Seismic Source Zones (Model 1). Red Lines: Modelled Faults, Magenta Polygon: Deep Earthquake Source. Yellow Polygons: Model 1 for Shallow Crustal Earthquake Sources.*

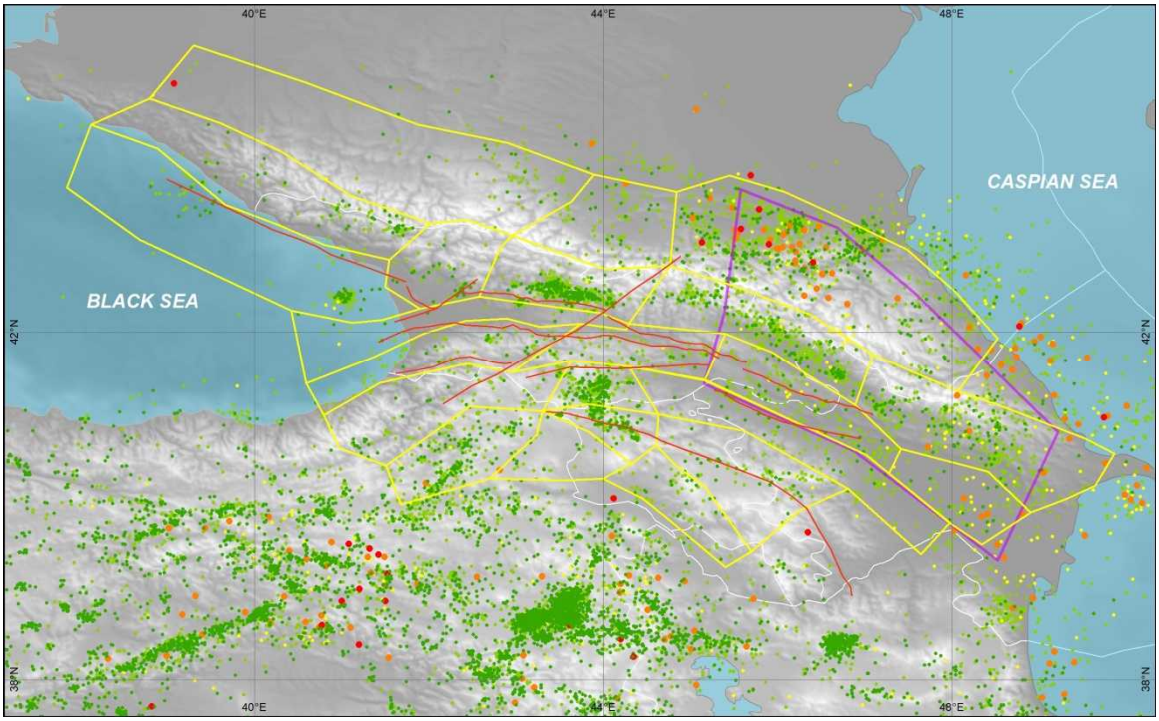


*Figure 10b. Delineation of Seismic Source Zones (Model 2).*

The deep seismicity in eastern Georgia is also characterized by an area source whose recurrence parameters are included in Table 2. The deep source is modeled at a distributed depth of 40km to 60km. Some earthquakes in this zone are deeper than 60km, therefore using a 60km maximum depth introduces slight conservatism, but we consider this acceptable given the uncertainties in depth determinations of earthquakes, particularly earlier in the catalogue.

Bounded Gutenberg-Richter relationship was used to calculate recurrence in each source zone. Table 2 presents the full set of recurrence parameters and example Gutenberg-Richter plots are shown in Figure 11.

*Table 2a. Recurrence Parameters for Source Zones (Model 1)*

| SOURCE ZONE NO. | SOURCE ZONE NAME | $M_{MAX}$ | G-R B-VALUE | G-R A-VALUE |
|---|---|---|---|---|
| 1 | Greater Caucasus - West | 7.8 | 0.660 | 2.347 |
| 2 | Greater Caucasus - Central | 7.4 | 0.751 | 2.678 |
| 3 | Northeast Black Sea | 7.4 | 0.980 | 3.686 |
| 4 | Western Main Caucasus | 7.6 | 0.925 | 4.131 |
| 5 | Eastern Main Caucasus | 7.8 | 0.901 | 3.902 |
| 6 | Rioni Valley | 7.4 | 0.680 | 2.172 |
| 7 | North Lesser Caucasus 1 | 7.6 | 0.763 | 2.544 |
| 8 | North Lesser Caucasus 2 | 7.5 | 0.703 | 2.425 |
| 9 | SW Georgia | 7.4 | 0.857 | 2.893 |
| 10 | Javakheti | 7.2 | 1.147 | 5.000 |
| 11 | Kartli | 7.6 | 0.802 | 2.909 |
| 12 | North Kartli | 7.6 | 0.904 | 3.401 |
| 13 | Terek | 7.6 | 0.790 | 2.732 |
| 14 | Kuban | 7.4 | 0.744 | 2.455 |
| 15 | Dagestan Fold and Thrust | 7.8 | 1.076 | 4.990 |
| 16 | Greater Caucasus – East | 7.8 | 0.982 | 4.342 |
| 17 | Kura | 7.4 | 0.613 | 2.181 |
| 18 | NE Turkey | 7.8 | 0.773 | 3.194 |
| 19 | Kars | 7.4 | 0.645 | 1.922 |
| 20 | North Armenia | 7.2 | 0.858 | 3.541 |
| 21 | Lesser Caucasus 1 | 7.6 | 0.789 | 2.713 |
| 22 | Lesser Caucasus 2 | 7.6 | 0.806 | 2.581 |
| 23 | Deep Seismicity | 7.6 | 0.904 | 3.543 |

*Table 2b. Recurrence Parameters for Source Zones (Model 2)*

| SOURCE ZONE NO. | SOURCE ZONE NAME | $M_{MAX}$ | G-R B-VALUE | G-R A-VALUE |
|---|---|---|---|---|
| 1 | Kuban Basin | 7.8 | 0.689 | 1.725 |
| 2 | Terek Basin | 7.8 | 0.872 | 3.276 |

| | | | | |
|---|---|---|---|---|
| 3 | Dagestan Fold and Thrust Belt | 7.8 | 1.084 | 4.984 |
| 4 | Thrust Front East | 7.8 | 0.945 | 4.122 |
| 5 | Greater Caucasus - West | 7.8 | 0.661 | 2.377 |
| 6 | Riona Uplift | 7.6 | 0.967 | 3.598 |
| 7 | Greater Caucasus - Central | 7.6 | 0.924 | 4.124 |
| 8 | Greater Caucasus - East | 7.9 | 0.910 | 4.027 |
| 9 | East Greater Caucasus | 7.6 | 0.941 | 4.064 |
| 10 | North Black Sea | 7.6 | 0.982 | 3.680 |
| 11 | Rioni Valley | 7.6 | 0.647 | 2.142 |
| 12 | Adjara Trialet | 7.6 | 0.789 | 2.811 |
| 13 | Alasani | 7.8 | 0.849 | 3.327 |
| 14 | Kura | 7.8 | 0.662 | 2.479 |
| 15 | Artvin | 7.8 | 0.829 | 2.959 |
| 16 | Javakheti | 7.2 | 0.997 | 4.537 |
| 17 | Kartli | 7.8 | 0.819 | 3.066 |
| 18 | Pambak Sevan Fault Region | 7.9 | 0.704 | 2.355 |
| 19 | Kars | 7.6 | 0.750 | 3.234 |
| 20 | Lesser Caucasus | 7.8 | 0.730 | 2.740 |
| 21 | Agri | 7.8 | 0.819 | 3.475 |
| 22 | Deep Seismicity | 7.6 | 0.904 | 3.543 |

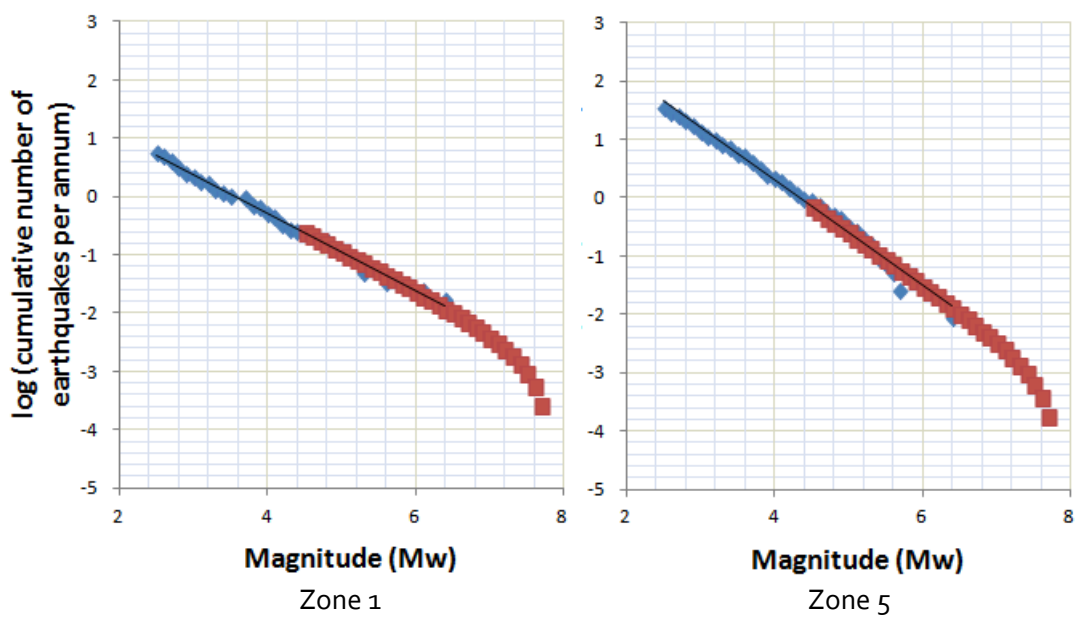


*Figure 11a. Cumulative number of earthquakes per annum plotted against magnitude for example source zones (Model 1). Blue diamonds indicate observed seismicity and red squares indicate modeled seismicity (bounded Gutenberg-Richter model).*

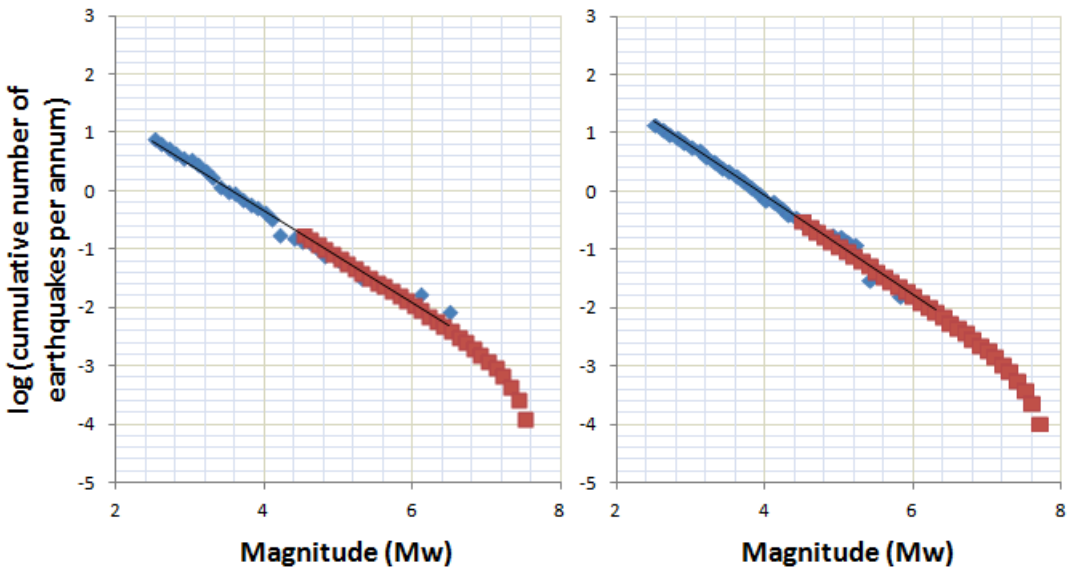


Zone 12 Zone 13

*Figure 11b. Cumulative number of earthquakes per annum plotted against magnitude for example source zones (Model 2). Blue diamonds indicate observed seismicity and red squares indicate modeled seismicity (bounded Gutenberg-Richter model).*

Uncertainties in source parameters listed in Table 2 are accounted for in a logic tree framework. The alternative source zone models are weighted 0.50 each. Uncertainty in the depth of the shallow crustal seismicity is accounted for by assigning 0.50 weight to 10km source depth, and 0.50 to 15km source weight. Two nodal planes are weighted 0.50 each, depending on the expected earthquake faulting mechanisms in each source zone. For earthquakes in the deep seismicity source zone, a broader depth range is used: depths of 40km, 50km, and 60km are weighted 0.33 each.

## GROUND MOTION CHARACTERIZATION

The choice of ground motion prediction equations (GMPEs) used in PSHA to characterize strong ground motion is dependent on the tectonic setting of the study area and availability of strong motion data. In order of decreasing amount of data, options are to: 1) empirically derive region-specific GMPEs, 2) choose regionally or globally derived GMPEs based on comparisons and/or calibrations against locally recorded strong motion data, and 3) choose regionally or globally derived GMPEs based on judgement taking into account the local attenuation characteristics.

Unfortunately, strong motion data are limited in Georgia. We use the available data to guide the GMPE choices, including two strong motion recordings from the 1990 Mw5.4 Javakheti region earthquake at 15km-20km distance, two strong motion recordings from the 1991 Mw6.9 Racha earthquake at 115km-130km distance, and numerous recordings from the smaller magnitude aftershocks of the Racha earthquake. This dataset is limited in terms of magnitude

and distance range, however there is an ongoing effort to increase the number of strong motion instruments in the country. As data becomes available from these instruments, better calibration/validation of the GMPEs will be possible, leading to a more robust strong motion characterization for Georgia.

Since there is not enough strong motion data for options (1) and (2) described above, ground motion characterization for this PSHA study uses globally derived GMPEs with the limited recorded data guiding the GMPE selection. Global GMPEs broadly fall into one of the following tectonic groupings: a) active tectonic regions with shallow crustal seismicity, b) stable continental regions, and c) subduction zones. Georgia is located in an active tectonic region with relatively high attenuation rates (low Q) for shallow crustal earthquakes (Figure 12).

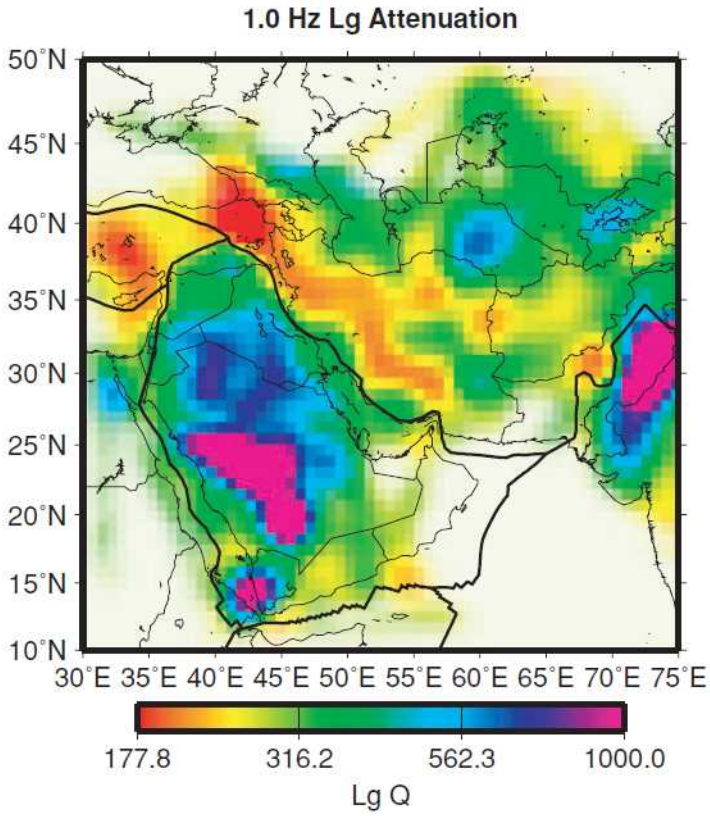


*Figure 12. Attenuation map of Lg Q at 1 Hz (from Pasyanos et al., 2009).*

Four GMPEs from Next Generation Attenuation (NGA) West-2 project (active tectonic regions) are used in this project: Abrahamson et al. (2014) – referred to as ASK14, Boore et al. (2014) – BSSA14, Campbell and Bozorgnia (2014) – CB14, and Chiou and Youngs (2014) – CY14. In addition, Akkar et al. (2014) – ASB14 relationship is used to characterize ground shaking from shallow crustal seismicity (Figure 13). The ASB14 relationship is mainly based on data from Europe and the Middle East and is weighted 0.50. The NGA West-2 relations are based on global data and are collectively weighted 0.50 (i.e. the weight of each individual NGA West-2 relationship is 0.125).

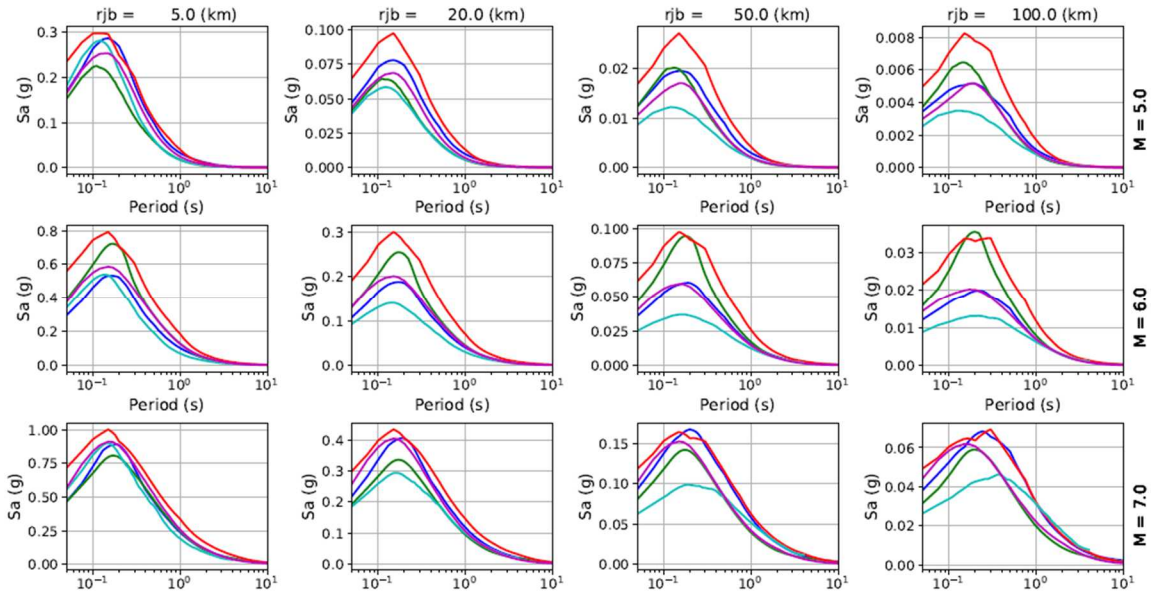


*Figure 13. GMPEs Used to Represent Ground Shaking from Shallow Crustal Seismicity at Various Distances (Rjb: Closest Distance to Surface Projection of Rupture) and Magnitudes (Mw). Red: CB14,Green: BSSA14, Blue: ASK14, Magenta: CY14, and Cyan: ASB14.*

To the east of Georgia, there are deep earthquakes that may be associated with subduction. Since there are no strong motion data available from these earthquakes, four subducting slab GMPEs from around the world are used with equal weights to characterize the deep earthquakes to the east. These are Atkinson and Boore (2003), Abrahamson et al. (2015), Garcia et al. (2005), and Zhao et al. (2006). The first two were developed with global datasets while Garcia et al. (2005) was developed with Mexican subducting slab strong motion data and Zhao et al. (2006) with Japanese data.

Ground motions from all GMPEs were computed for Vs30 = 801m/s, since the draft update of the building code of Georgia uses it as the reference site condition. Vs30 is defined as the average shear-wave velocity of the upper 30 m of the site.

## MODEL IMPLEMENTATION AND RESULTS

Various free and open-source PSHA software are available to implement the source and ground motion characterizations and run probabilistic analyses, such as OpenQuake (Pagani et al., 2014), OpenSHA (Field et al., 2003), and EqHaz (Assatourians and Atkinson, 2013). OpenQuake was used for this study.

The ground motions are presented for five probabilities of exceedance: 2% in 50 years (corresponding to a return period of 2,475 years), 5% in 50 years (975-year return period), 10% in 50 years (475-year return period), 20% in 50 years (225-year return period), and 40% in 50 years (100-year return period). Results are presented in a series of hazard maps of peak ground acceleration (PGA), and spectral accelerations at periods of 0.2 sec and 1.0 sec for each

probability of exceedance (Figures 14 through 18). Full suite of maps for all spectral accelerations (0.1 sec, 0.2 sec, 0.5 sec, 2.0 sec, and 4.0 sec) and PGA can be found in Appendix A. In addition, the results are presented for selected cities in terms of uniform hazard spectra (UHS) in Figure 19; and hazard curves for PGA and spectral accelerations at 0.2 sec and 1.0 sec in Figure 20. Full city results in terms of UHS and hazard curves are presented in Appendices B and C, respectively. Hazard deaggregations are presented in Figure 21 for Tbilisi, Kutaisi and Batumi at 10% probability of exceedance in 50 years. Appendix D includes deaggregations at 2% probability of exceedance for the same three cities.

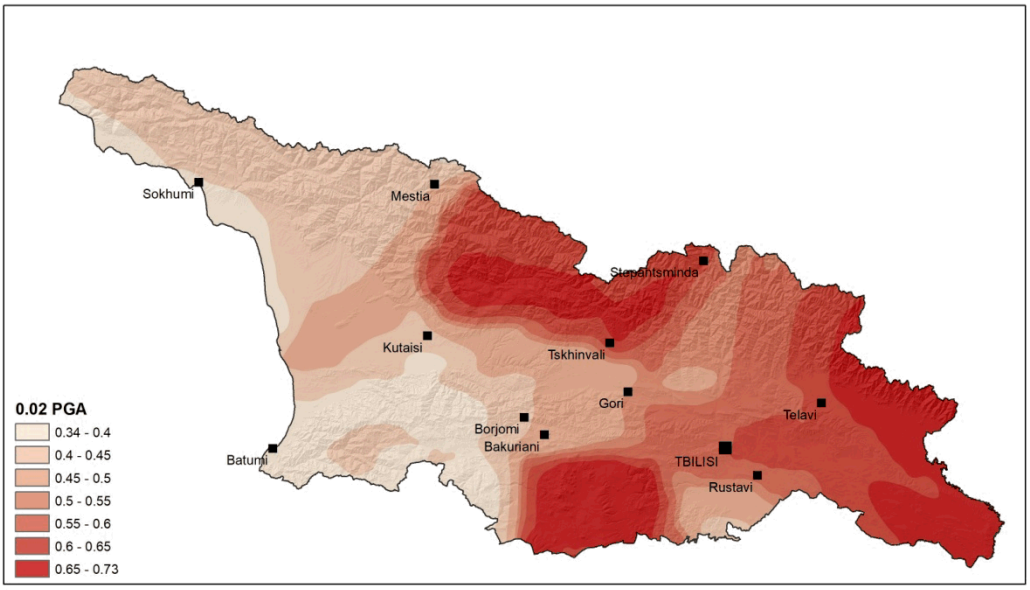


(a)

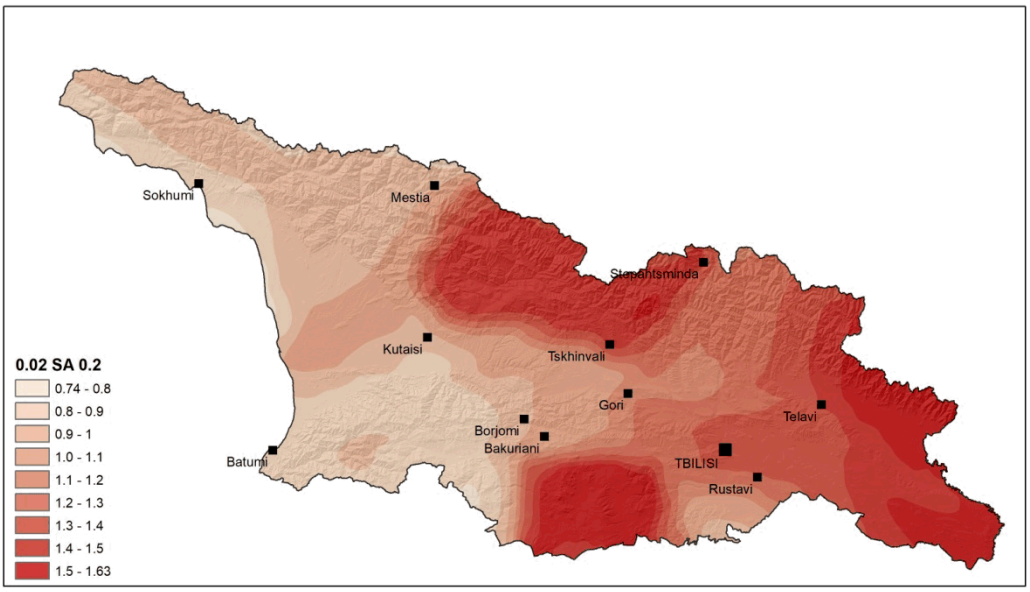


(b)

*Figure 14. Probabilistic seismic hazard in Georgia with a 2% chance of exceedance in 50 years in terms of (a) PGA, (b) Spectral Acceleration at 0.2 sec*

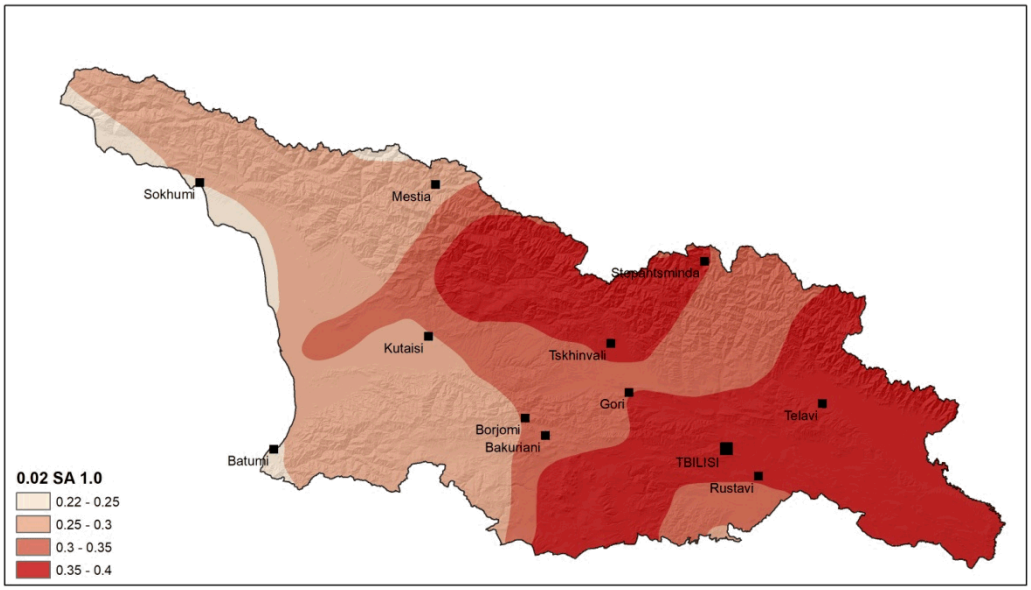


(c)

*Figure 14 (cont). Probabilistic seismic hazard in Georgia with a 2% chance of exceedance in 50 years in terms of (c) Spectral Acceleration at 1.0 sec*

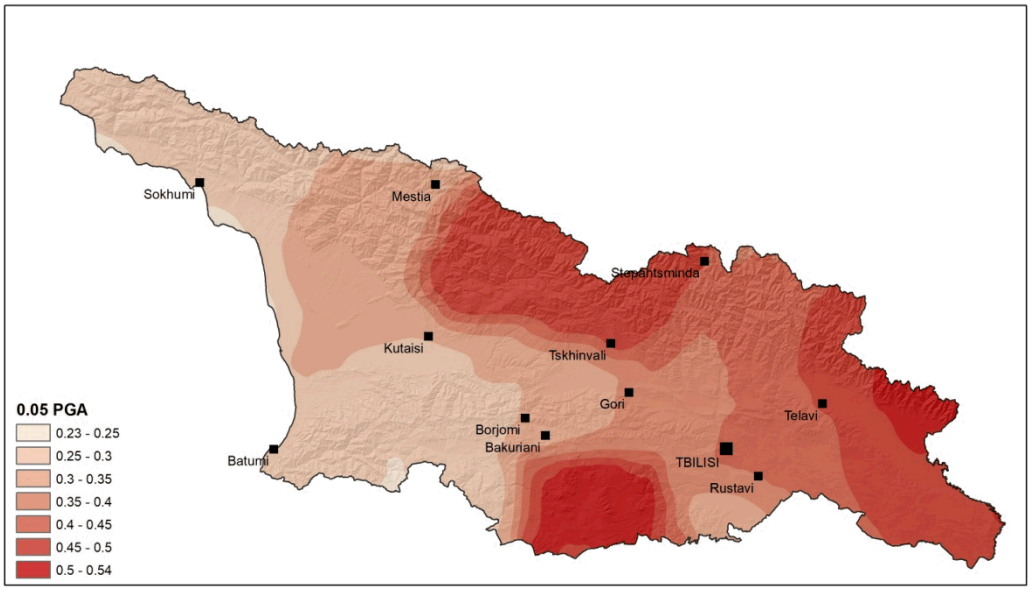


(a)

*Figure 15. Probabilistic seismic hazard in Georgia with a 5% chance of exceedance in 50 years in terms of (a) PGA*

(b)

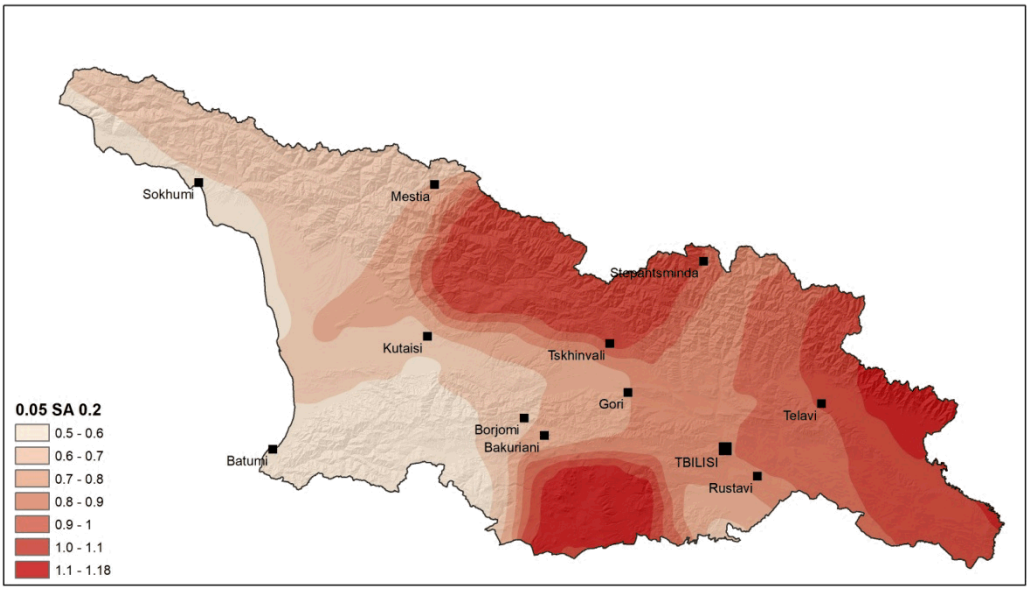


(c)

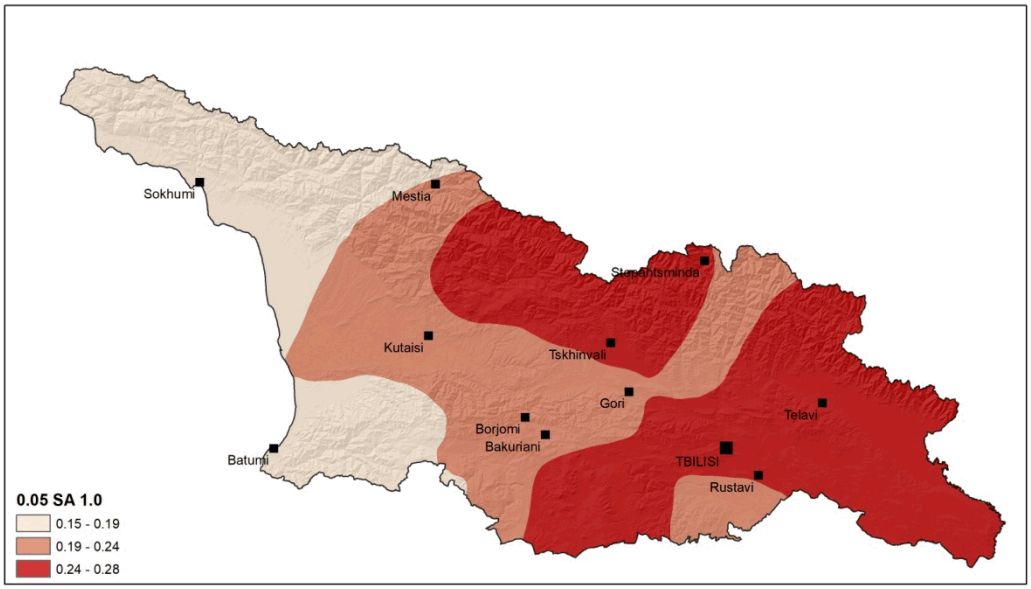


*Figure 15 (cont). Probabilistic seismic hazard in Georgia with a 5% chance of exceedance in 50 years in terms of (b) Spectral Acceleration at 0.2 sec, (c) Spectral Acceleration at 1.0 sec*

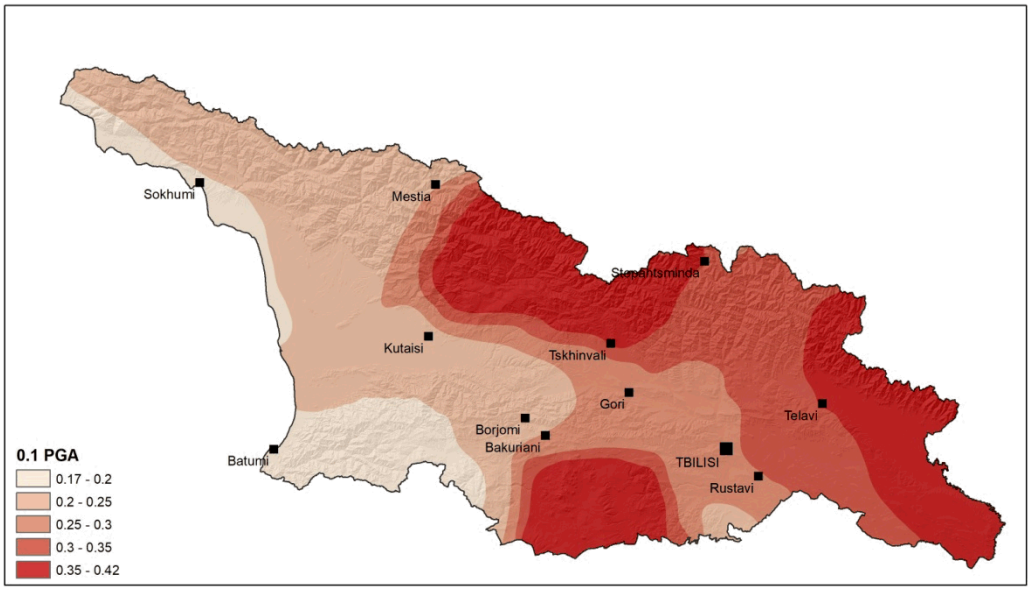


(a)

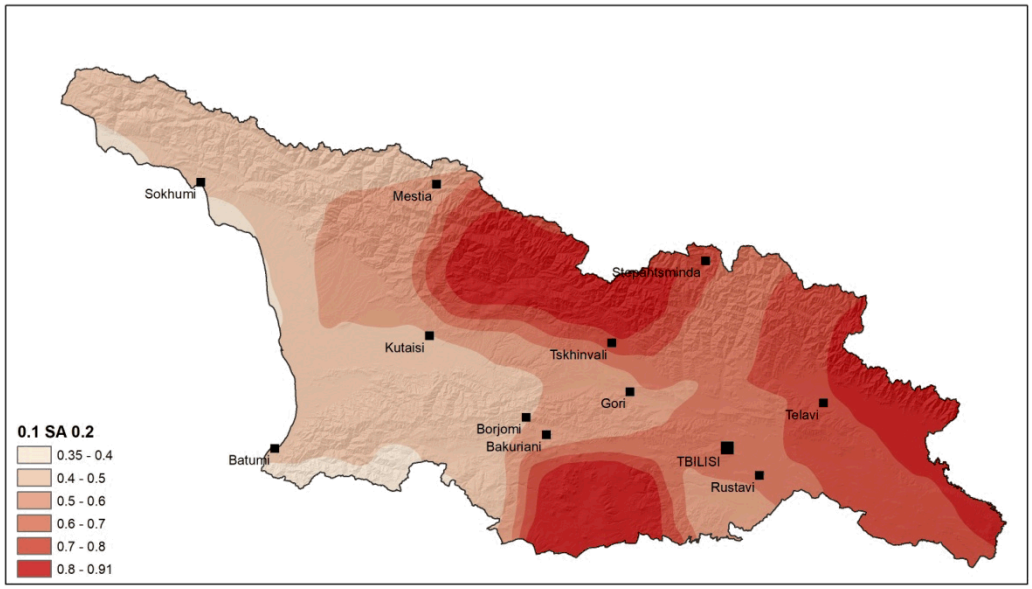


(b)

*Figure 16. Probabilistic seismic hazard in Georgia with a 10% chance of exceedance in 50 years in terms of (a) PGA, (b) Spectral Acceleration at 0.2 sec*

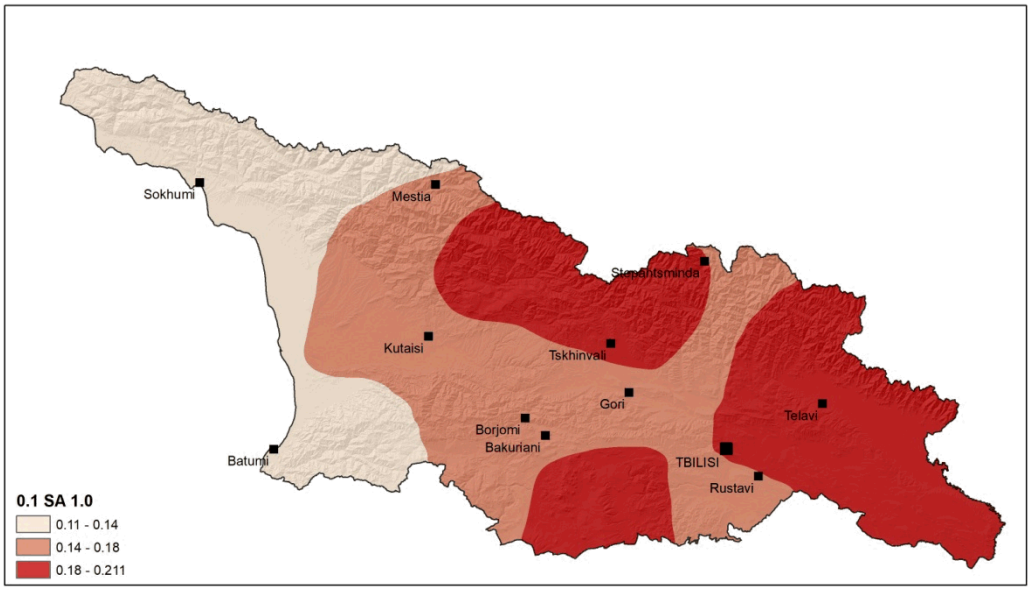


(c)

*Figure 16 (cont). Probabilistic seismic hazard in Georgia with a 10% chance of exceedance in 50 years in terms of (c) Spectral Acceleration at 1.0 sec*

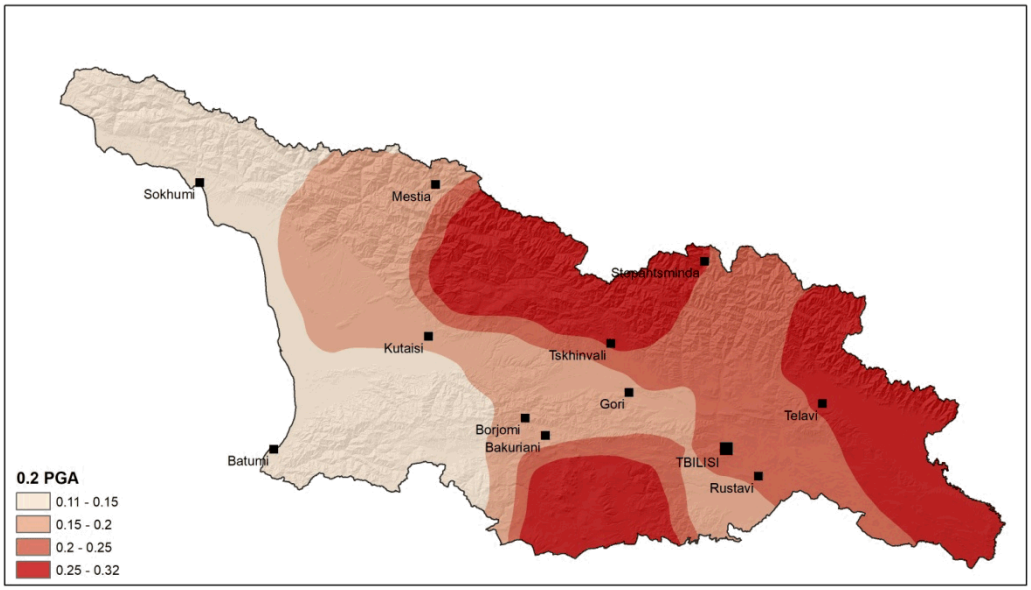


(a)

*Figure 17. Probabilistic seismic hazard in Georgia with a 20% chance of exceedance in 50 years in terms of (a) PGA*

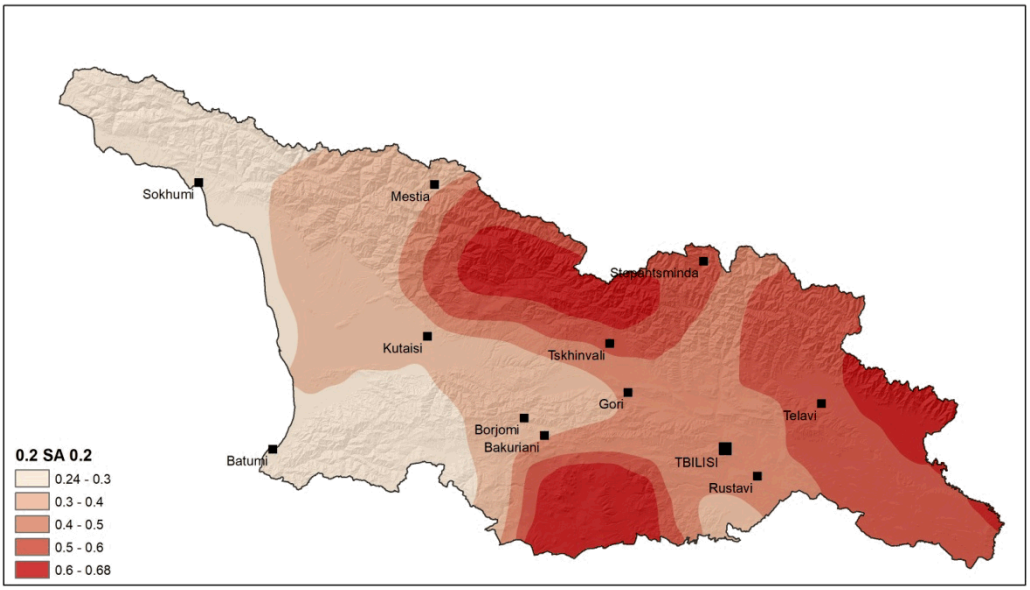


(b)

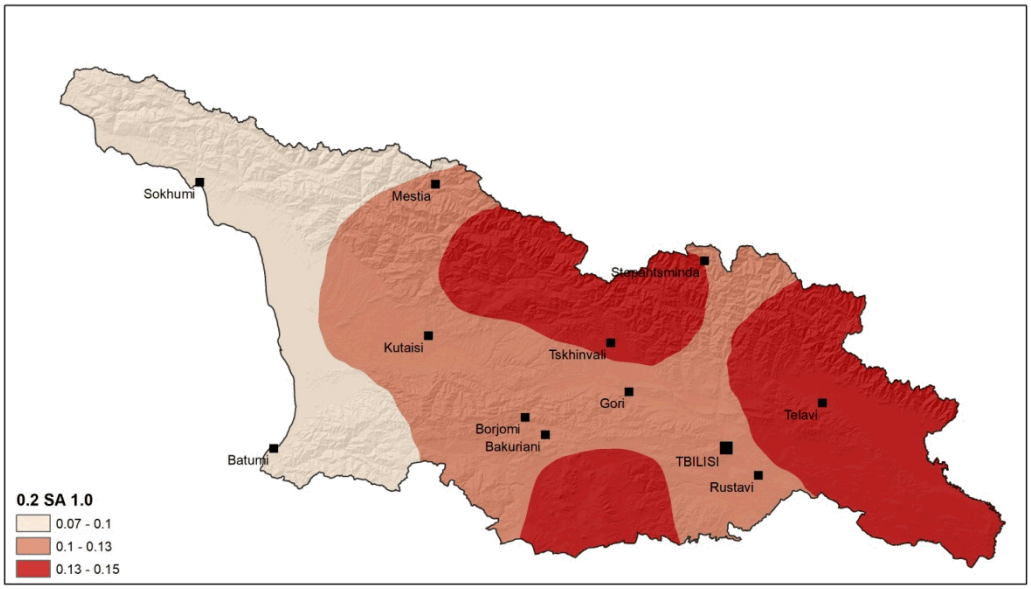


(c)

*Figure 17 (cont). Probabilistic seismic hazard in Georgia with a 20% chance of exceedance in 50 years in terms of (b) Spectral Acceleration at 0.2 sec, (c) Spectral Acceleration at 1.0 sec*

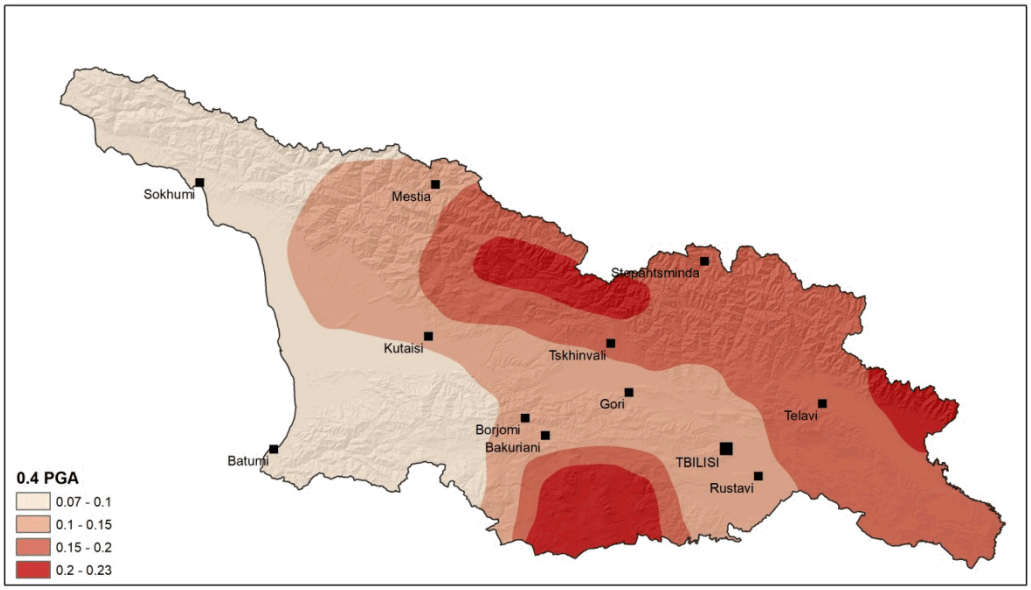


(a)

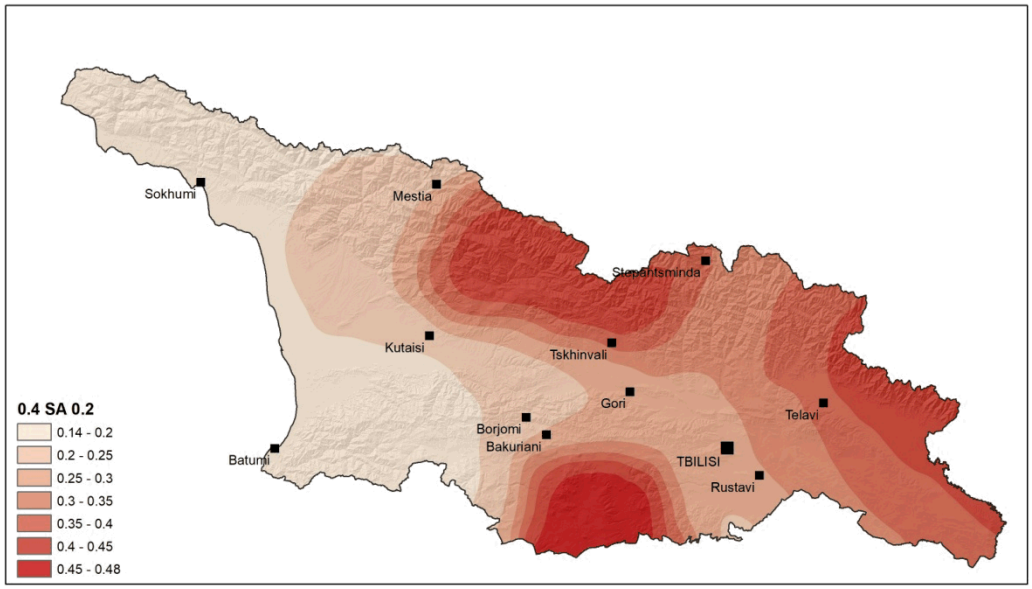


(b)

*Figure 18. Probabilistic seismic hazard in Georgia with a 40% chance of exceedance in 50 years in terms of (a) PGA, (b) Spectral Acceleration at 0.2 sec*

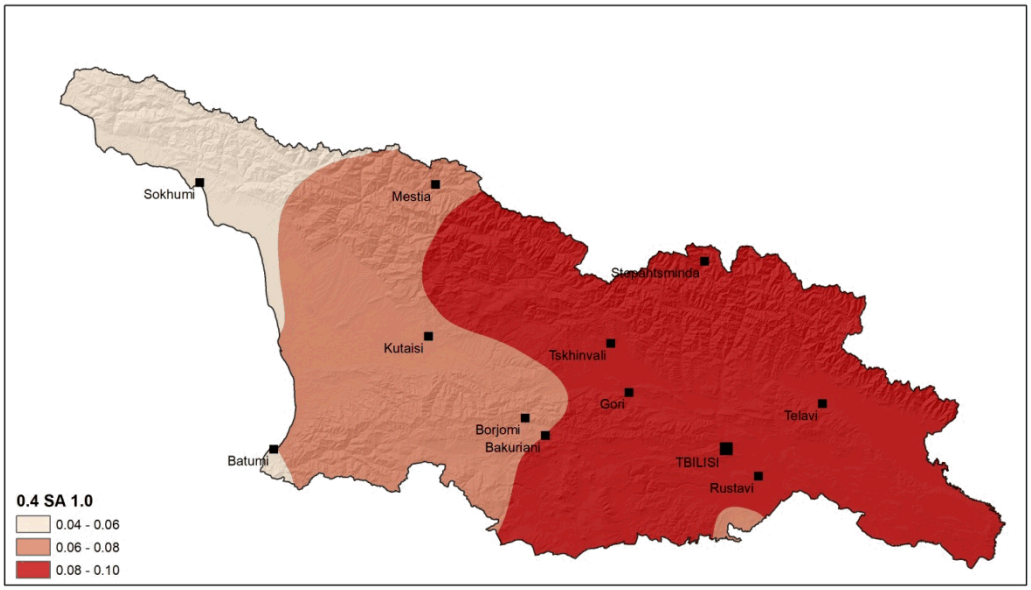


(c)

*Figure 18 (cont). Probabilistic seismic hazard in Georgia with a 40% chance of exceedance in 50 years in terms of (c) Spectral Acceleration at 1.0 sec*

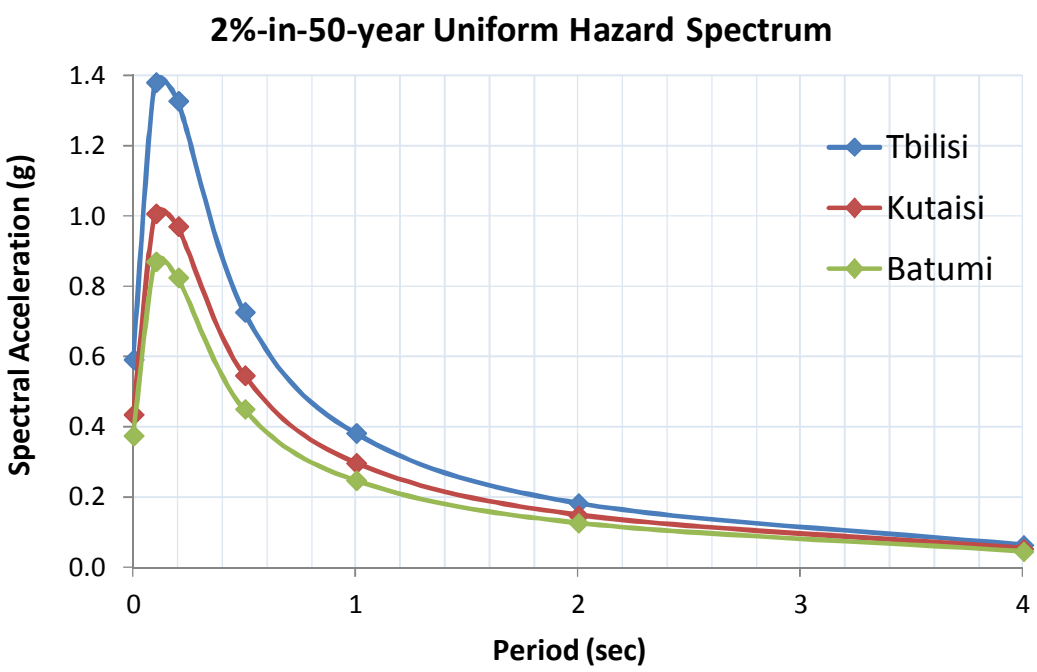


(a)

*Figure 19. Uniform hazard spectra for selected cities with a probability of exceedance of (a) 2% in 50 years*

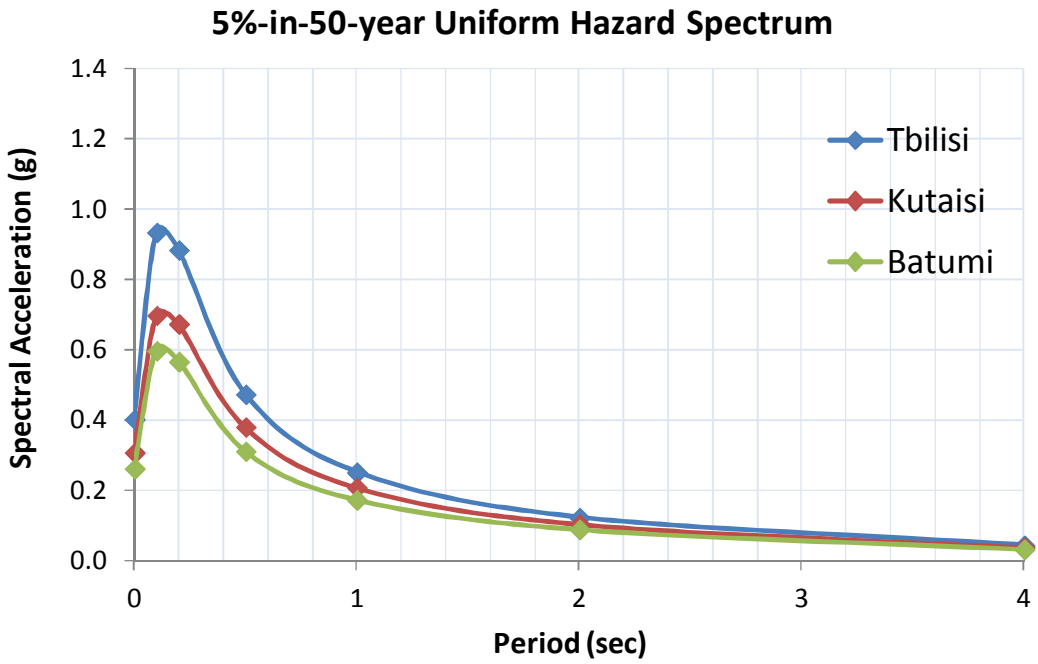


(b)

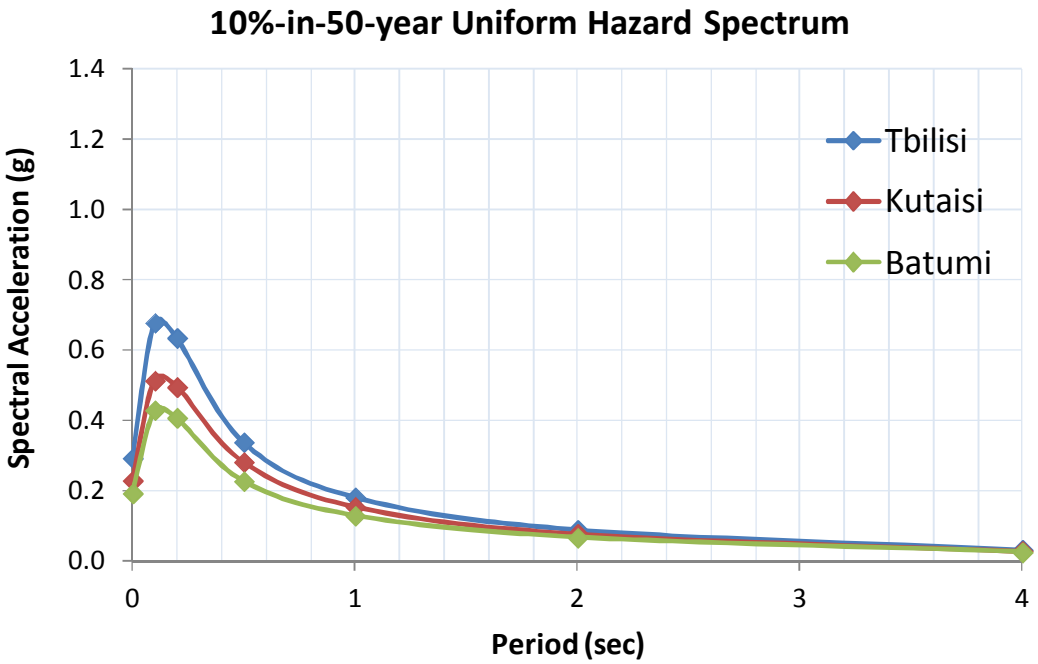


(c)

*Figure 19 (cont). Uniform hazard spectra for selected cities with a probability of exceedance of (b) 5% in 50 years, (c) 10% in 50 years*

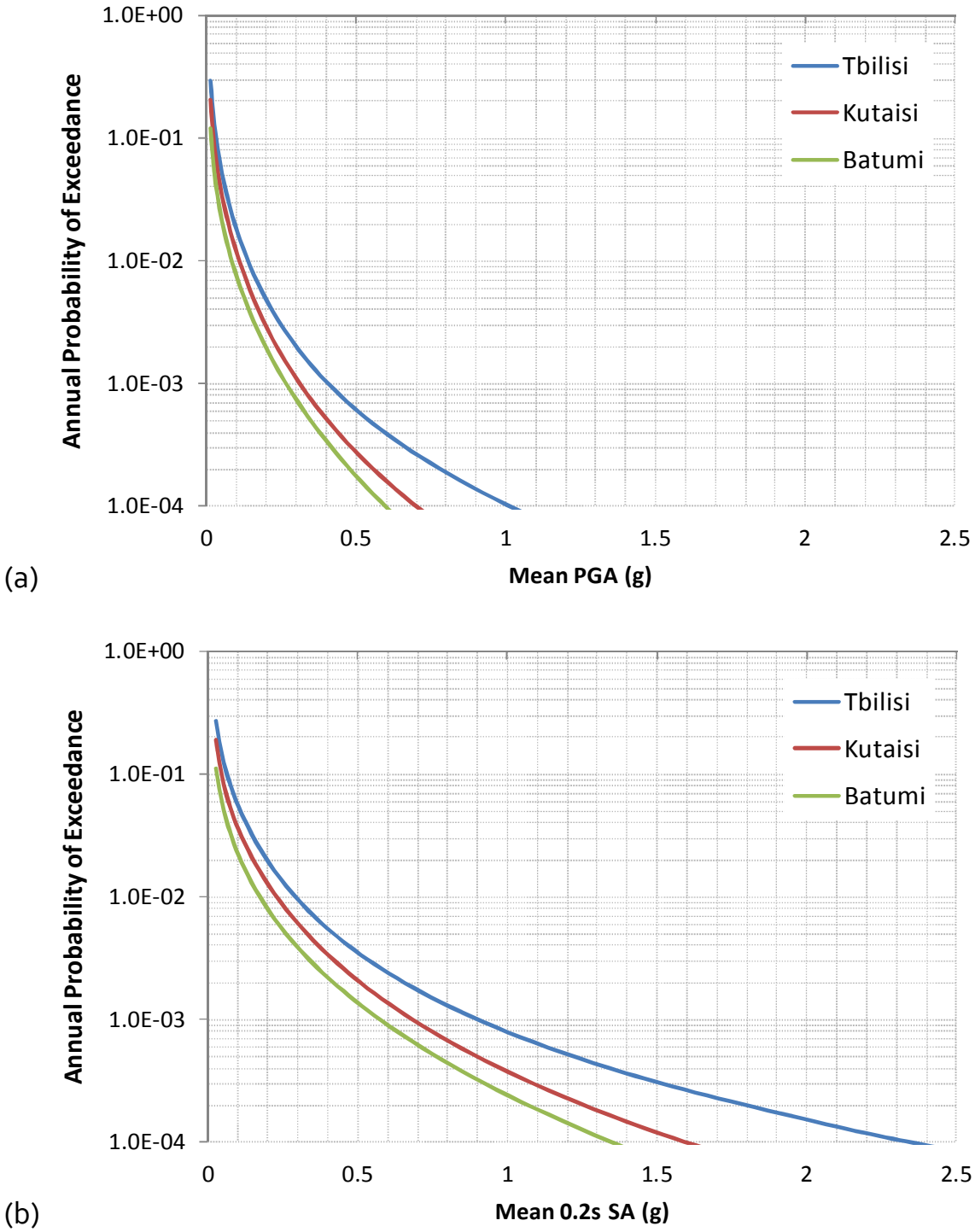


*Figure 20. Hazard curves for selected cities. (a) PGA, (b) Spectral Acceleration at 0.2 sec*

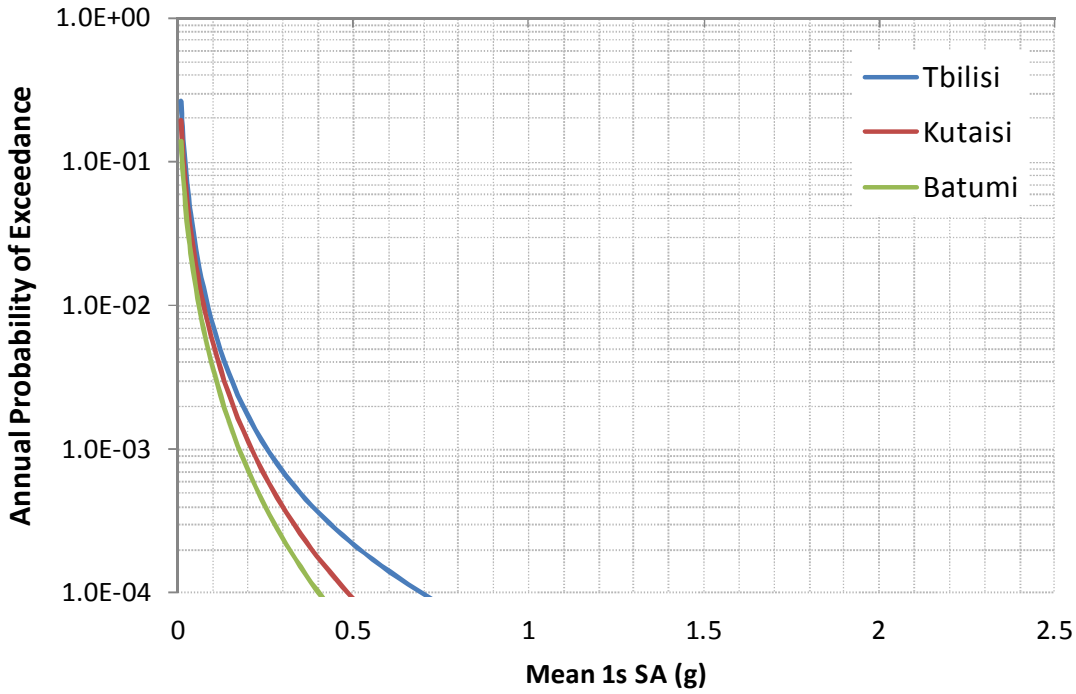


(c)

*Figure 20 (cont). Hazard curves for selected cities. (c) Spectral Acceleration at 1.0 sec*

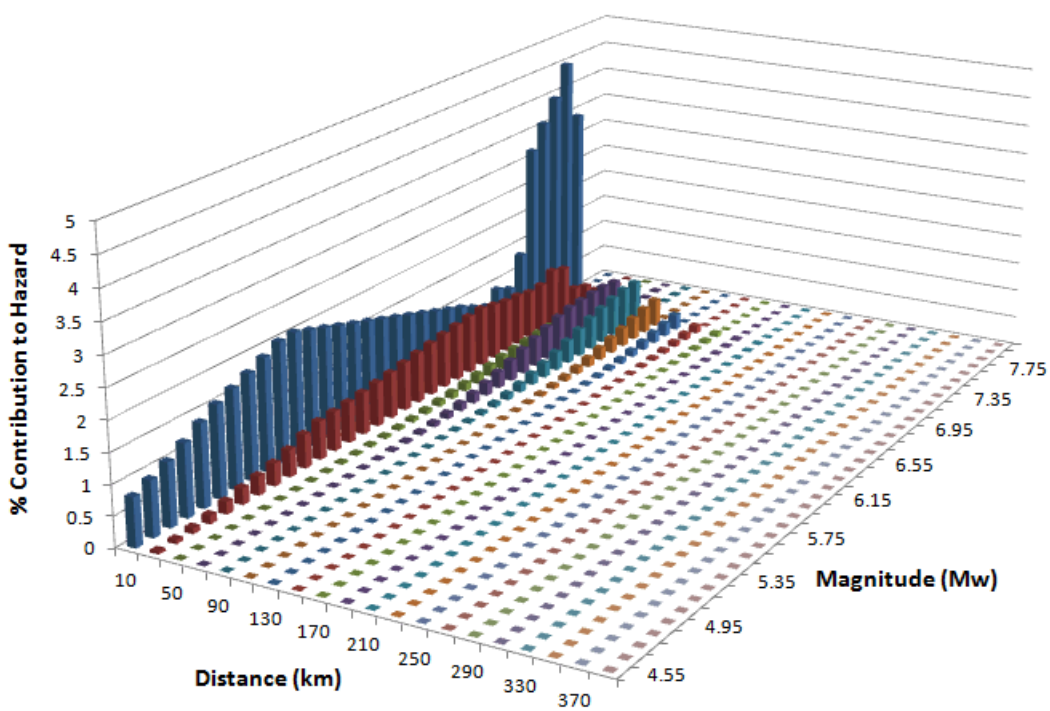


(a)

*Figure 21. Hazard deaggregations for 10%-in-50-year PGA for selected cities. (a) Tbilisi (mean magnitude: 6.55, mean distance: 30km, mode magnitude: 7.65, mode distance: 10km)*

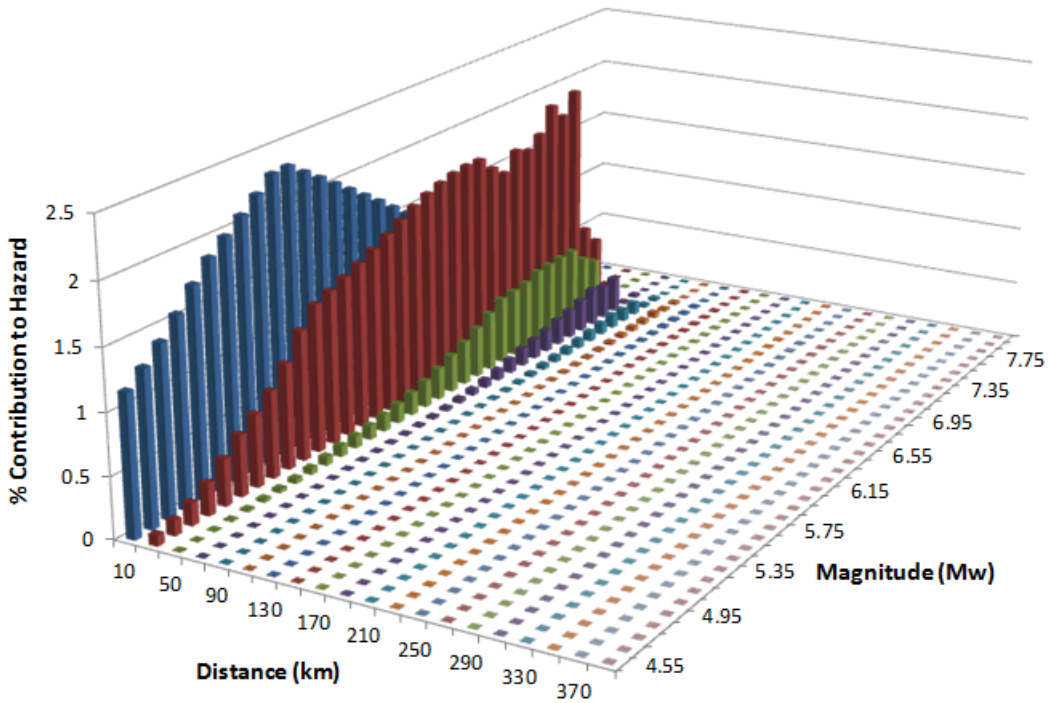


(b)

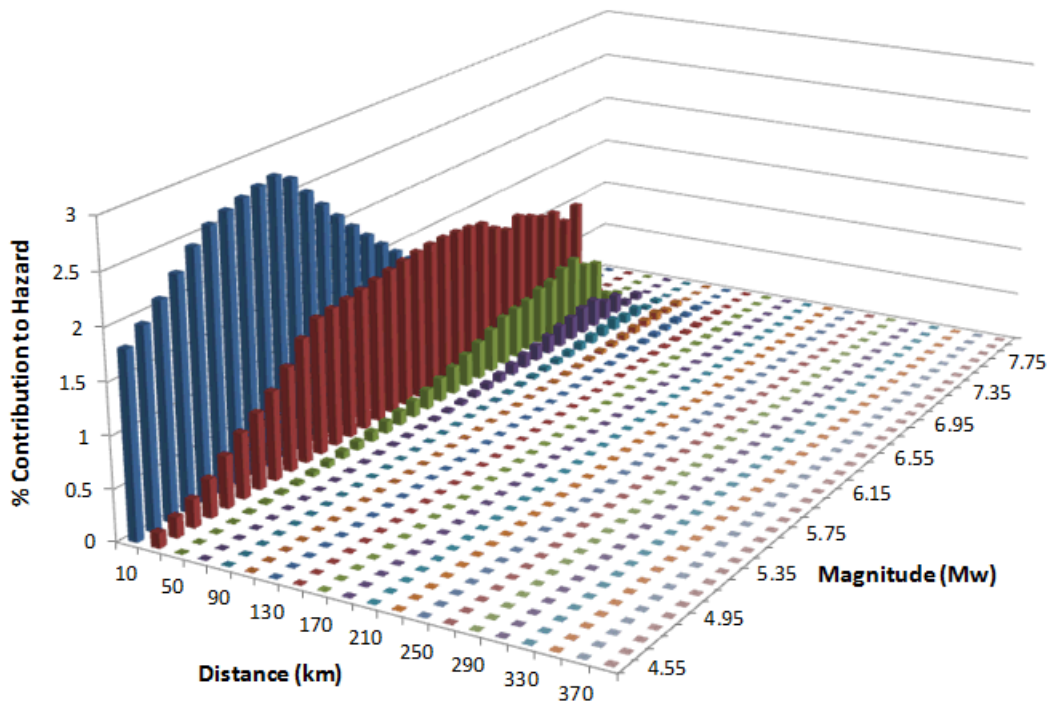


(c)

*Figure 21 (cont). Hazard deaggregations for 10%-in-50-year PGA for selected cities. (b) Kutaisi (mean magnitude: 6.24, mean distance: 25km, mode magnitude: 5.55, mode distance: 10km), (c) Batumi (mean magnitude: 6.07, mean distance: 24km, mode magnitude: 5.45; mode distance: 10km)*

## CONCLUSIONS

Hazard results generally reflect the change in rate of seismic activity in the Greater Caucasus from west to east, and Javakheti region's high levels of seismic activity is apparent in the hazard to the south. In the three major cities, Tbilisi, Kutaisi, and Batumi, the largest contribution to hazard is from moderate earthquakes (Mw6.0 to Mw6.5) nearby (within 30km). However in Tbilisi, larger magnitude earthquakes (Mw > 7.0) also contribute to hazard, particularly for longer period ground motions and at lower probabilities of exceedance.

National hazard maps for two neighbouring countries were updated recently, Turkey (AFAD, 2018) and Armenia (unpublished), both of which use 10% chance of exceedance in 50 years for seismic design. The hazard map for Georgia at this probability level generally compares well with the hazard map for Turkey at the border regions to the southwest, and is somewhat higher than the hazard map for Armenia in the south.

Reflecting recent scientific advances in characterization of seismic sources and ground motions, and using up-to-date engineering parameters and hazard analysis concepts, this study represents a significant improvement over Georgia's existing national hazard maps. It also provides the seismic hazard information in a format that is compatible with the requirements of the new building code of Georgia. It is important to note that more information is becoming available, pertinent to the understanding of seismic hazard, as more studies are being conducted in the region. Therefore, it is imperative for these hazard models to be updated regularly.

## ACKNOWLEDGEMENTS

We would like to thank the Ministry of Education and Ministry of Economy and Urban Development of Georgia for their support and interest in this project. We would also like to thank all regional participants whose experience and knowledge we greatly benefited from, including Prof. Dr. Ali Kocyigit, Assoc. Prof. Dr. Zeynep Gulerce, Dr. Hektor Babayan, Dr. Murat Nurlu, and Dr. Dogan Kalafat. The Georgian Building Code Committee very closely observed the development of this project by participating in and organizing numerous meetings and discussions during our visits to Georgia. We would like to particularly thank Mr. Irakli Urushadze and Mr. David Gigineishvili for their valuable input. We are grateful to Dr. Andrea Chiang for running the hazard analyses on high performance computing at the LLNL; and to Mr. Carlos Herrera for assisting with Figure 3.

## DISCLAIMER

This is a project report and the application of the results is the responsibility of the reader. All information and data provided as part of this report (presented in any form, including any attachments to this report or other email communications) are the authors' best estimates on a subject that is susceptible to large uncertainties and varying interpretations. In no event shall the authors of this report be liable to any party for direct, indirect, special, incidental, or consequential damages, including injuries, loss of life, loss of property or any form of financial loss, arising out of the use of the information and data described herein.

This work was performed under the auspices of the U.S. Department of Energy by Lawrence Livermore National Laboratory under Contract DE-AC52-07NA27344. This is LLN-TR-XXXX.

## REFERENCES

ABRAHAMSON, N. A., N. GREGOR, K. ADDO (2016). BC Hydro ground motion prediction equations for subduction earthquakes, *Earthquake Spectra*, Vol. 32(1): 23-44.

ABRAHAMSON, N. A., W. J. SILVA, R. KAMAI (2014). Summary of the ASK14 ground motion relation for active crustal regions, *Earthquake Spectra*, 30: 1025–1055.

ADAMIA, S. H., G. GUJABIDZE (2004). Geological Map of Georgia, 1: 500,000 Scale.

ADAMIA, S., G. ZAKARIADZE, T. CHKHOTUA, A. CHABUKIANI, N. SADRADZE, N. TSERETELI, A. GVENTSADZE (2011). Geology of the Caucasus: A Review. *Turk. J. Earth Sci.*, 20: 489–544.

AFAD (2018). Earthquake hazard map of Turkey. Department of Earthquake Directorate, Disaster and Emergency Management Authority, Republic of Turkey.

AKKAR, S. M. A. SANDIKKAYA, J. J. BOMMER (2014) Empirical ground-motion models for point- and extended-source crustal earthquake scenarios in Europe and the Middle East, *Bulletin of Earthquake Engineering*, 12(1): 359–387.

ALANIA, V. M., A. O. CHABUKIANI, R. L. CHAGELISHVILI, O. V. ENUKIDZE, K. O. GOGRICHIANI, A. N. RAZMADZE, N. S. TSERETELI (2017). Growth structures, piggy-back basins and growth strata of the Georgian part of the Kura foreland fold–thrust belt: implications for Late Alpine kinematic evolution, *Geological Society, London, Special Publications*, 428(1), 171.

ASSATOURIANS, K., G. M. ATKINSON (2013). EqHaz: An open-source probabilistic seismic-hazard code based on the Monte Carlo simulation approach. *Seismological Research Letters*, 84(3): 516-524.

ATKINSON, G. M., D. BOORE (2003). Empirical ground-motion relations for subduction-zone earthquakes and their application to Cascadia and other regions. *Bulletin of the Seismological Society of America*, 93(4): 1703-1929.

BALASSANIAN, S. Y., A. H. MARTIROSYAN, S. N. NAZARETIAN, A. R. ARAKELIAN, A. S. AVANESSIAN, V. A. IGUMNOV, E. RUTTENER (1998). Seismic Hazard Assessment in Armenia. *Natural Hazards*, 18: 227-236.

BANKS, C., A. ROBINSON, M. WILLIAMS (1997). Structure and regional tectonics of the Achara-Trialeti fold belt and the adjacent Rioni and Kartli foreland basins, Republic of Georgia. In: **Regional and Petroleum Geology of the Black Sea and Surrounding Region** (A. G. Robinson, Editor). American Association of Petroleum Geologists Memoir 68, 331-336.

BONDÁR, I., D. STORCHAK (2011). Improved location procedures at the International Seismological Centre, *Geophysical Journal International*, 186: 1220-1244.

BONDÁR, I., P. MÓNUS, C. S. CZANIK, M. KISZELY, Z. GRÁCZER, Z. WÉBER, AND THE ALPARRAY WORKING GROUP (2018). Relocation of Seismicity in the Pannonian Basin Using a Global 3D Velocity Model, *Seismological Research Letters*, 89: 2284-2293, doi:10.1785/0220180143.

BOORE, D. M., J. P. STEWART, E. SEYHAN, G. A. ATKINSON (2014). NGA-West2 equations for predicting PGA, PGV,and 5% damped PSA for shallow crustal earthquakes, *Earthquake Spectra*, 30: 1057–1085.

CAMPBELL, K. W., Y. BOZORGNIA (2014). NGA-West2 ground motion model for the average horizontal components of PGA, PGV, and 5% damped linear acceleration response spectra, *Earthquake Spectra*, 30: 1087–1115.

CAPUTO, M., I. GAMKRELIDZE, V. MALVEZZI, V. SGRIGNA, G. SHENGELIA, D. ZILPIMIANI, D. (2000) Geostructural basis and geophysical investigations for the seismic hazard assessment and prediction in the Caucasus, *Il Nuovo Cimento*, 23 C (2): 191-215.

CHIOU, B. S.-J., R. R. YOUNGS (2014). Update of the Chiou and Youngs NGA model for the average horizontal component of peak ground motion and response spectra, *Earthquake Spectra*, 30: 1117–1153.

COWGILL, E., A. M. FORTE, N. NIEMI, B. AVDEEV, A. TYE, C. TREXLER, Z. JAVAKHISHVILI, M. ELASHVILI, T. GODOLADZE (2016). Relict basin closure and crustal shortening budgets during continental collision: an example from Caucasus sediment provenance. *Tectonics*, 35 (12): 2918–2947.

DOTDUYEV, S.I. (1986). Nappe structure of the Greater Caucasus range, *Geotectonics*, 20: 420–430.

ENGDAHL, E. R., A. VILLASEÑOR (2002). Chapter 41, Global Seismicity: 1900–1999, In **International Handbook of Earthquake Engineering and Seismology, Part A** (W. H. K. Lee, H. Kanamori, P. C. Jennings, and C. Kisslinger, Editors), Academic Press, London, England, 665–690.

FIELD, E. H., T. H. JORDAN, C. A. CORNELL (2003), OpenSHA: A developing community-modeling environment for seismic hazard analysis, *Seismological Research Letters*, 74(4): 406-419.

FORTE, A. M., E. COWGILL, T. BERNARDIN, O. KREYLOS, B. HAMANN (2010), Late Cenozoic deformation of the Kura fold-thrust belt, southern Greater Caucasus, *Geological Society of America Bulletin*, 122(3/4): 465-486.

FORTE, A. M., E. COWGILL, K. X. WHIPPLE (2014). Transition from a singly vergent to doubly vergent wedge in a young orogen: The Greater Caucasus, *Tectonics*, 33(11): 2077-2101.

GAMKRELIDZE P. D. (1957). The main features of the tectonic structure of Georgia // Tr. GIN Ser. Geol. T. X (XY). Tbilisi: Metsniereba. 100 p.

GAMKRELIDZE, I.P. (1986). Geodynamic evolution of the Caucasus and adjacent areas in Alpine time, Tectonophysics, 127(3-4): 261-277.

GAMKRELIDZE, I., M. PRUIDZE, M. GAMKRELIDZE, M. LOLADZE (2013). Tectonic Map of Georgia 1:500 000.

GARCIA, D., S. K. SINGH, M. HARRAIZ, M. ORDAZ, J. F. PACHECO (2005). Inslab earthquakes of Central Mexico: Peak ground-motion parameters and response spectra. *Bulletin of the Seismological Society of America*, 95(6): 2272-2282.

GARDNER, J.K, L. KNOPOFF (1974). Is the sequence of earthquakes in Southern California, with aftershocks removed, Poissonian? *Bulletin of the Seismological Society of America*, 64: 1363–1367

GIARDINI, D., G. GRÜNTHAL, K. M. SHEDLOCK, P. ZHANG (1999). The GSHAP global seismic hazard map, *Annali di Geofisica*, 42(6): 1225-1230.

GODOLADZE, T., E. SANDVOL, I. BONDAR, R. GOK (in preparation). Improved seismic catalog in the Caucasus.

GÖK, R., A. KAVIANI, E. M. MATZEL, M. E. PASAYANOS, K. MAYEDA, G. YETIRMISHLI, I. EL-HUSSAIN, A. AL-AMRI, F. AL-JERI,T. GODOLADZE (2016). Moment magnitude of local/regional events from 1D coda calibrations in the broader Middle East region, *Bull. Seismol. Soc. Am.* 106(5): 1926 – 1938, doi:10.1785/0120160045.

HAFKENSCHEID, E., M. J. R. WORTEL, W. SPAKMAN (2006). Subduction history of the Tethyan region derived from seismic tomography and tectonic reconstructions. *Journal of Geophysical Research B, Solid Earth and Planets*, 111(B08401), doi: 10.1029/ 2005JB003791.

JACKSON, J. (1992). Partitioning of strike-slip and convergent motion between Eurasia and Arabia in eastern Turkey and the Caucasus, *Journal of Geophysical Research*, 97: 12,471-12,479.

KARAKHANYAN, A.S., V. G. TRIFONOV, H. PHILIP, A. AVAGYAN, K. HESSAMI, F. JAMALI, M. S. BAYRAKTUTAN, H. BAGDASSARIAN, S. ARAKELIAN, V. DAVTIAN, A. ADILKHANYAN (2004). Active faulting and natural hazards in Armenia, eastern Turkey and northwestern Iran. *Tectonophysics*, 380: 189–219.

KADIROV, F., M. FLOYD, A. ALIZADEH, I. GULIEV, R. REILINGER, S. KULELI, R. KING, M. N. TOKSOZ (2012). Kinematics of the eastern Caucasus near Baku, Azerbaijan, *Natural Hazards*, 63: 997–1006, doi:10.1007/s11069-012-0199-0.

KADIROV, F. A., M. FLOYD, R. REILINGER, A. A. ALIZADEH, I.S. GULIYEV, S. G. MAMMADOV, R. T. SAFAROV (2015). Active geodynamics of the Caucasus region: Implications for earthquake hazards in Azerbaijan, *Proceedings of Azerbaijan National Academy of Sciences, the Sciences of Earth*, No.3.

KAZMIN, V. G., N. F. TIKHONOVA (2006). Late Cretaceous-Eocene Marginal Seas in the Black-Sea-Caspian Region: Paleotectonic reconstructions. *Geotectonics*, 40: 162–182.

KOÇYIGIT, A., A. YILMAZ, S. ADAMIA, S. KULOSHVILI (2001). Neotectonics of east Anatolia plateau (Turkey) and Lesser Caucasus: implication for transition from thrusting to strike-slip faulting. *Geodin. Acta* 14: 177-195.

KONDORSKAYA, N. V., N. V. SHEBALIN (1977). New Catalog of Large Earthquakes in the USSR Area. Nauka, Publishing House, Moscow. pp. 536 (in Russian).

MARTIN, R. J. III (2007). Caucasus Seismic Information Network: Data and Analysis, Final Report. Submitted by New England Research, Inc. (Principal Investigator: R. J. Martin III). Submitted to Department of Energy. Contract No. DE-AC52-03NA99600.

MAYEDA, K., W. R. WALTER (1996). Moment, energy, stress drop, and source spectra of western United States earthquakes from regional coda envelopes, *J. Geophys. Res.*, 101: 11,195–11,208.

MAYEDA, K., A. HOFSTETTER, J. L. O'BOYLE, W. R. WALTER (2003). Stable and transportable regional magnitudes based on coda-derived moment rate spectra, *Bull. Seismol. Soc. Am.*, 93: 224–239.

MELLORS, R., J. JACKSON, S. MYERS, R. GOK, K. PRIESTLEY, G. YETIRMISHLI, N. TURKELLI, T. GODOLADZE (2012). Deep earthquakes beneath the Northern Caucasus: Evidence of active or recent subduction in Western Asia, *Bulletin of the Seismological Society of America*, 102(2): 862-866.

MOSAR, J., T. KANGARLI, M. BOCHUD, U. A. GLASMACHER, A. RAST, M. BRUNET, M. SOSSON (2010). Cenozoic-recent tectonics and uplift in the greater Caucasus: a perspective from Azerbaijan. *Geological Society, London, Special Publications*, 340: 261-280. doi:10.1144/SP340.12.

NALIVKIN, D.V. (1973). Geology of the U.S.S.R. (N. Rast, Tran.), Edinburgh, Oliver & Boyd.

NALIVKIN, D. V. (1976). Geologic Map of the Caucasus, Ministry of Geology, USSR.

NEMČOK, M., B. GLONTI, A. YUKLER, B. MARTON (2013). Development history of the foreland plate trapped between two converging orogens; Kura Valley, Georgia, case study: *Geological Society, London, Special Publications*, v. 377, doi:10.1144/SP377.9.

NIKISHIN, A. M., P. A. ZIEGLER, D. I. PANOV, B. P. NAZAREVICH, M.-F. BRUNET, R. A. STEPHENSON, S. N. BOLOTOV, M. V. KOROTAEV, P. L. TIKHOMIROV (2001). Mesozoic and Cainozoic evolution of the Scythian Platform – Black Sea – Caucasus domain. In: Ziegler, P., Cavazza, W., Robertson, A. H. F. & Crasquin-Soleau, S. (Eds) **Peri-Tethys Memoir 6: Peri-Tethyan Rift/Wrench Basins and Passive Margins.** Mémoires du Muséum National d'Histoire Naturelle, Paris, 186: 295–346.

PAGANI, M., D. MONELLI, G. WEATHERILL, L. DANCIU, H. CROWLEY, V. SILVA, P. HENSHAW, L. BUTLER, M. NASTASI, L. PANZERI, M. SIMIONATO, D. VIGANO (2014). OpenQuake Engine: An open hazard (and risk) software for the Global Earthquake Model, *Seismological Research Letters*, 85(3): 692-702.

PASYANOS, M. E., E. M. MATZEL, W. R. WALTER, A. J. RODGERS (2009). Broad-band Lg attenuation modelling in the Middle East, *Geophysical Journal International*, 177(3): 1166-1176.

PHILIP, H., A. CISTERNAS, A. GVISKIANI, A. GORSHKOV (1989). The Caucasus: an actual example of the initial stages of continental collision. *Tectonophysics*, 161: 1–21.

PHILIP, H., A. AVAGYAN, A. KARAKHANIAN, J.-F. RITZ, S. REBAI (2001). Estimating slip rates and recurrence intervals for strong earthquakes along an intracontinental fault: example of the Pambak–Sevan–Sunik fault (Armenia). *Tectonophysics*, 343: 205–232.

REASENBERG, P. (1985). Second-order moment of central California seismicity, 1969-82, *Journal of Geophysical Research*, 90: 5479-5495.

REILINGER, R., S. MCCLUSKY, P. VERNANT (2004). GPS constraints on continental deformation in the Eastern Mediterranean and Caucasus region, *Eos. Trans.* AGU, 85, Fall Meet. Suppl. Abstract G31D-04.

REILINGER, R.E., S.C. MCCLUSKY, P. VERNANT, S. LAWRENCE, S. ERGINTAV, R. CAKMAK, H. OZENER, F. KADIROV, I. GULIEV, R. STEPANIAN, M. NADARIYA, G. HAHUBIA, S. MAHMOUD, K. SAKR, A. ARRAJEHI, D. PARADISSIS, A. AL-AYDRUS, M. PRILEPIN, T. GUSEVA, E. EVREN, A. DMIROTSA, S.V. FILIKOV, F. GOMEZ, R. AL-GHAZZI, G. KARAM, (2006). GPS constraints on continental deformation in the Africa-Arabia-Eurasia continental collision zone and implications for the dynamics of plate interactions. *Journal of Geophysical Research*, Vol. 111, B05411, doi:10.1029/2005JB004051.

SESETYAN, K., L. DANCIU, M. B. DEMIRCIOGLU TUMSA, D. GIARDINI, M. ERDIK, S. AKKAR, L. GULEN, M. ZARE, S. ADAMIA, A. ANSARI, A. ARAKELYAN, A. ASKAN, M. AVANESYAN, H. BABAYAN, T. CHELIDZE, R. DURGARYAN, A. ELIAS, H. HAMZEHLOO, K. HESSAMI, D. KALAFAT, O. KALE, A. KARAKHANYAN, M. ASIF KHAN, T. MAMMADLI, M. AL-QARYOUTI, M. SAYAB, N. TSERETELI, M. UTKUCU, O. VARAZANASHVILI, M. WASEEM, H. YALCIN, M. T. YILMAZ (2018). The 2014 seismic hazard model of the Middle East: overview and results, *Bulletin of Earthquake Engineering*, https://doi.org/10.1007/s10518-018-0346-4.

SOKHADZE, G., M. FLOYD, T. GODOLADZE, R. KING, E. S. COWGILL, Z. JAVAKHISHVILI, G. HAHUBIA, R.REILINGER (2018). Active convergence between the Lesser and Greater Caucasus in Georgia: Constraints on the tectonic evolution of the Lesser–Greater Caucasus continental collision. *Earth and Planetary Science Letters*, Vol. 481, 154–161.

SOSSON, M. Y. ROLLAND, C. MULLER, T. DANELIAN, R. MELKONYAN, S. KEKELIA, S. ADAMIA, V. BABAZADEH, T. KANGARLI, A. AVAGYAN, G. GALOYAN, J. MOSAR (2010). Subductions, obduction and collision in the Lesser Caucasus (Armenia, Azerbaijan, Georgia), new insights: Geological Society, London, Special Publications, v. 340, p. 329–352, doi:10.1144/SP340.14.

STAMPFLI, G. M., G. BOREL, W. CAVAZZA, J. MOSAR, P. ZIEGLER (2001). Palaeotectonic and palaeogeographic evolution of the western Tethys and Peri-Tethyan domain. *Episodes*. 24: 222–228.

TIBALDI, A., V. ALANIA, F. L. BONALI, O. ENUKIDZE, N. TSERETELI, N. KVAVADZE, O. VARAZANASHVILI (2017). Active inversion tectonics, simple shear folding and back-thrusting at Rioni Basin, Georgia. *J. Struct. Geol.* 96: 35–53.

UHRHAMMER, R. (1986). Characteristics of Northern and Central California seismicity, *Earthquake Notes*, 57(1): 21.

WELLS, D. L., K. J. COPPERSMITH (1994). New empirical relationships among magnitude, rupture length, rupture width, rupture area, and surface displacement, *Bulletin of the Seismological Society of America*, 84: 974-1002.

ZARE, M., H. AMINI, P. YAZDI, K. SESETYAN, M. B. DEMIRCIOGLU, D. KALAFAT, M. ERDIK, D. GIARDINI, M. A. KHAN, N. TSERETELI (2014). Recent developments of the Middle East catalog, *Journal of Seismology*, 18: 749-772.

ZHAO, J. X., J. ZHANG, A. ASANO, Y. OHNO, T. OOUCHI, T. TAKAHASHI, H. OGAWA, K. IRIKURA, H. K. THIO, P. G. SOMERVILLE, Y. FUKUSHIMA, Y. FUKUSHIMA (2006). Attenuation relations of strong ground motion in Japan using site classification based on predominant period. *Bulletin of the Seismological Society of America*, 96(3): 898-913.

## APPENDIX A

The full set of hazard maps for five return periods and seven ground motion parameters are presented below.

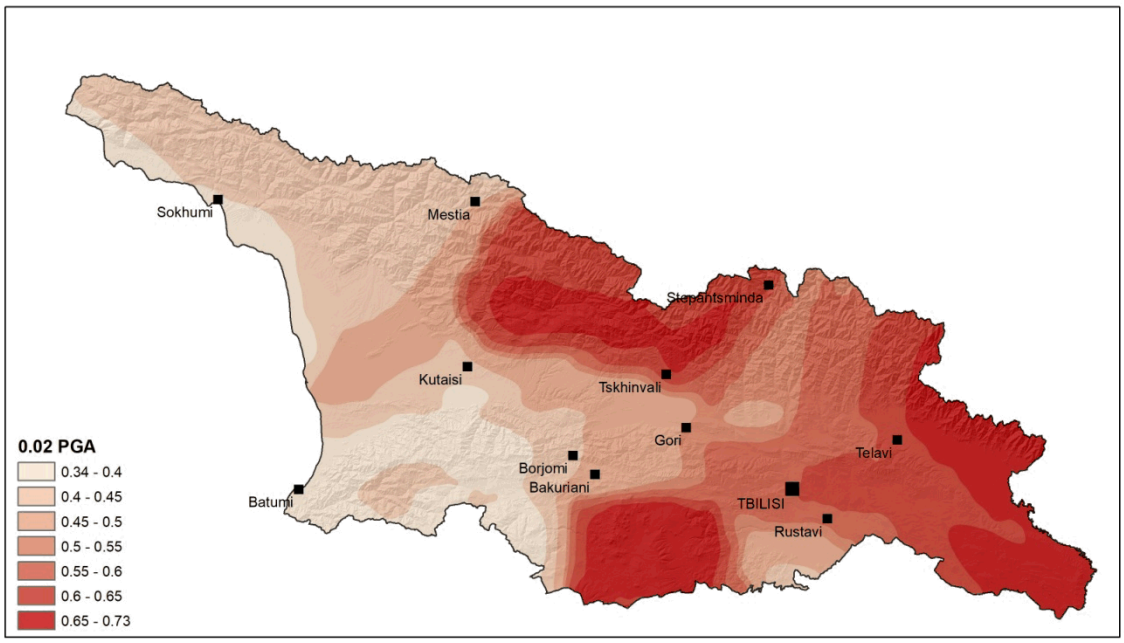


*Figure A1. Probabilistic seismic hazard with a 2% chance of exceedance in 50 years in terms of PGA*

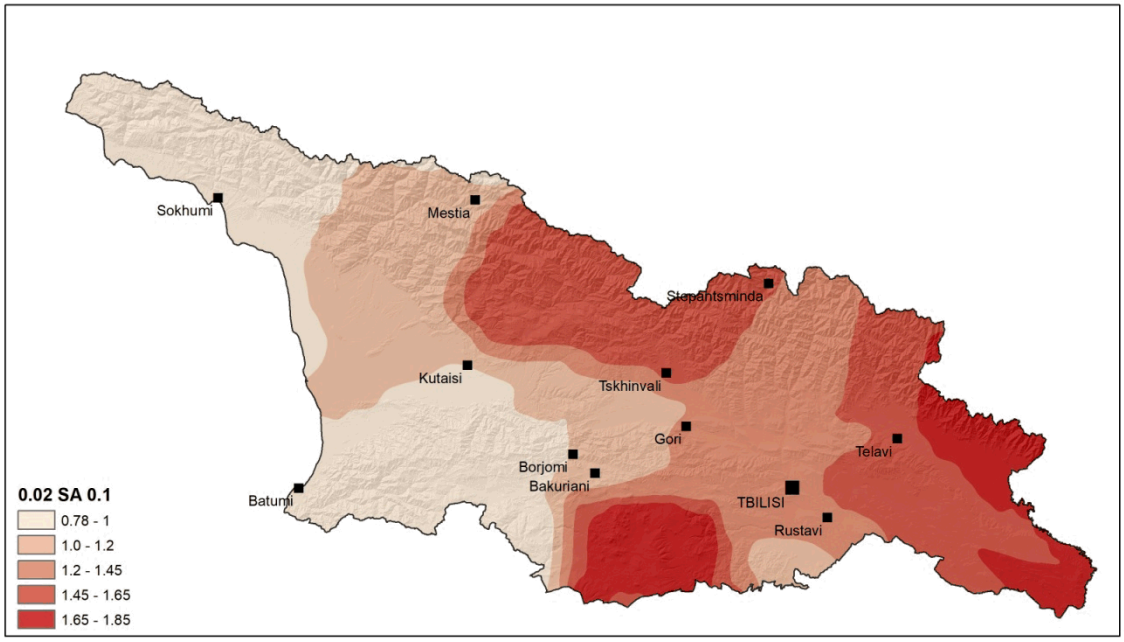


*Figure A2. Probabilistic seismic hazard with a 2% chance of exceedance in 50 years in terms of Spectral Acceleration at 0.1 sec*

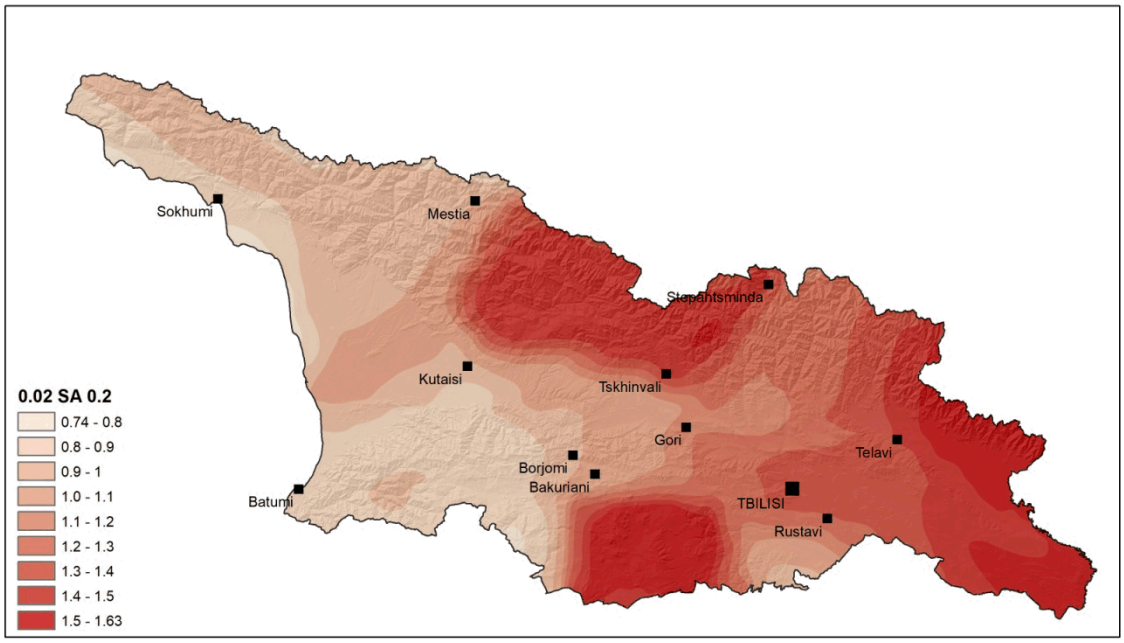


*Figure A3. Probabilistic seismic hazard in Georgia with a 2% chance of exceedance in 50 years in terms of Spectral Acceleration at 0.2 sec*

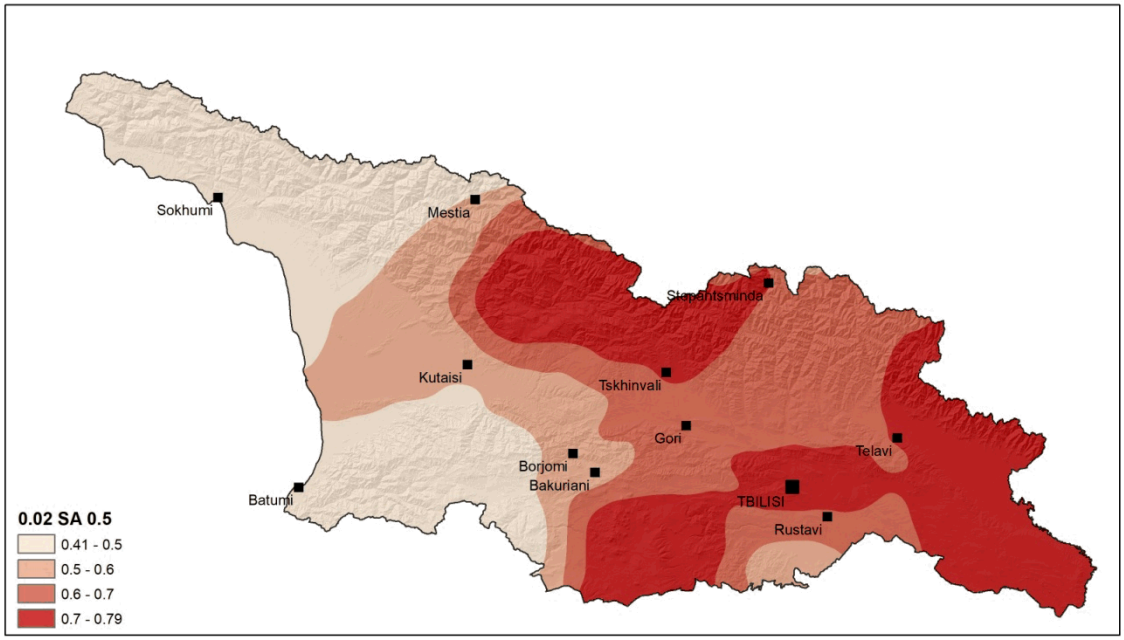


*Figure A4. Probabilistic seismic hazard in Georgia with a 2% chance of exceedance in 50 years in terms of Spectral Acceleration at 0.5 sec*

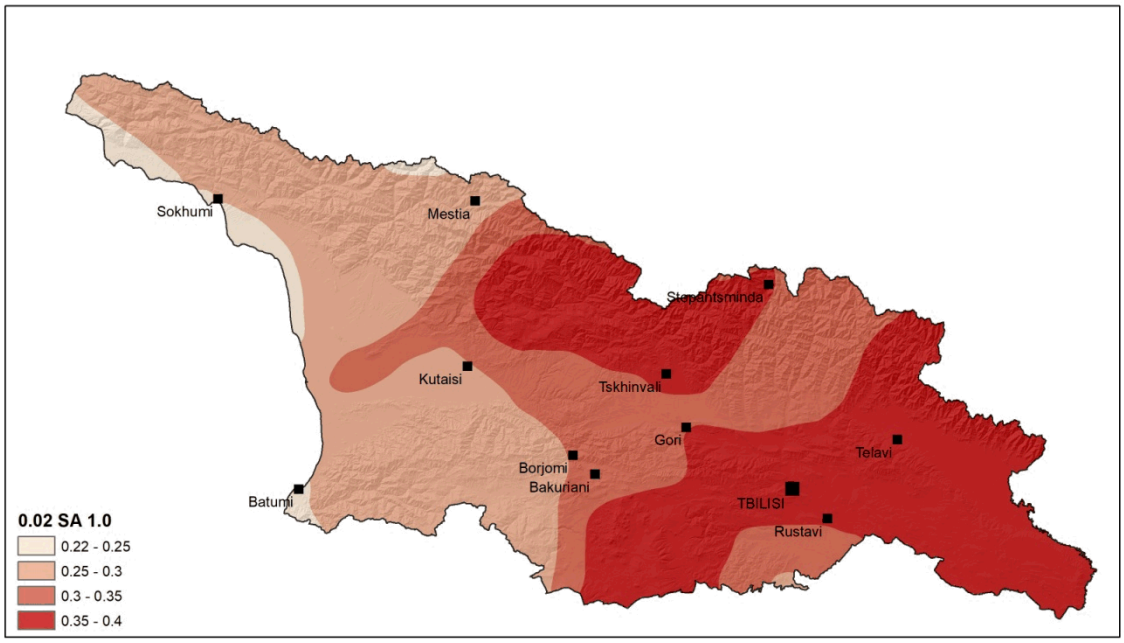


*Figure A5. Probabilistic seismic hazard in Georgia with a 2% chance of exceedance in 50 years in terms of Spectral Acceleration at 1.0 sec*

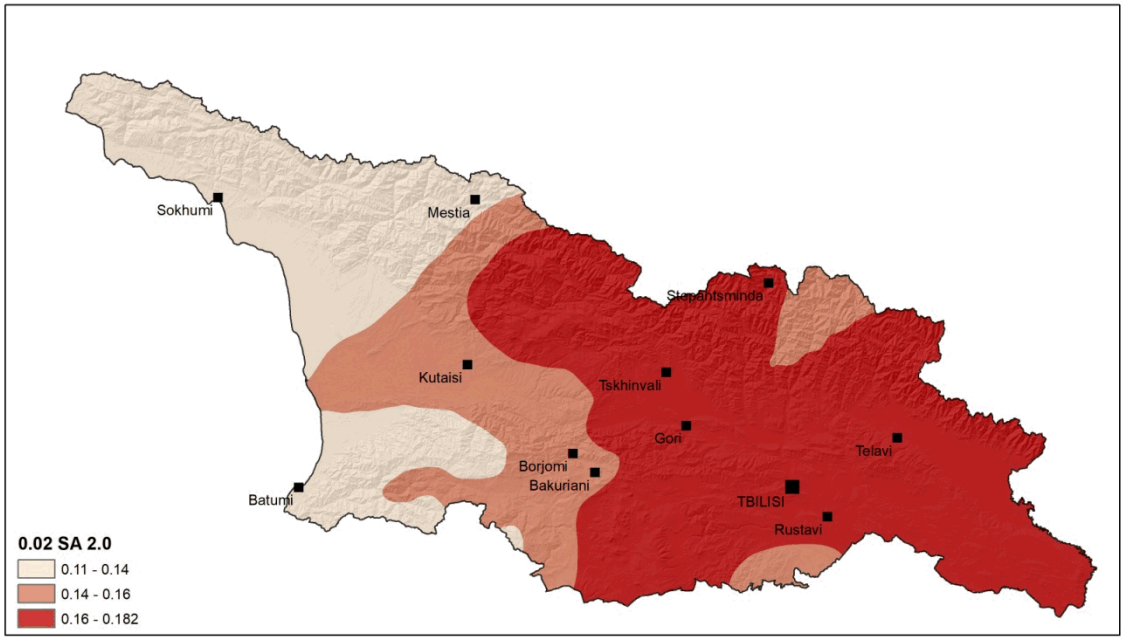


*Figure A6. Probabilistic seismic hazard in Georgia with a 2% chance of exceedance in 50 years in terms of Spectral Acceleration at 2.0 sec*

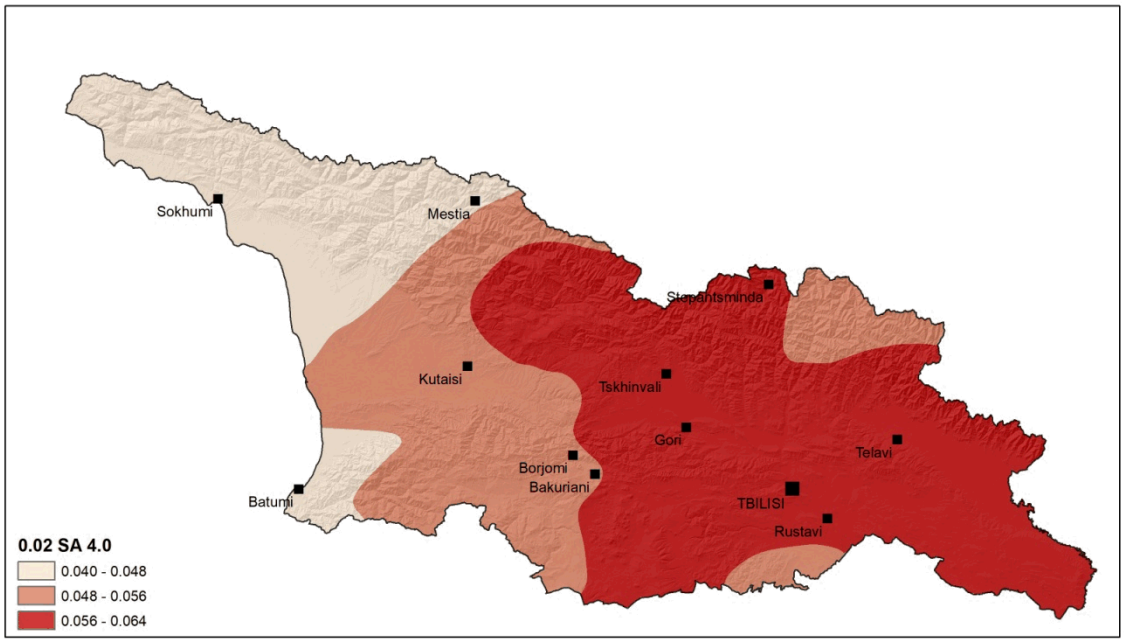


*Figure A7. Probabilistic seismic hazard in Georgia with a 2% chance of exceedance in 50 years in terms of Spectral Acceleration at 4.0 sec*

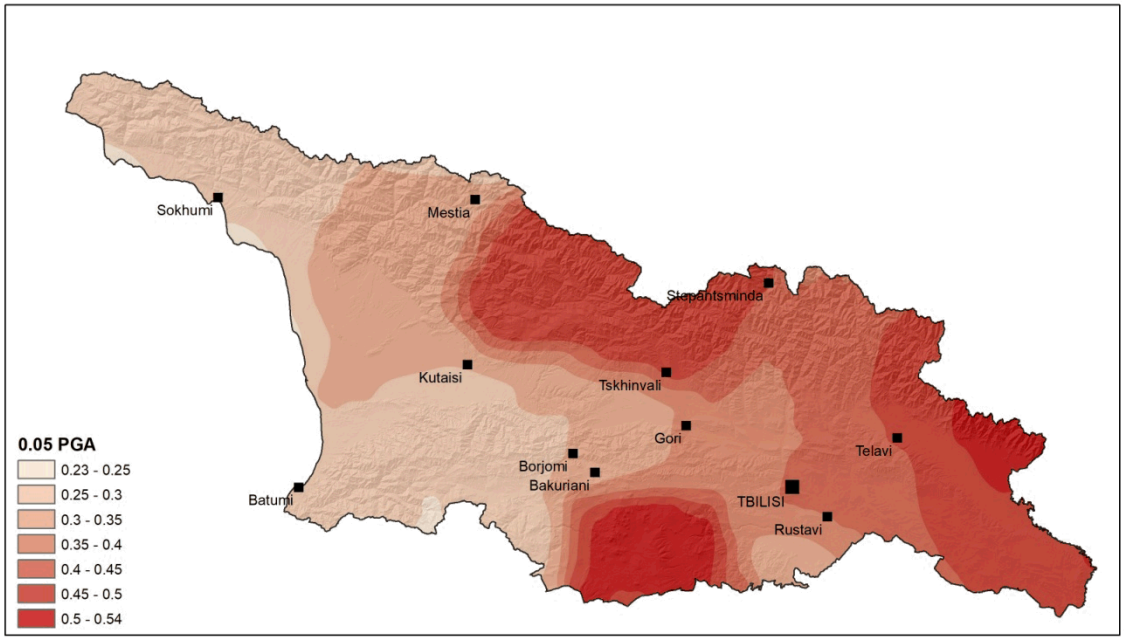


*Figure A8. Probabilistic seismic hazard in Georgia with a 5% chance of exceedance in 50 years in terms of PGA*

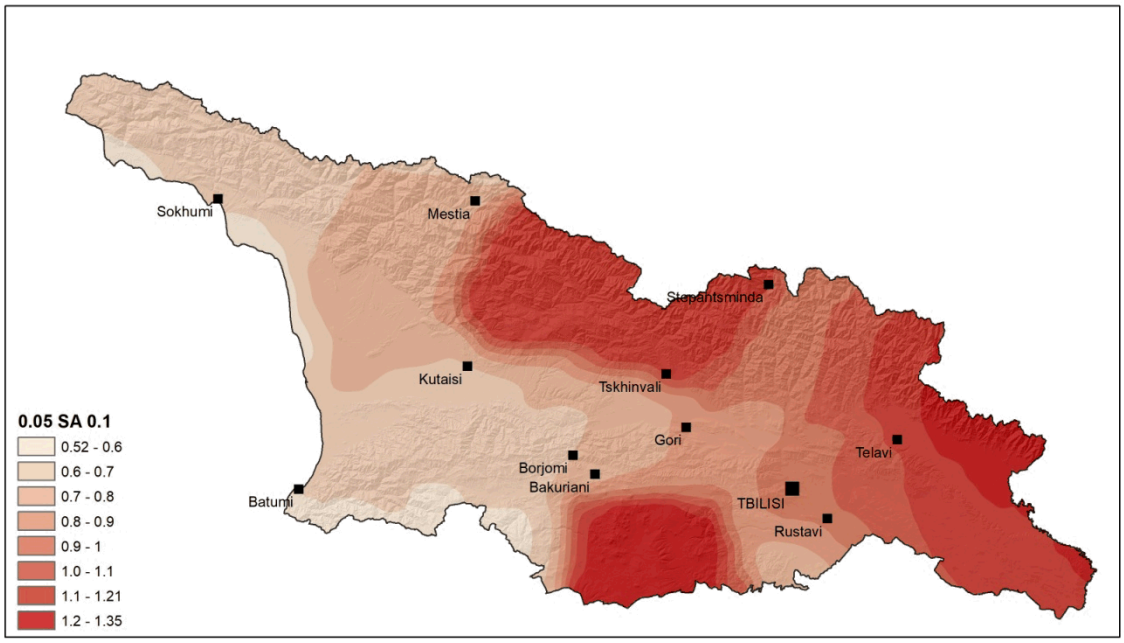


*Figure A9. Probabilistic seismic hazard in Georgia with a 5% chance of exceedance in 50 years in terms of Spectral Acceleration at 0.1 sec*

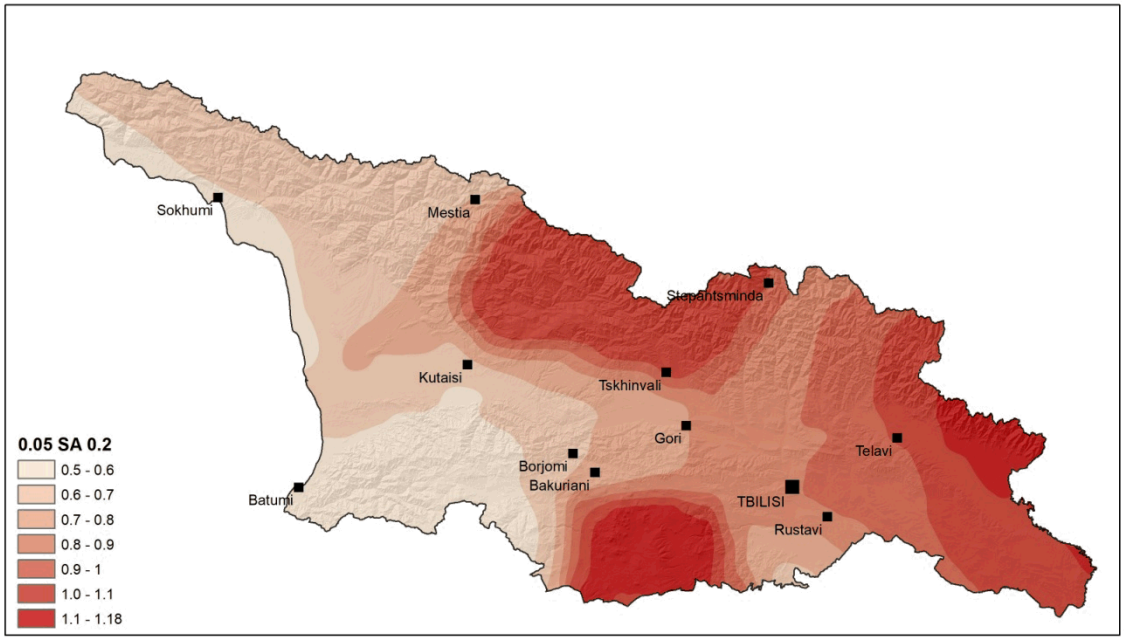


*Figure A10. Probabilistic seismic hazard in Georgia with a 5% chance of exceedance in 50 years in terms of Spectral Acceleration at 0.2 sec*

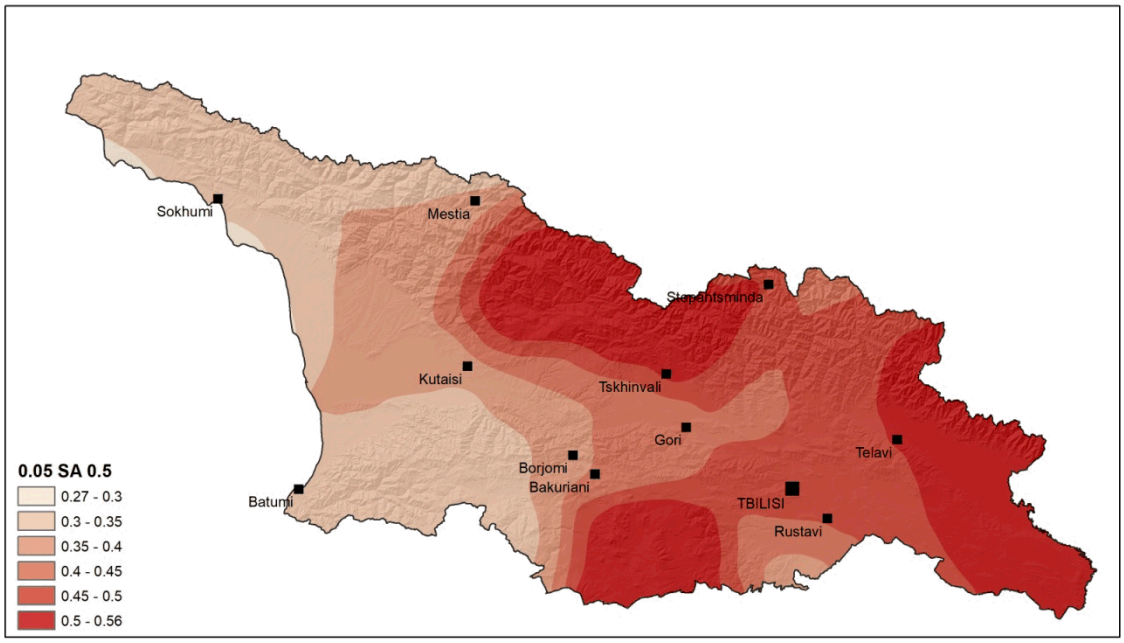


*Figure A11. Probabilistic seismic hazard in Georgia with a 5% chance of exceedance in 50 years in terms of Spectral Acceleration at 0.5 sec*

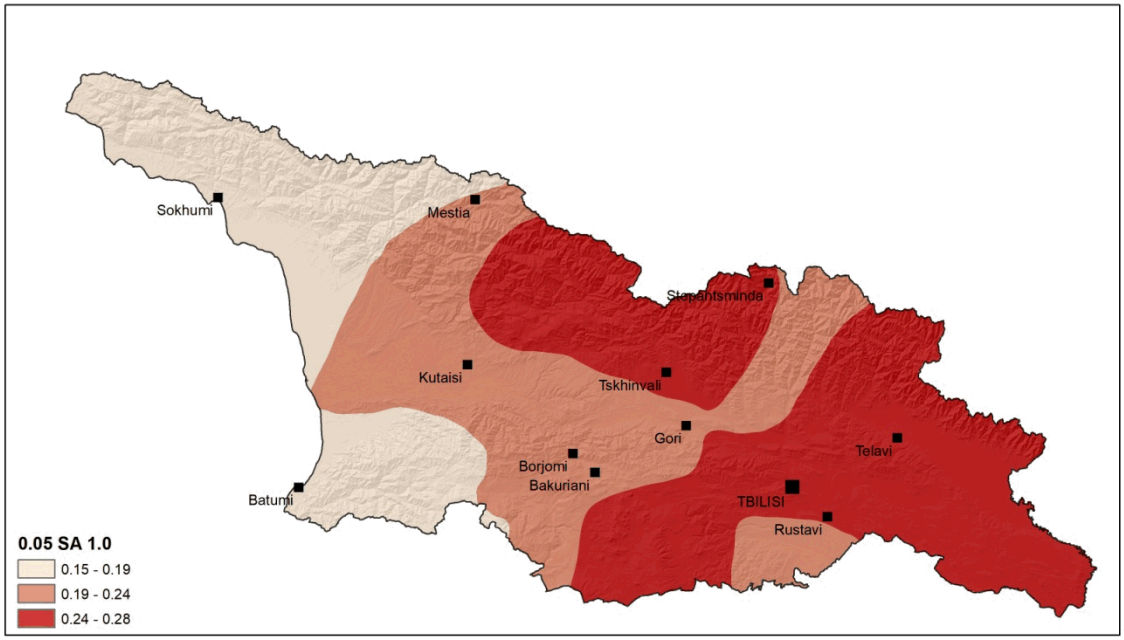


*Figure A12. Probabilistic seismic hazard in Georgia with a 5% chance of exceedance in 50 years in terms of Spectral Acceleration at 1.0 sec*

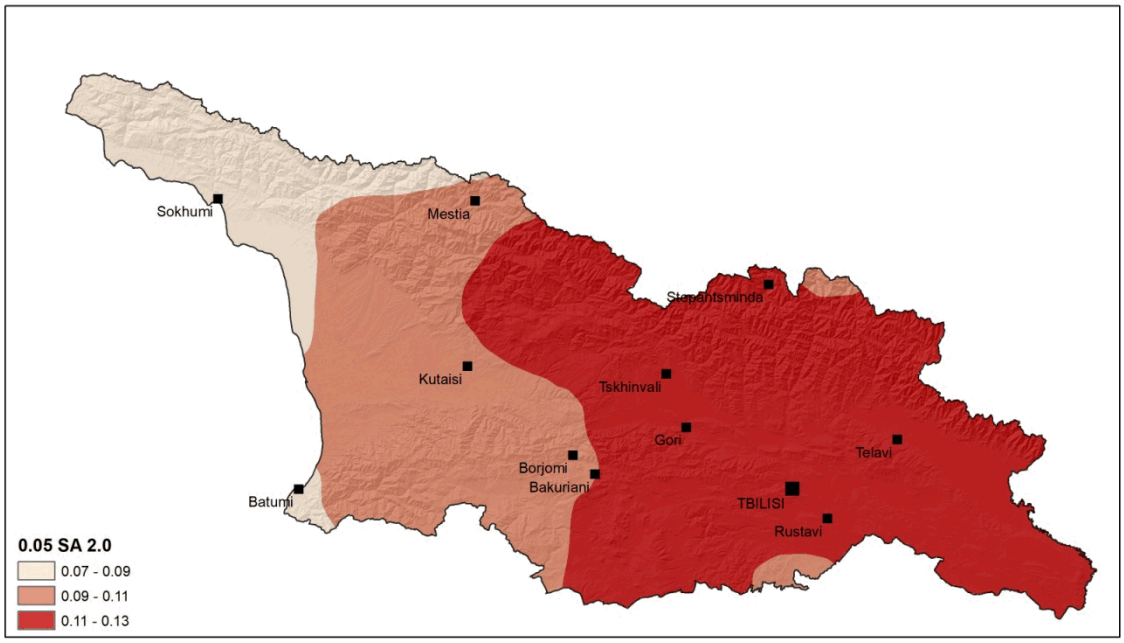


*Figure A13. Probabilistic seismic hazard in Georgia with a 5% chance of exceedance in 50 years in terms of Spectral Acceleration at 2.0 sec*

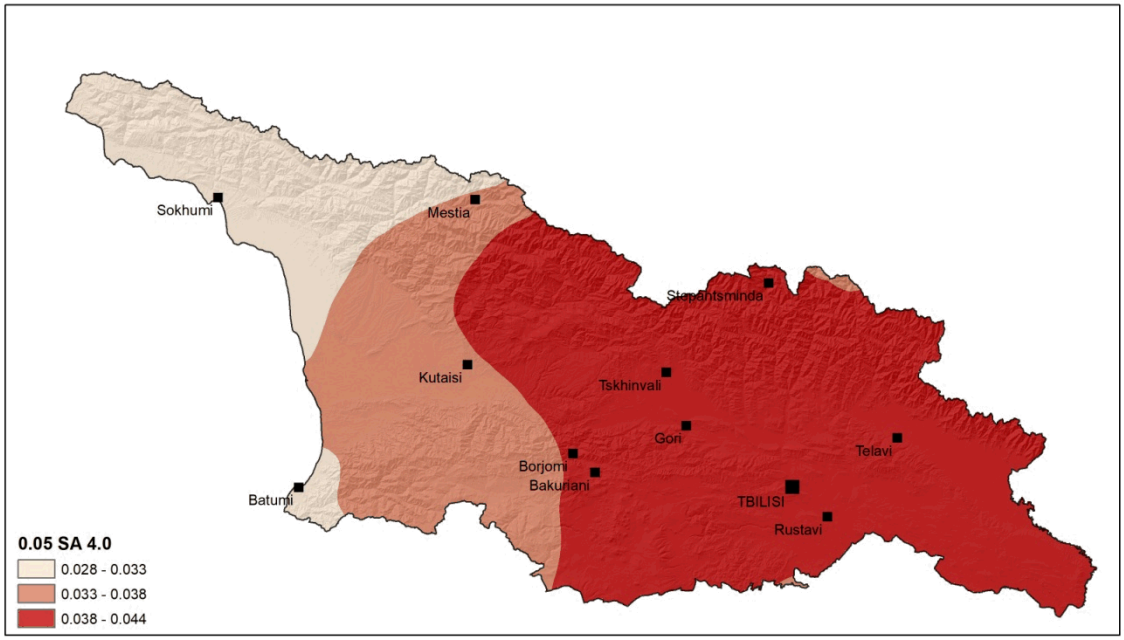


*Figure A14. Probabilistic seismic hazard in Georgia with a 5% chance of exceedance in 50 years in terms of Spectral Acceleration at 4.0 sec*

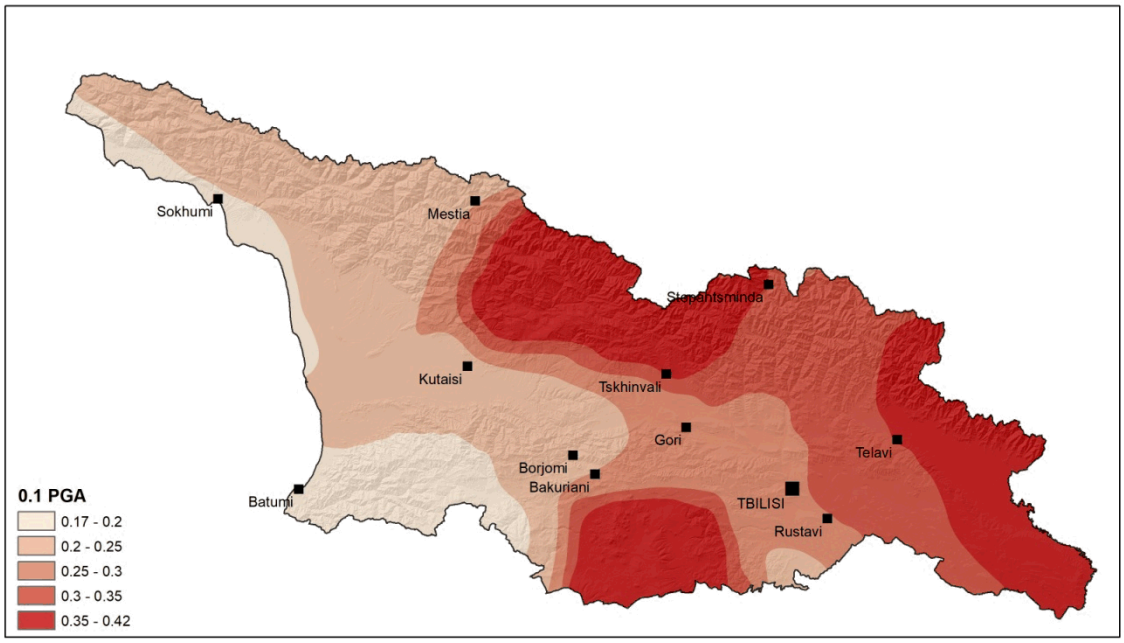


*Figure A15. Probabilistic seismic hazard in Georgia with a 10% chance of exceedance in 50 years in terms of PGA*

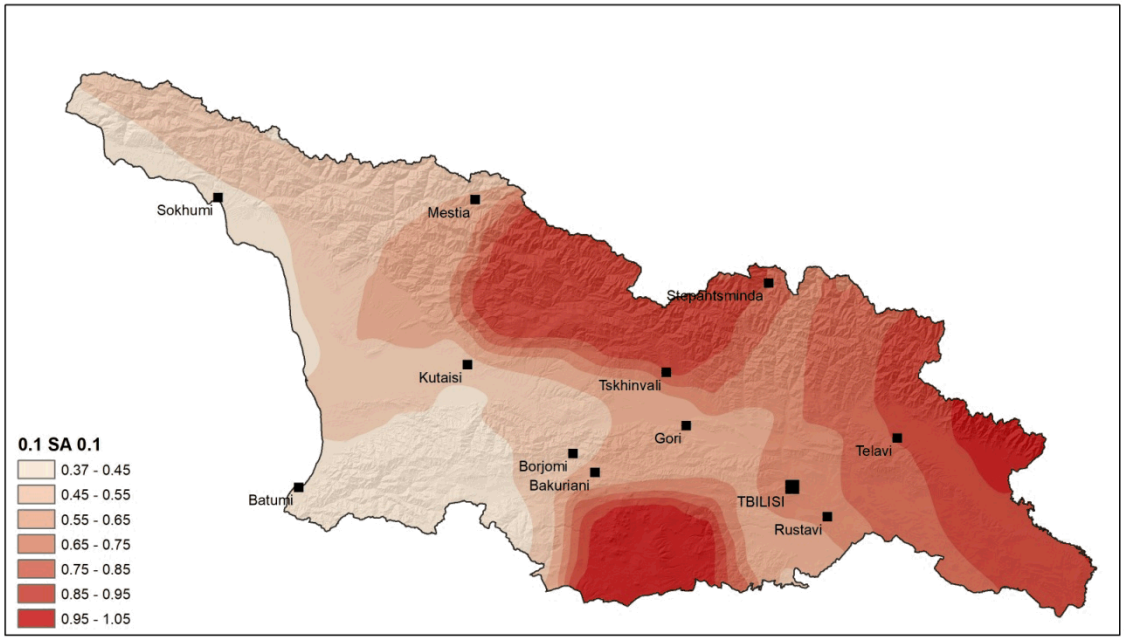


*Figure A16. Probabilistic seismic hazard in Georgia with a 10% chance of exceedance in 50 years in terms of Spectral Acceleration at 0.1 sec*

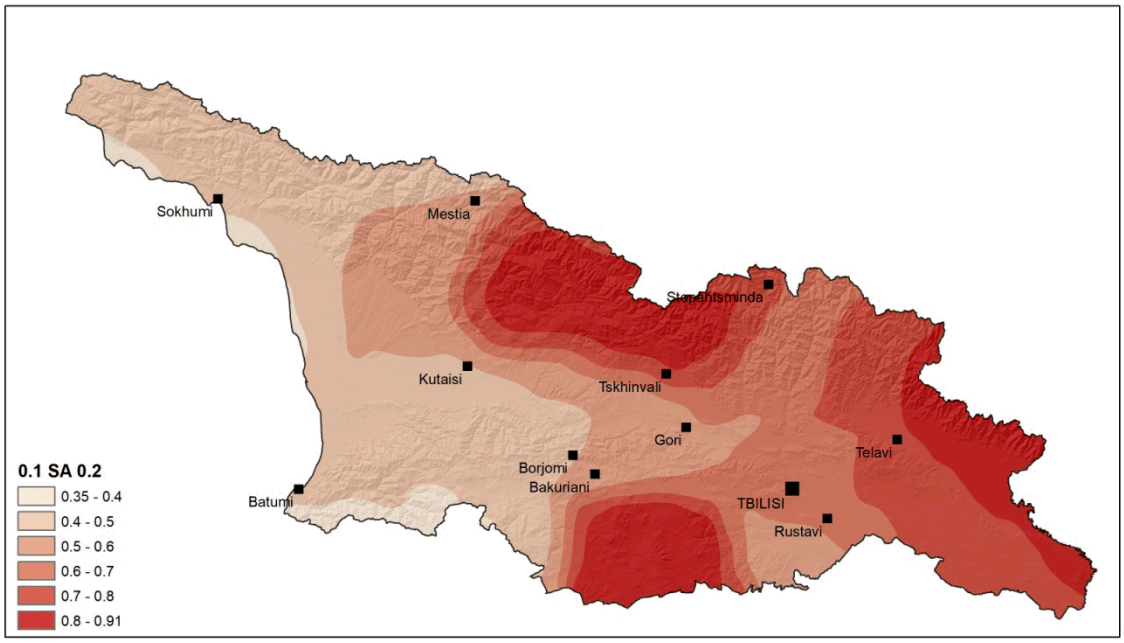


*Figure A17. Probabilistic seismic hazard in Georgia with a 10% chance of exceedance in 50 years in terms of Spectral Acceleration at 0.2 sec*

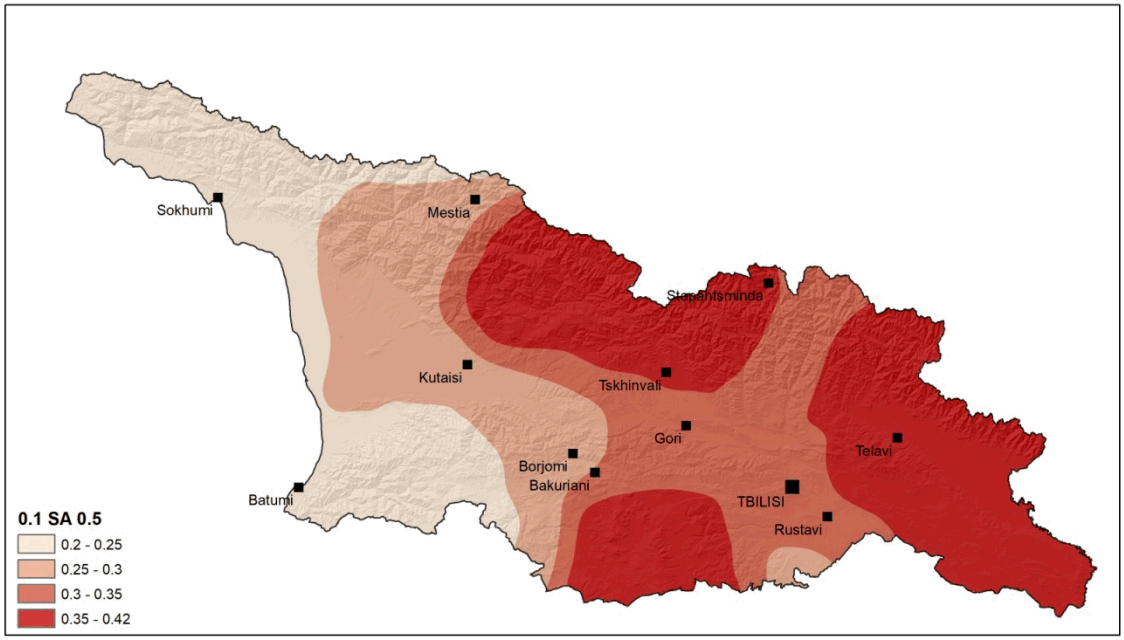


*Figure A18. Probabilistic seismic hazard in Georgia with a 10% chance of exceedance in 50 years in terms of Spectral Acceleration at 0.5 sec*

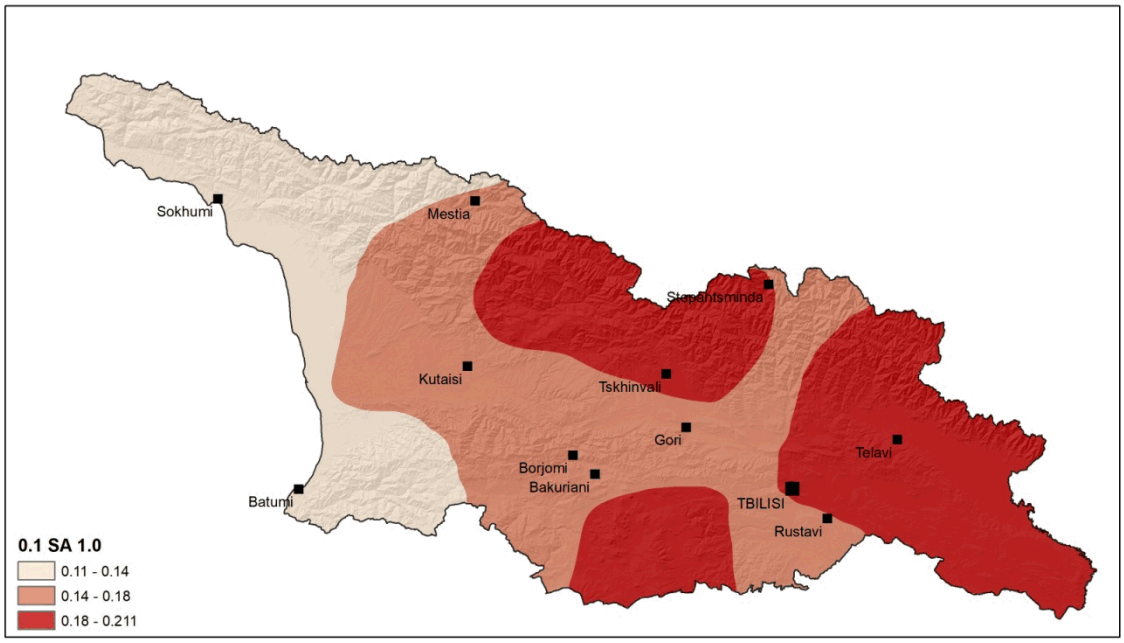


*Figure A19. Probabilistic seismic hazard in Georgia with a 10% chance of exceedance in 50 years in terms of Spectral Acceleration at 1.0 sec*

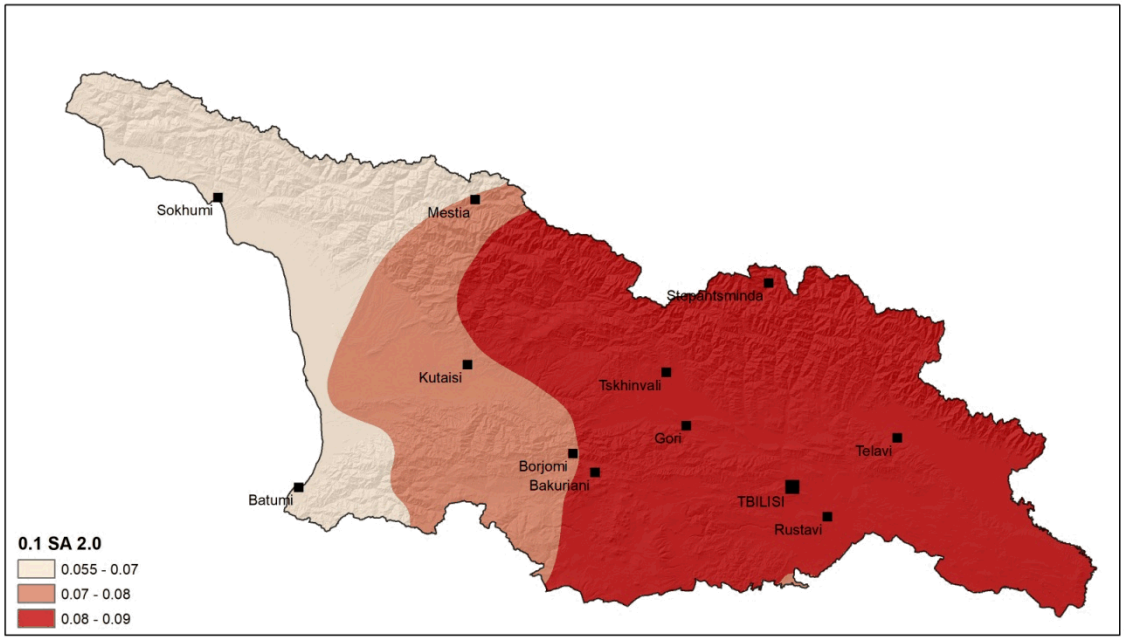


*Figure A20. Probabilistic seismic hazard in Georgia with a 10% chance of exceedance in 50 years in terms of Spectral Acceleration at 2.0 sec*

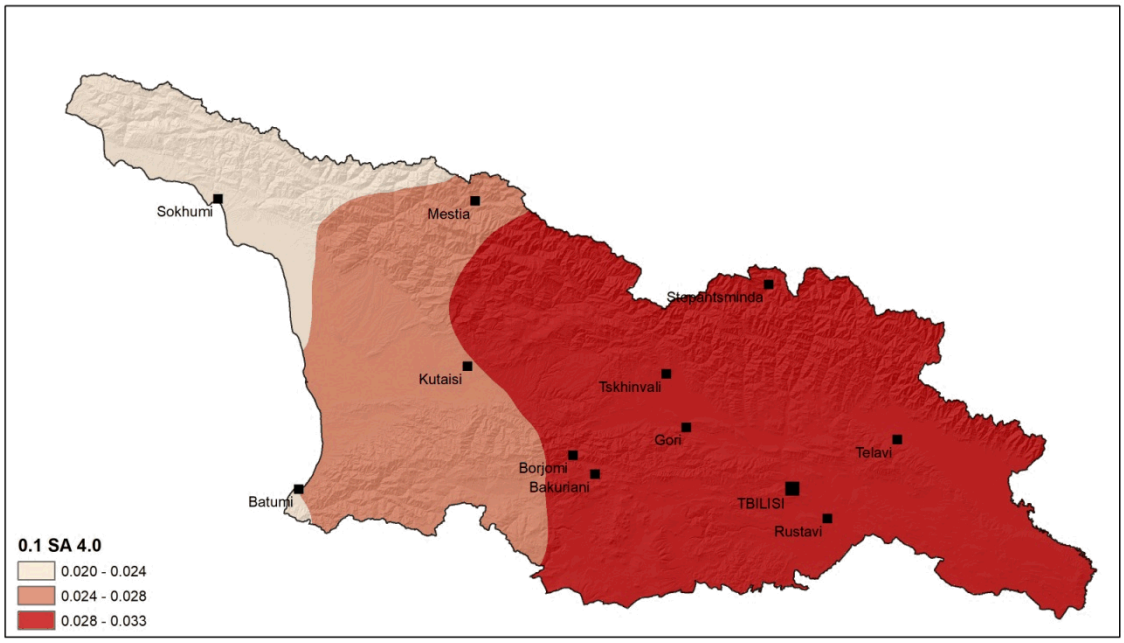


*Figure A21. Probabilistic seismic hazard in Georgia with a 10% chance of exceedance in 50 years in terms of Spectral Acceleration at 4.0 sec*

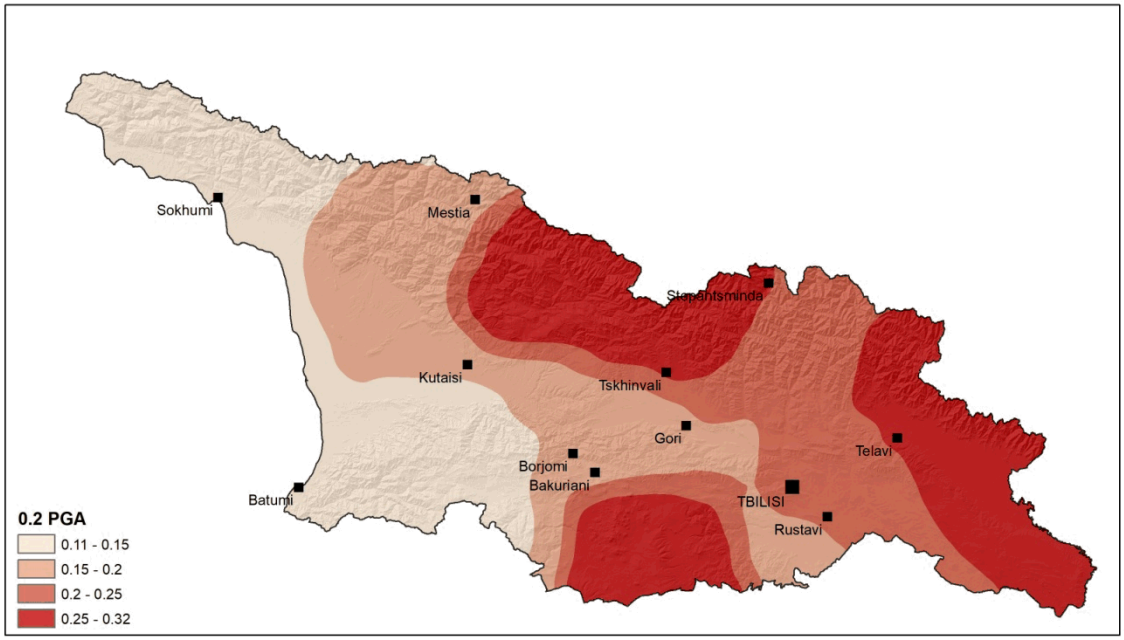


*Figure A22. Probabilistic seismic hazard in Georgia with a 20% chance of exceedance in 50 years in terms of PGA*

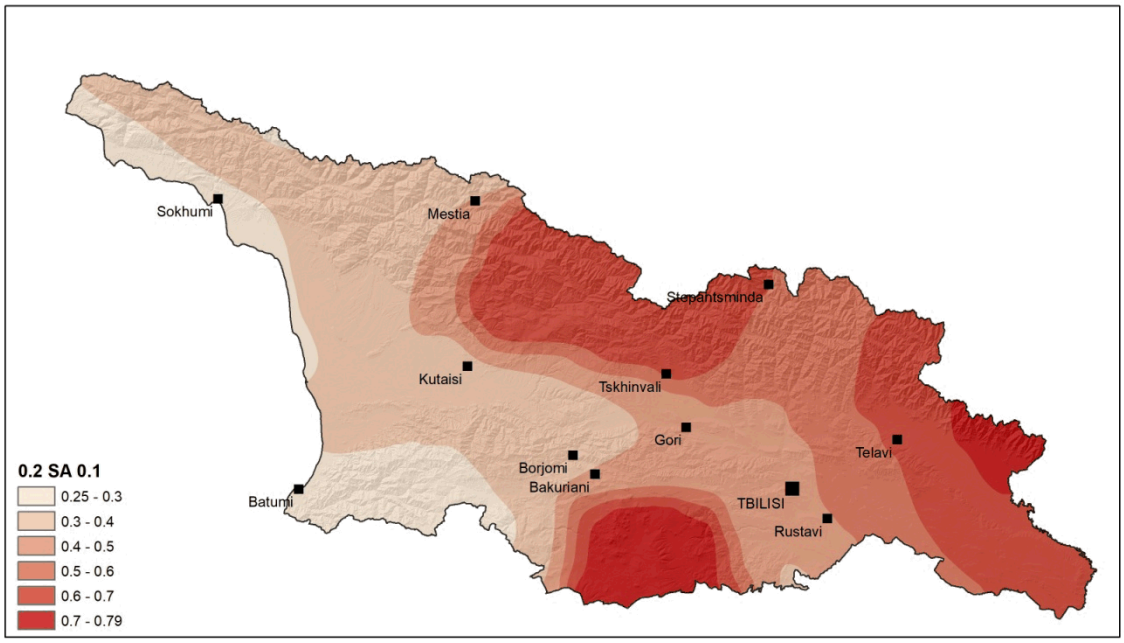


*Figure A23. Probabilistic seismic hazard in Georgia with a 20% chance of exceedance in 50 years in terms of Spectral Acceleration at 0.1 sec*

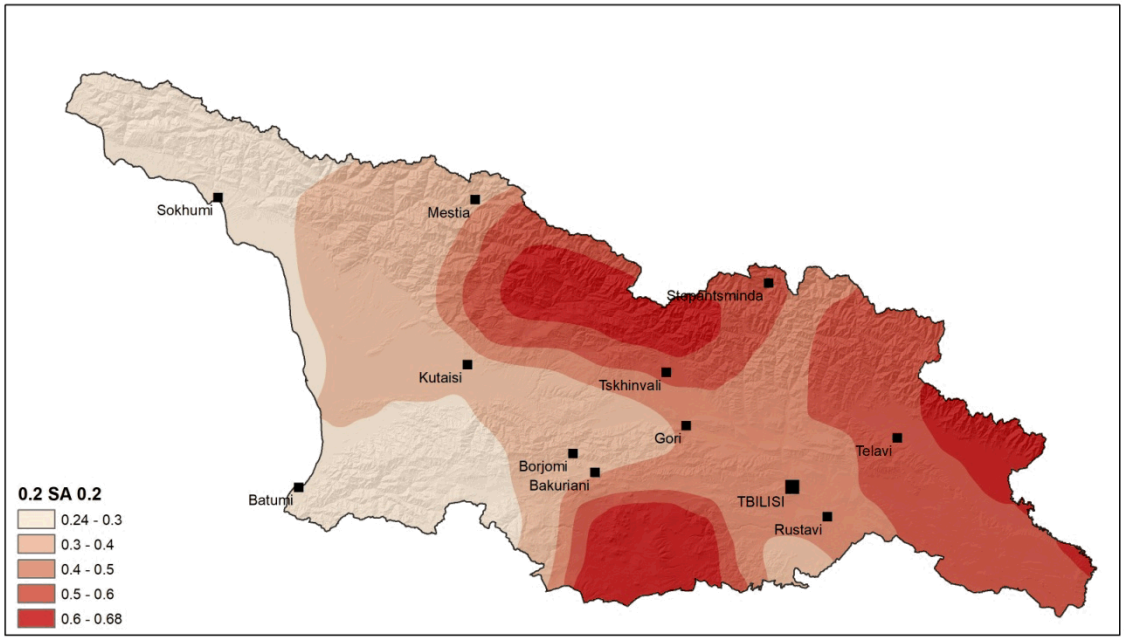


*Figure A24. Probabilistic seismic hazard in Georgia with a 20% chance of exceedance in 50 years in terms of Spectral Acceleration at 0.2 sec*

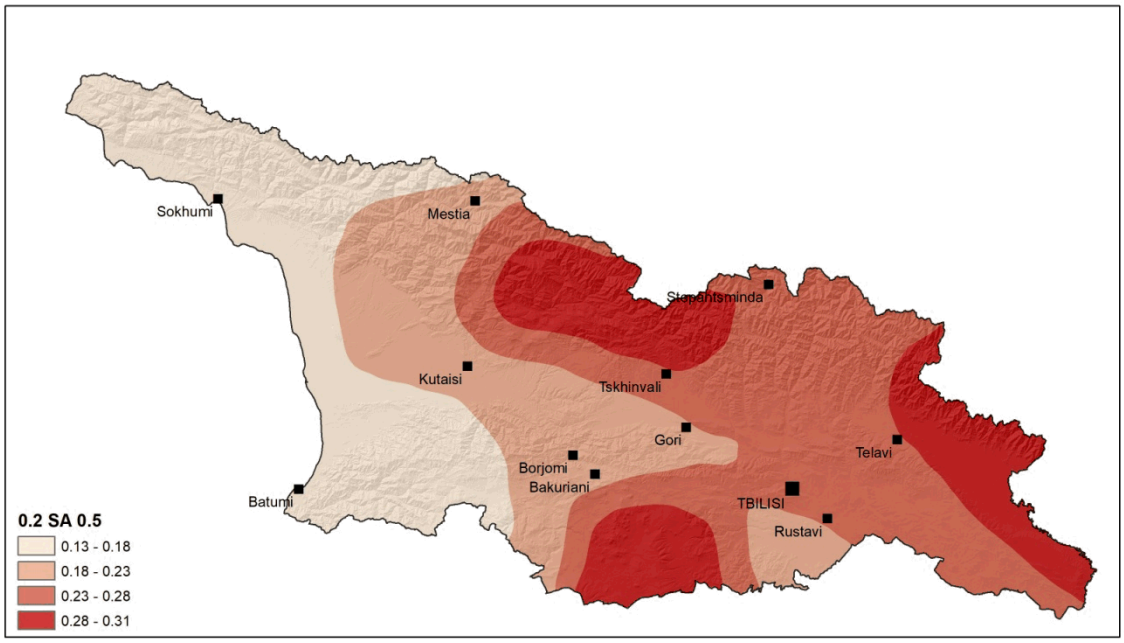


*Figure A25. Probabilistic seismic hazard in Georgia with a 20% chance of exceedance in 50 years in terms of Spectral Acceleration at 0.5 sec*

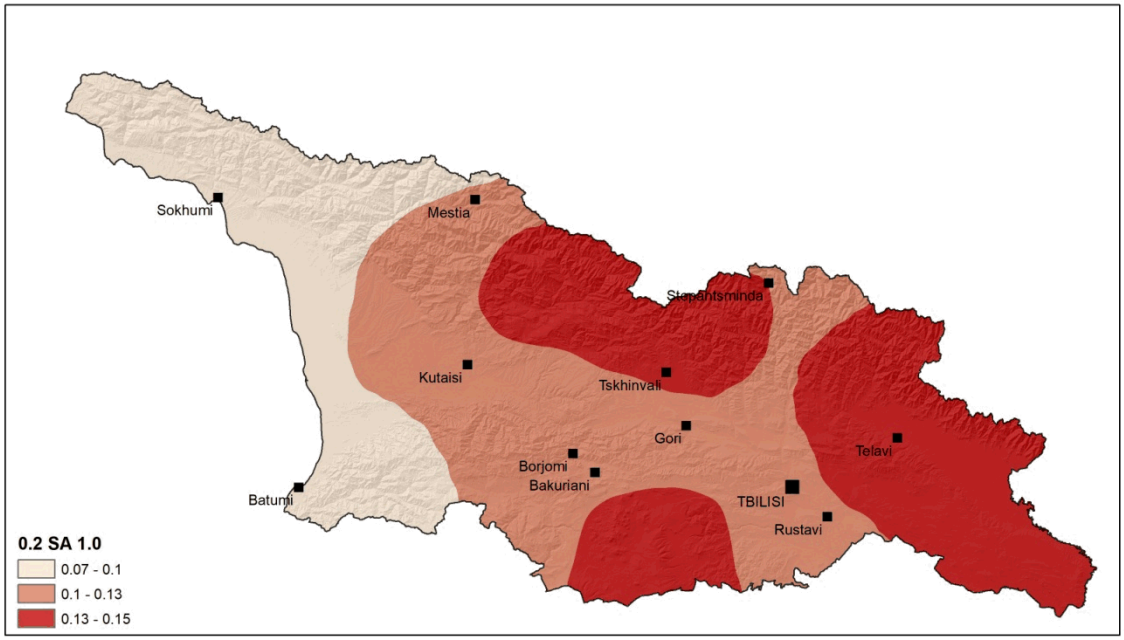


*Figure A26. Probabilistic seismic hazard in Georgia with a 20% chance of exceedance in 50 years in terms of Spectral Acceleration at 1.0 sec*

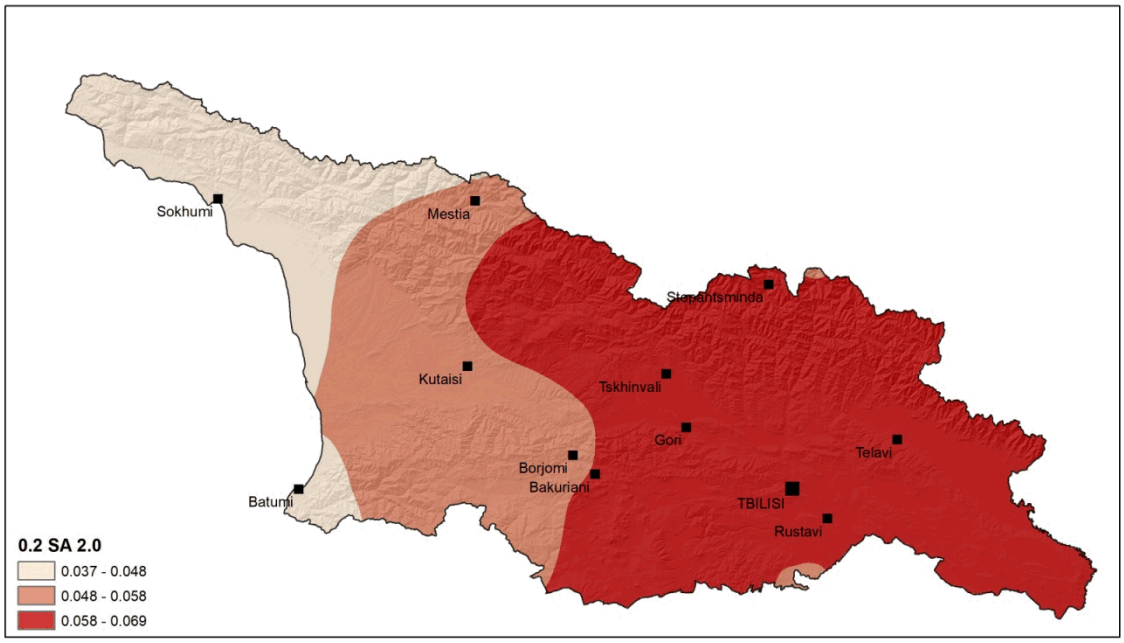


*Figure A27. Probabilistic seismic hazard in Georgia with a 20% chance of exceedance in 50 years in terms of Spectral Acceleration at 2.0 sec*

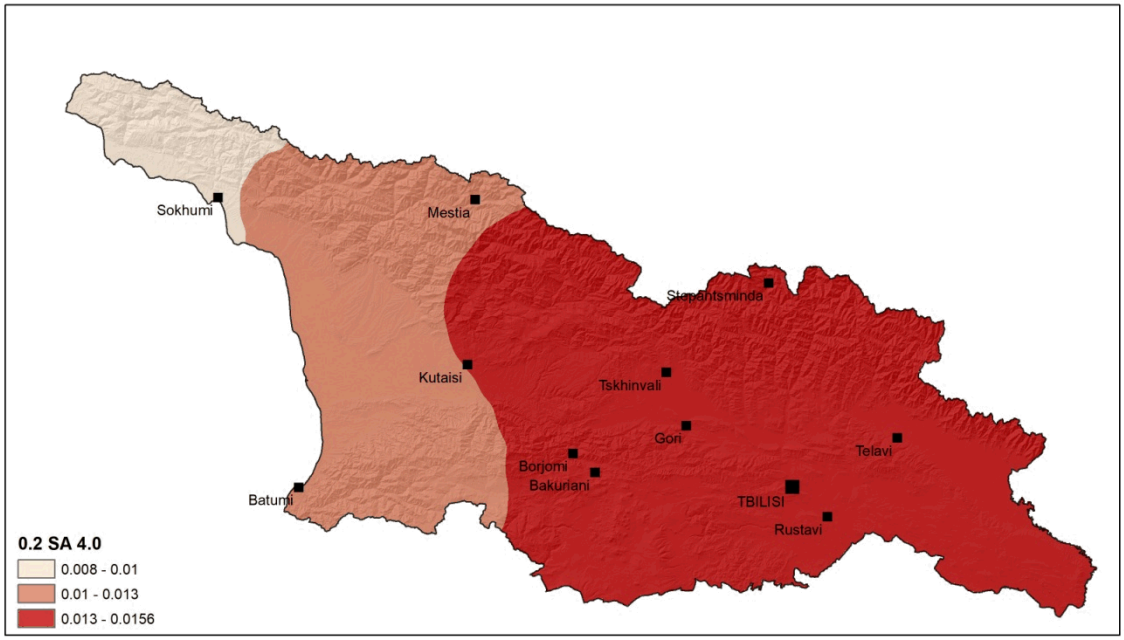


*Figure A28. Probabilistic seismic hazard in Georgia with a 20% chance of exceedance in 50 years in terms of Spectral Acceleration at 4.0 sec*

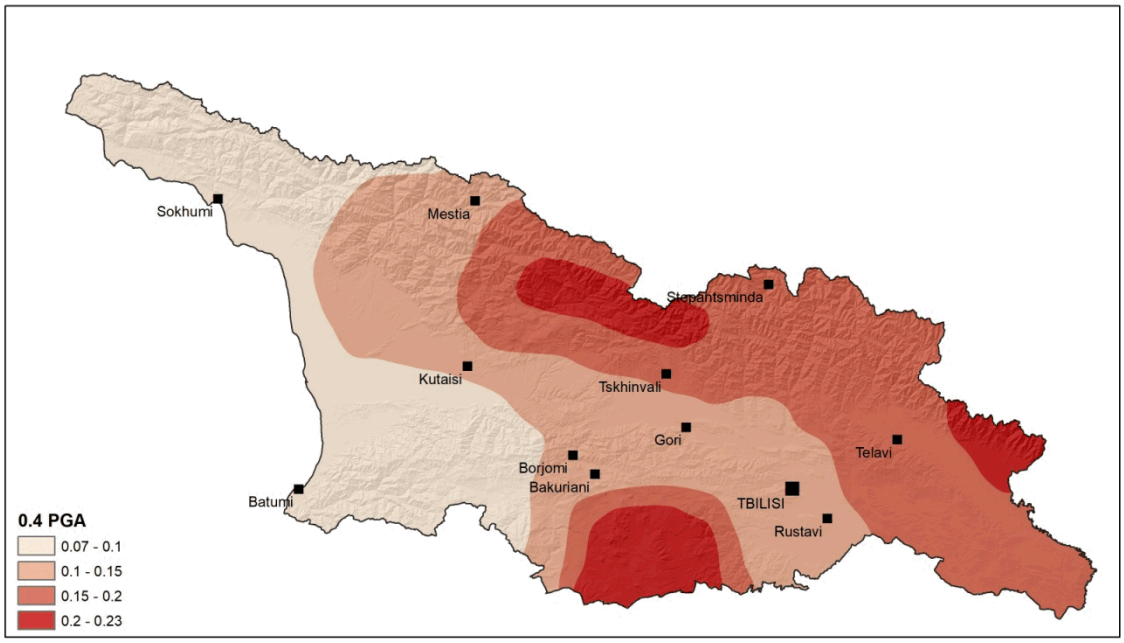


*Figure A29. Probabilistic seismic hazard in Georgia with a 40% chance of exceedance in 50 years in terms of PGA*

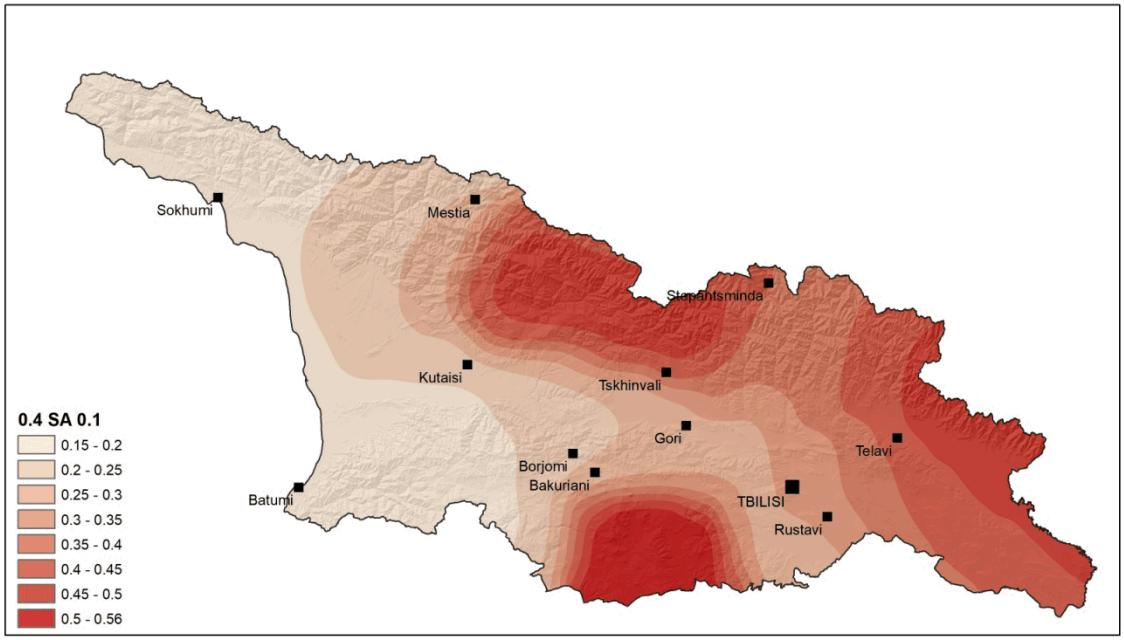


*Figure A30. Probabilistic seismic hazard in Georgia with a 40% chance of exceedance in 50 years in terms of Spectral Acceleration at 0.1 sec*

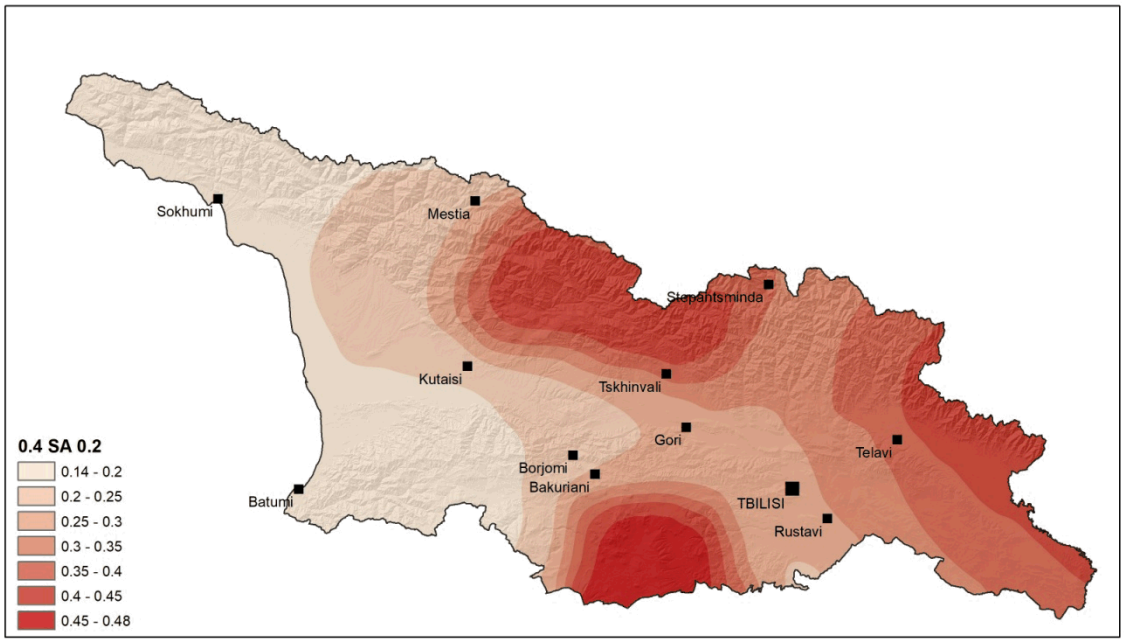


*Figure A31. Probabilistic seismic hazard in Georgia with a 40% chance of exceedance in 50 years in terms of Spectral Acceleration at 0.2 sec*

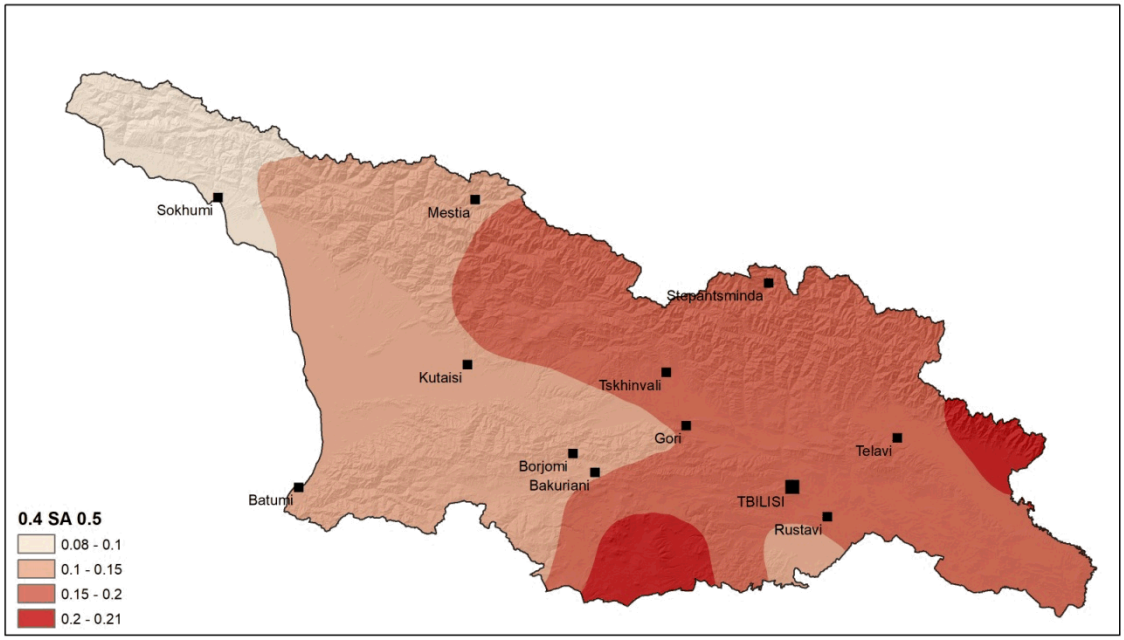


*Figure A32. Probabilistic seismic hazard in Georgia with a 40% chance of exceedance in 50 years in terms of Spectral Acceleration at 0.5 sec*

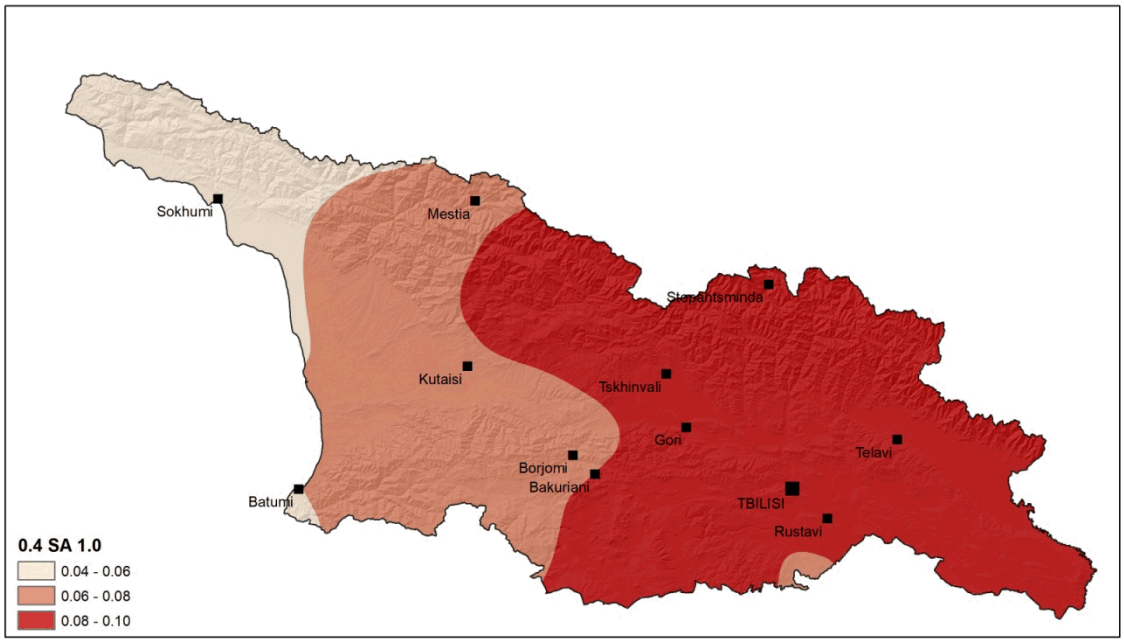


*Figure A33. Probabilistic seismic hazard in Georgia with a 40% chance of exceedance in 50 years in terms of Spectral Acceleration at 1.0 sec*

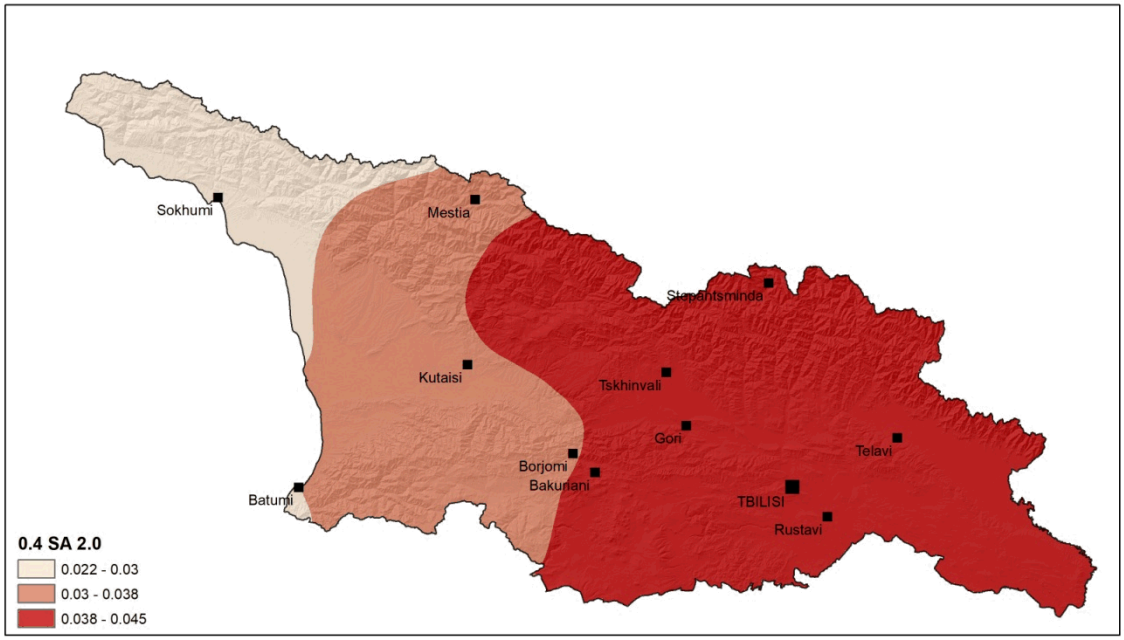


*Figure A34. Probabilistic seismic hazard in Georgia with a 40% chance of exceedance in 50 years in terms of Spectral Acceleration at 2.0 sec*

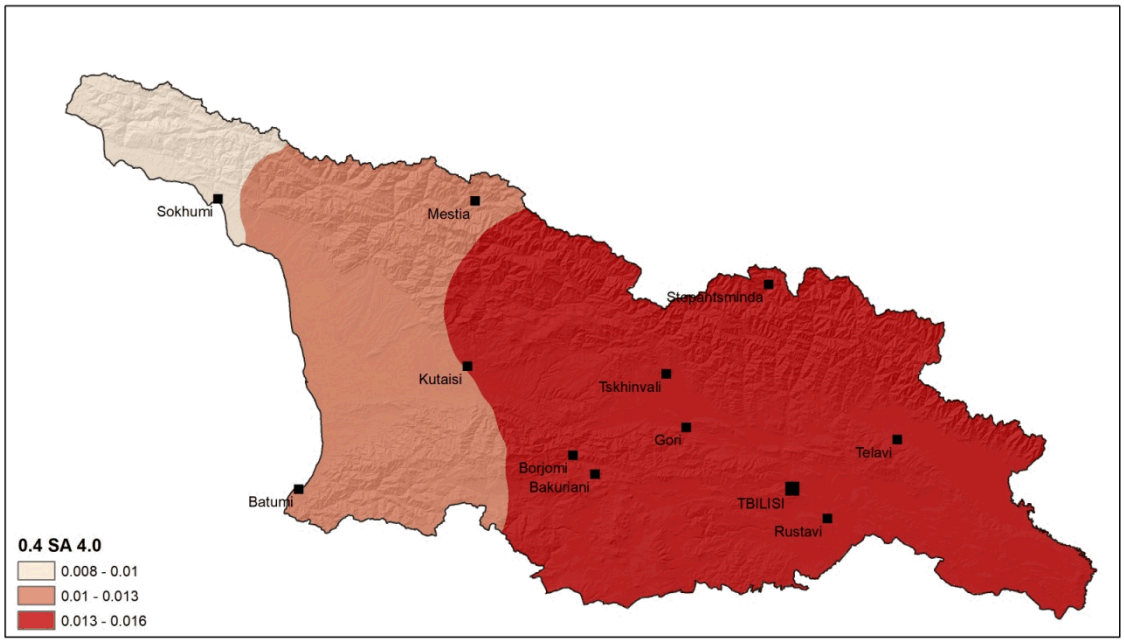


*Figure A35. Probabilistic seismic hazard in Georgia with a 40% chance of exceedance in 50 years in terms of Spectral Acceleration at 4.0 sec*

Uniform hazard spectra for 12 cities at five return periods are presented below.

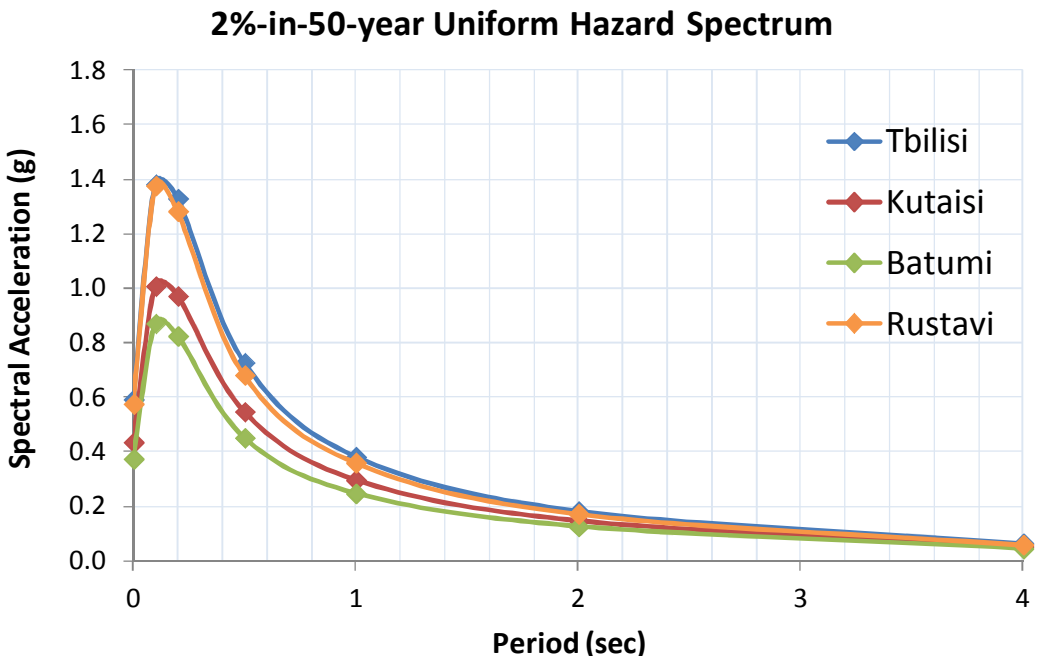


*Figure B1a. Uniform hazard spectrum with a 2% chance of exceedance in 50 years for Tbilisi, Kutaisi, Batumi and Rustavi*

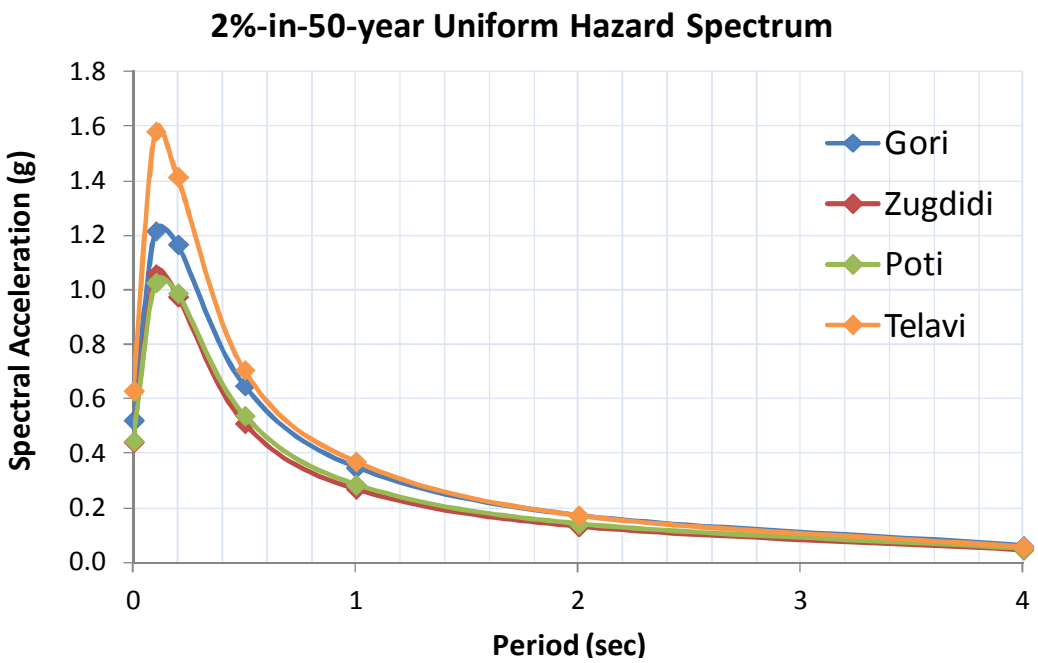


*Figure B1b. Uniform hazard spectrum with a 2% chance of exceedance in 50 years for Gori, Zugdidi, Poti and Telavi*

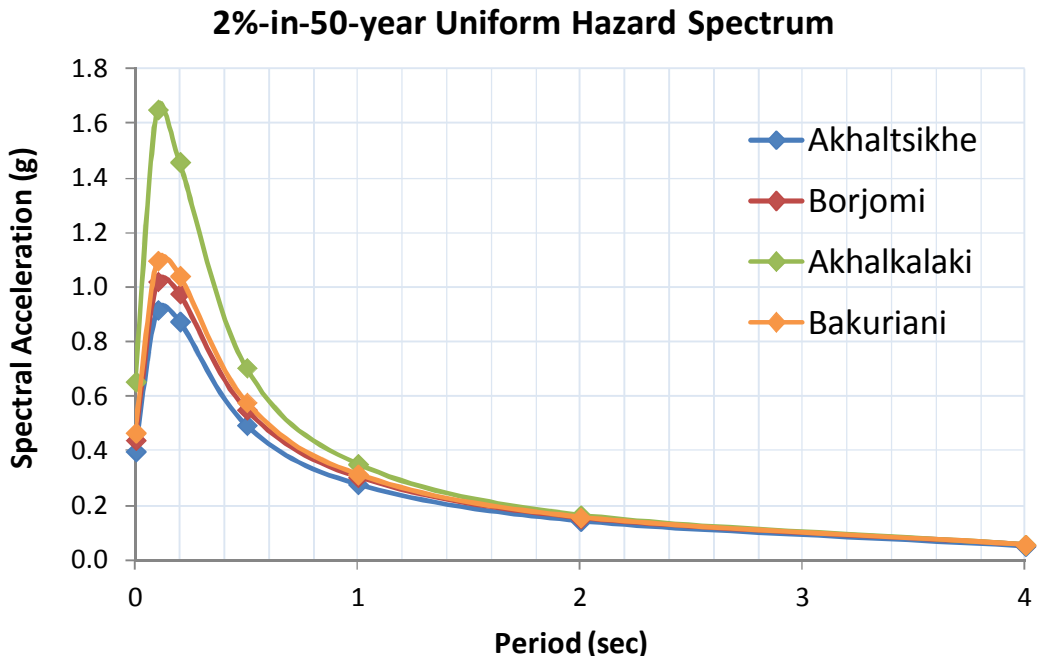


*Figure B1c. Uniform hazard spectrum with a 2% chance of exceedance in 50 years for Akhaltsikhe, Borjomi, Akhalkalaki and Bakuriani*

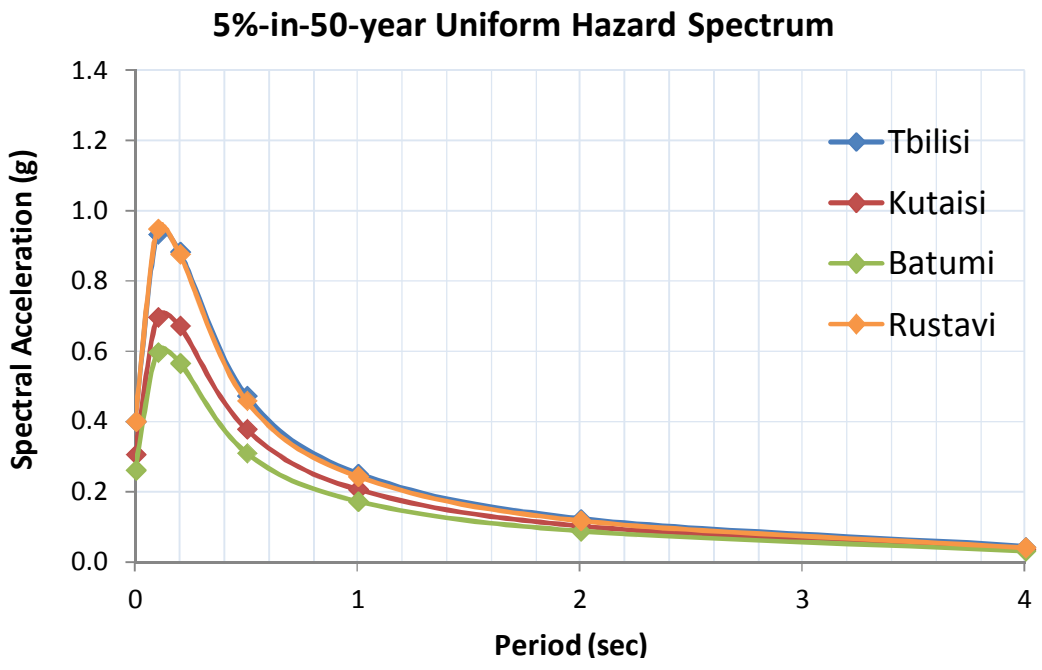


*Figure B2a. Uniform hazard spectrum with a 5% chance of exceedance in 50 years for Tbilisi, Kutaisi, Batumi and Rustavi*

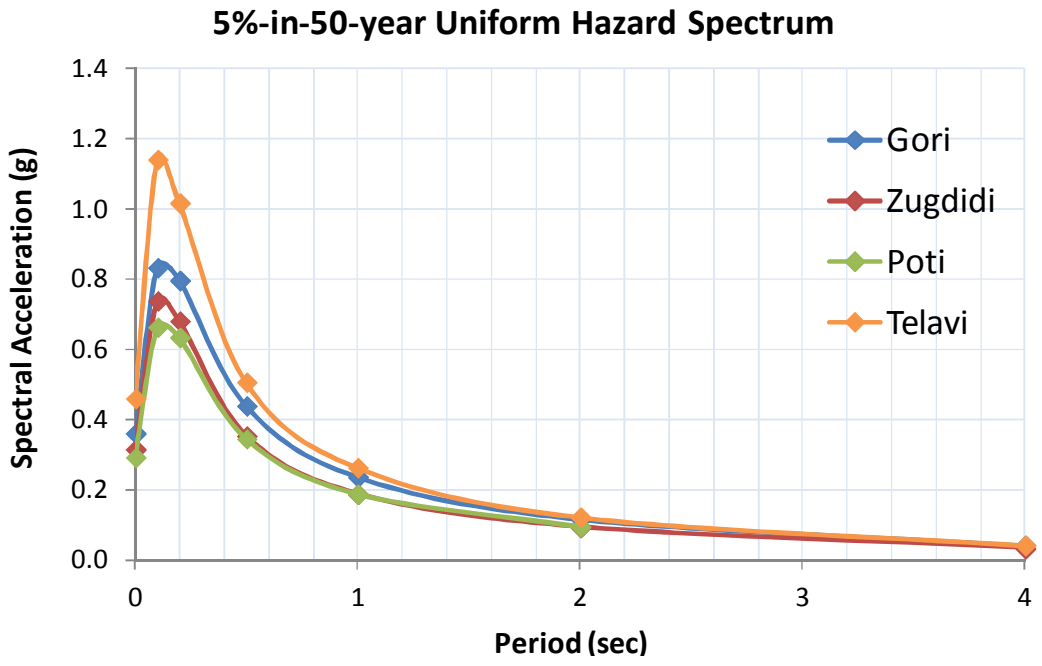


*Figure B2b. Uniform hazard spectrum with a 5% chance of exceedance in 50 years for Gori, Zugdidi, Poti and Telavi*

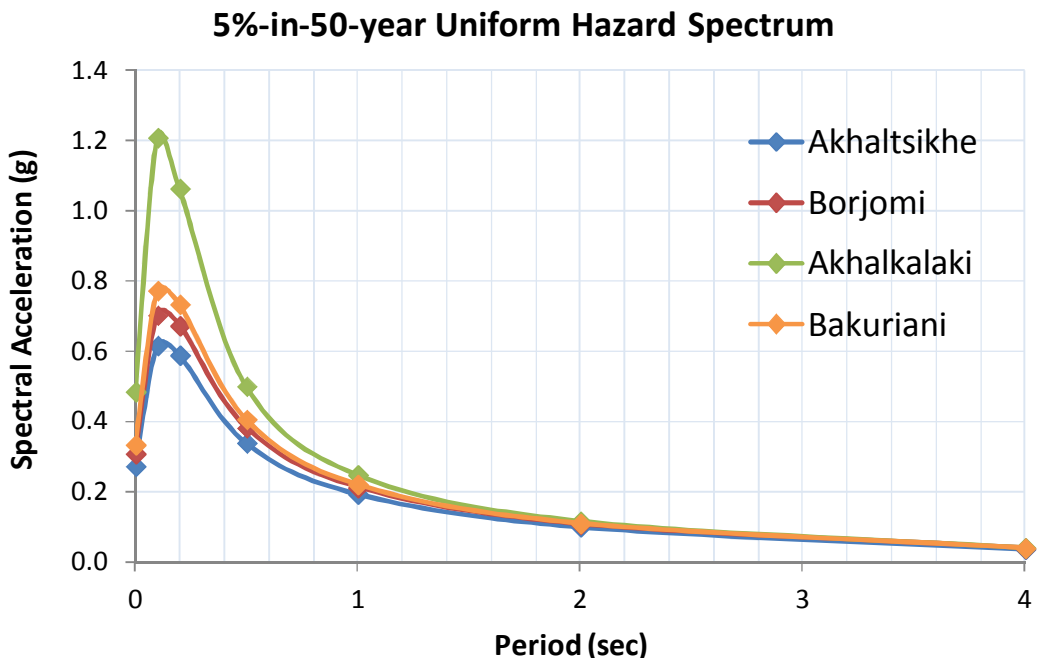


*Figure B2c. Uniform hazard spectrum with a 5% chance of exceedance in 50 years for Akhaltsikhe, Borjomi, Akhalkalaki and Bakuriani*

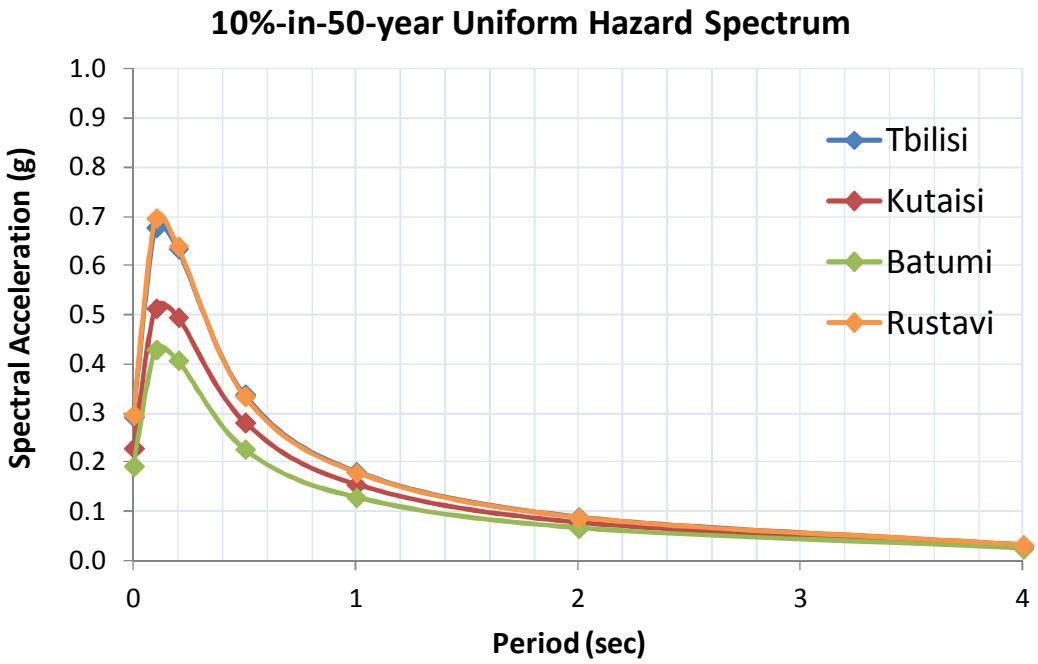


*Figure B3a. Uniform hazard spectrum with a 10% chance of exceedance in 50 years for Tbilisi, Kutaisi, Batumi and Rustavi*

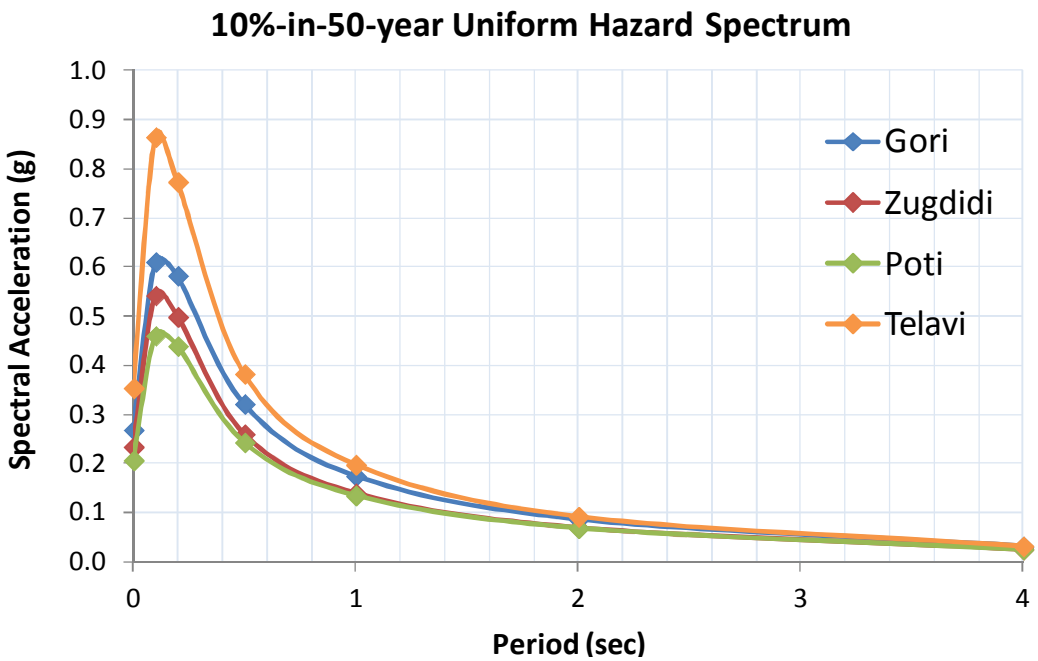


*Figure B3b. Uniform hazard spectrum with a 10% chance of exceedance in 50 years for Gori, Zugdidi, Poti and Telavi*

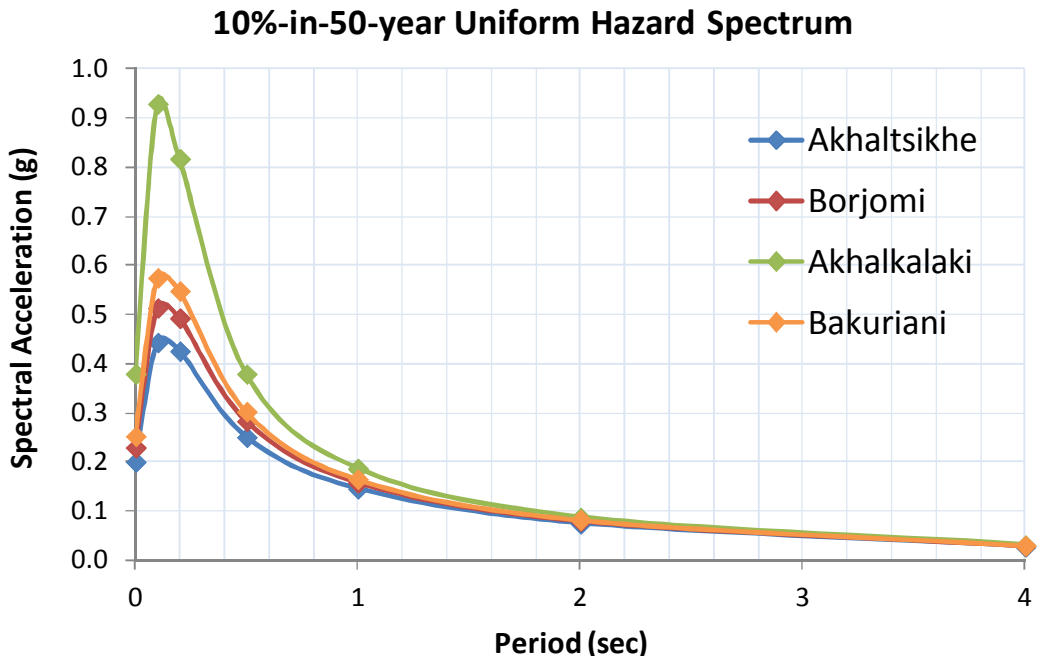


*Figure B3c. Uniform hazard spectrum with a 10% chance of exceedance in 50 years for Akhaltsikhe, Borjomi, Akhalkalaki and Bakuriani*

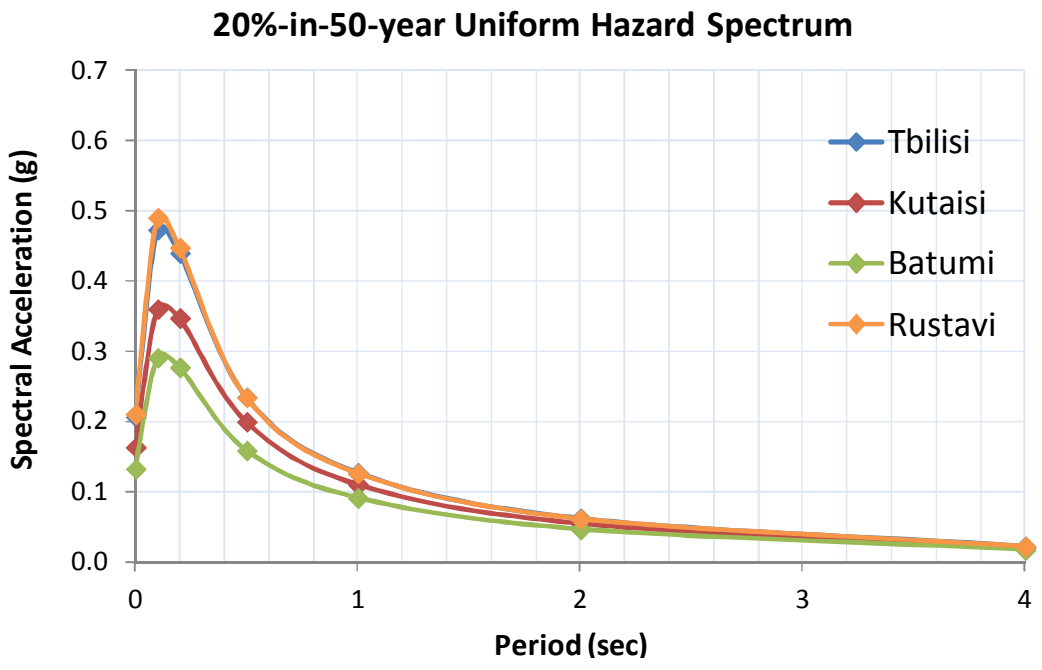


*Figure B4a. Uniform hazard spectrum with a 20% chance of exceedance in 50 years for Tbilisi, Kutaisi, Batumi and Rustavi*

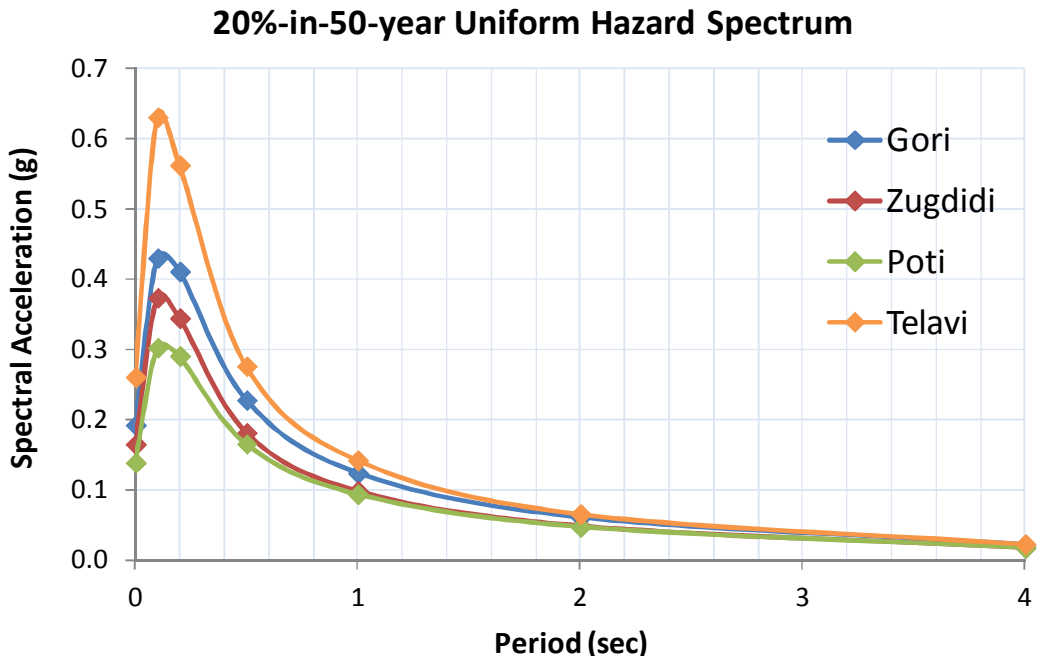


*Figure B4b. Uniform hazard spectrum with a 20% chance of exceedance in 50 years for Gori, Zugdidi, Poti and Telavi*

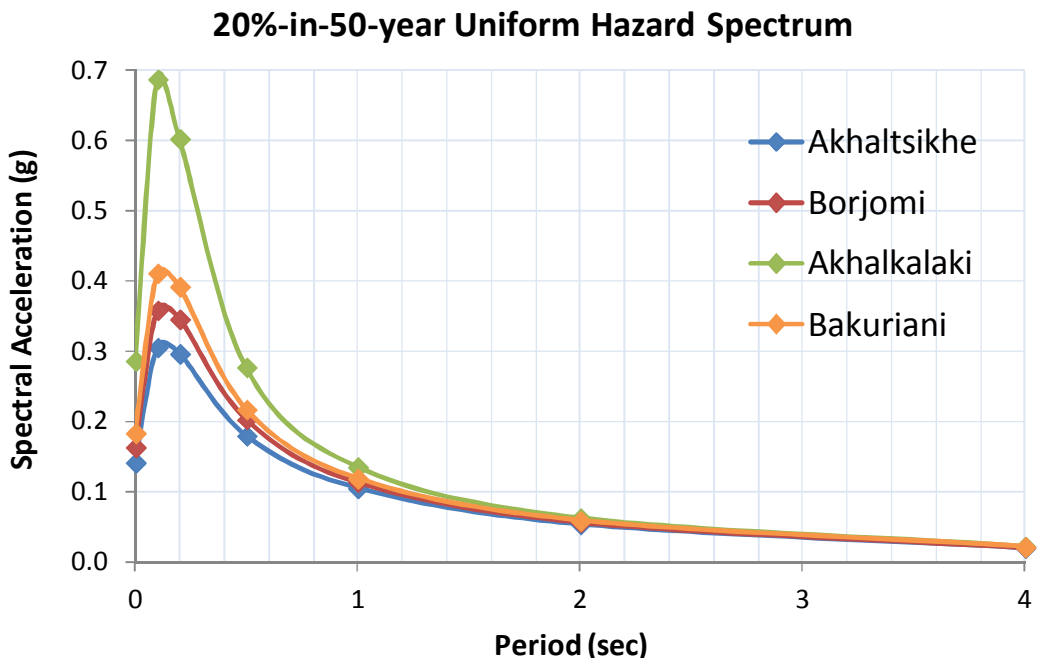


*Figure B4c. Uniform hazard spectrum with a 20% chance of exceedance in 50 years for Akhaltsikhe, Borjomi, Akhalkalaki and Bakuriani*

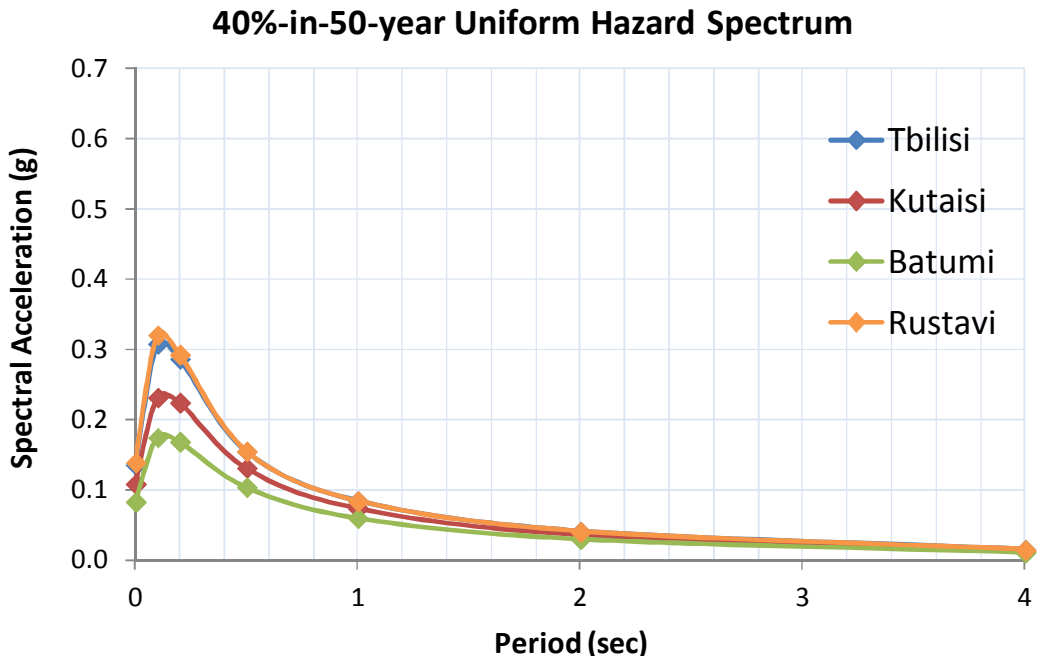


*Figure B5a. Uniform hazard spectrum with a 40% chance of exceedance in 50 years for Tbilisi, Kutaisi, Batumi and Rustavi*

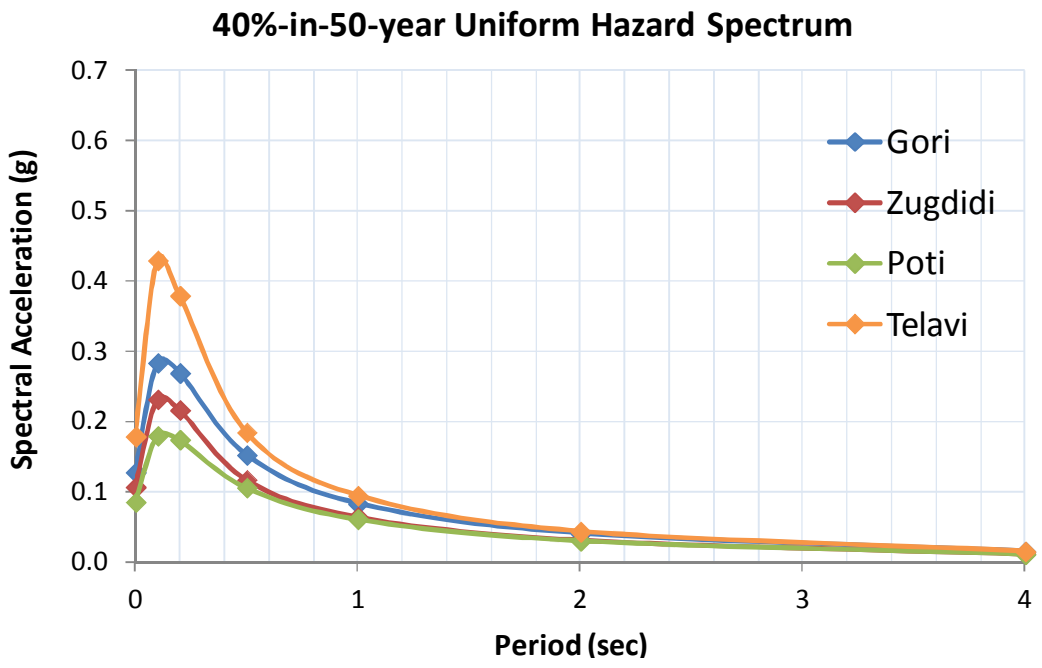


*Figure B5b. Uniform hazard spectrum with a 40% chance of exceedance in 50 years for Gori, Zugdidi, Poti and Telavi*

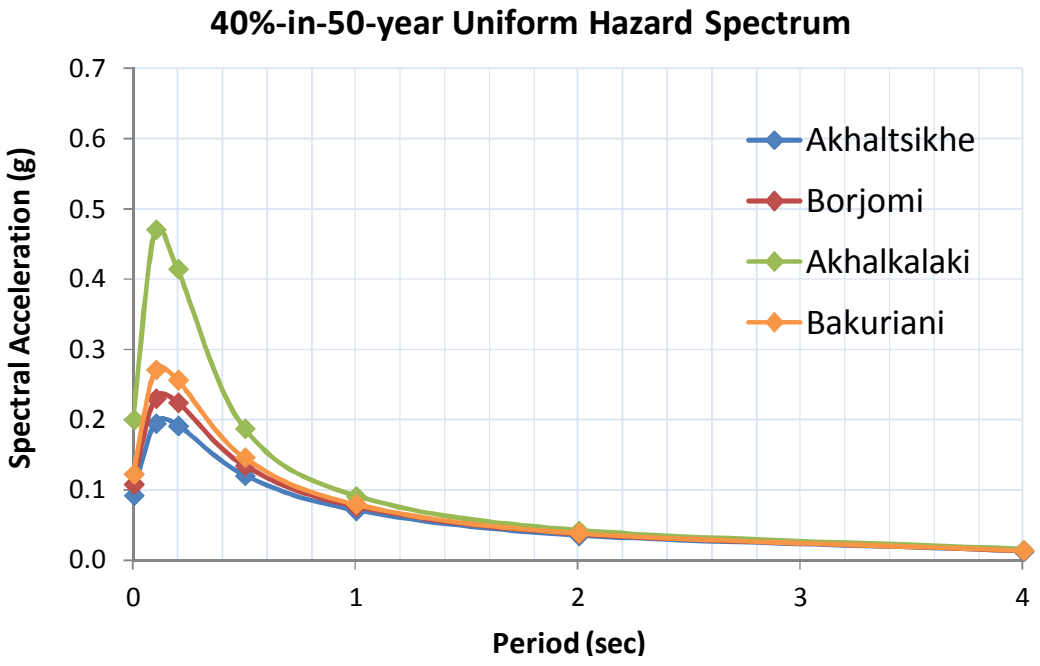


*Figure B5c. Uniform hazard spectrum with a 40% chance of exceedance in 50 years for Akhaltsikhe, Borjomi, Akhalkalaki and Bakuriani*

Hazard curves for 12 cities for PGA, Sa(0.2sec) and Sa(1.0sec) are presented below.

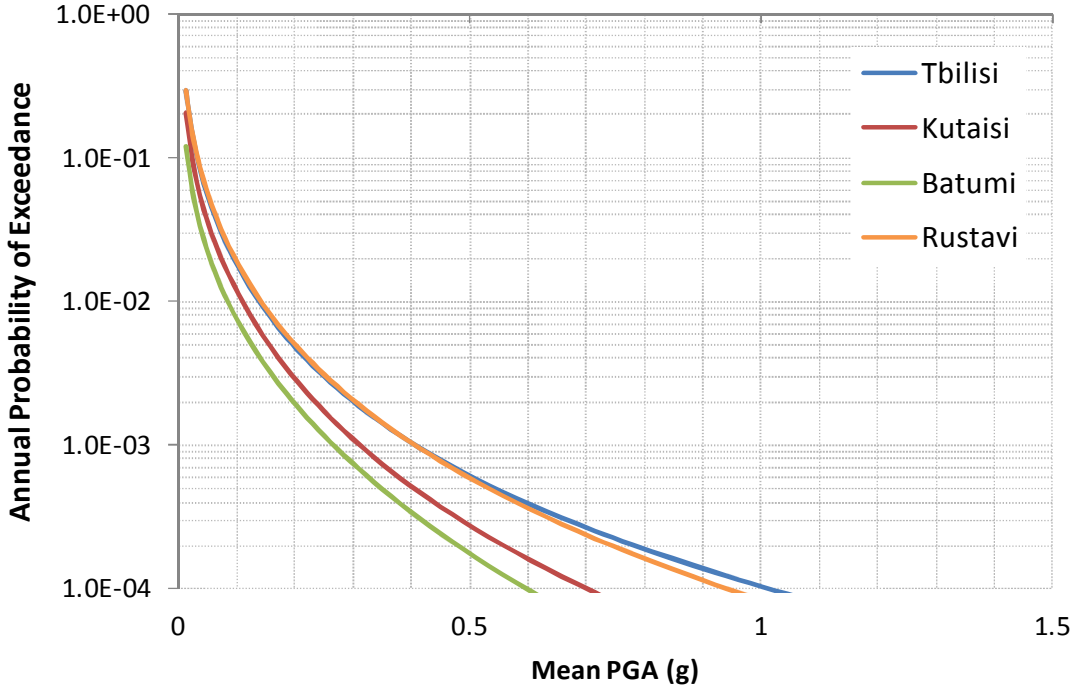


*Figure C1a. Hazard curves for PGA for Tbilisi, Kutaisi, Batumi and Rustavi*

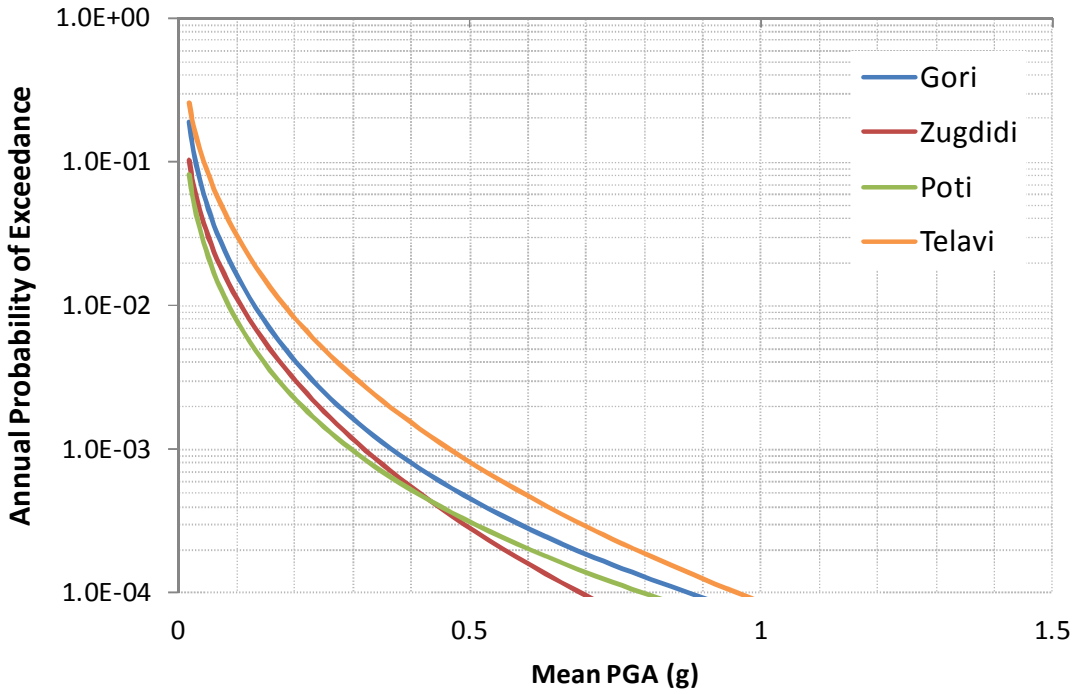


*Figure C1b. Hazard curves for PGA for Gori, Zugdidi, Poti and Telavi*

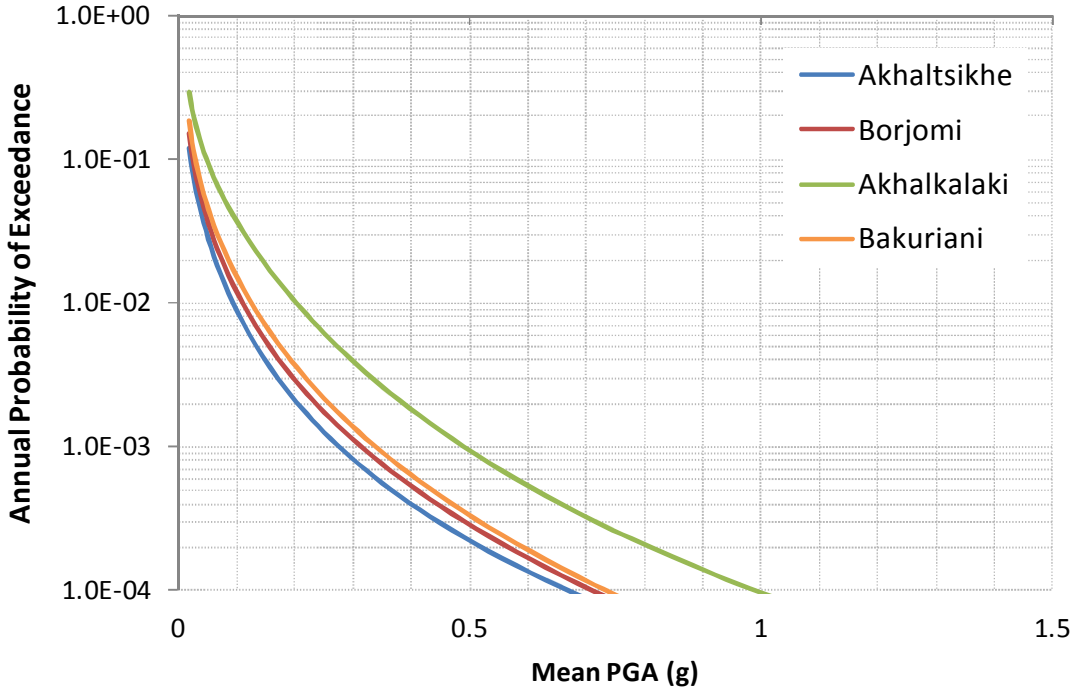


*Figure C1c. Hazard curves for PGA for Akhaltsikhe, Borjomi, Akhalkalaki and Bakuriani*

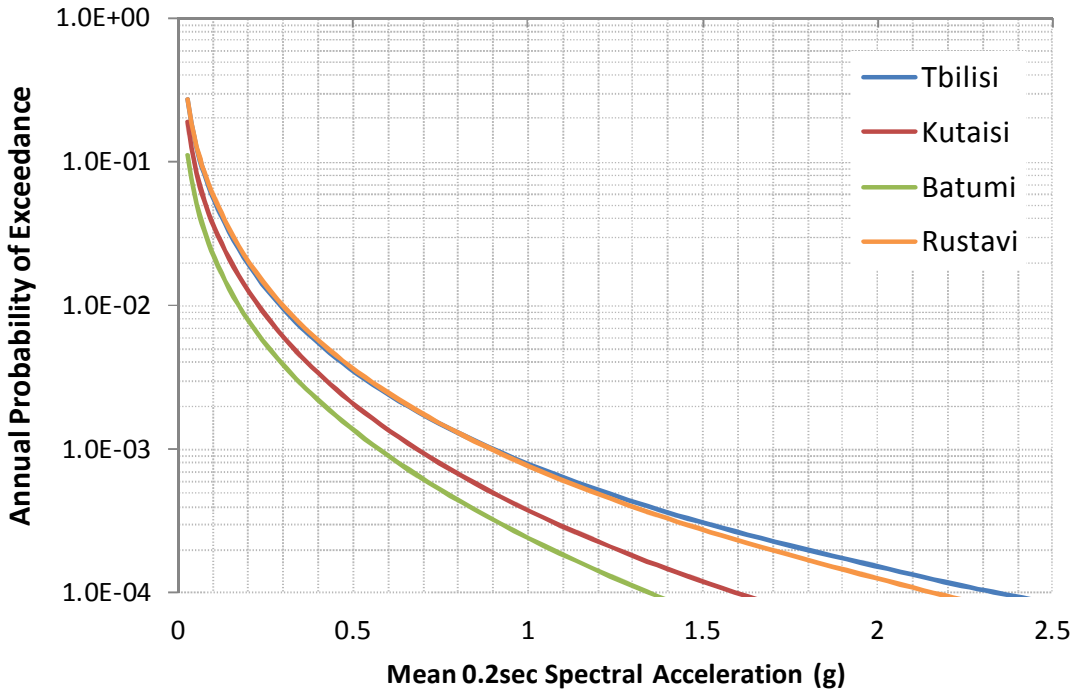


*Figure C2a. Hazard curves for Spectral Acceleration at 0.2sec for Tbilisi, Kutaisi, Batumi and Rustavi*

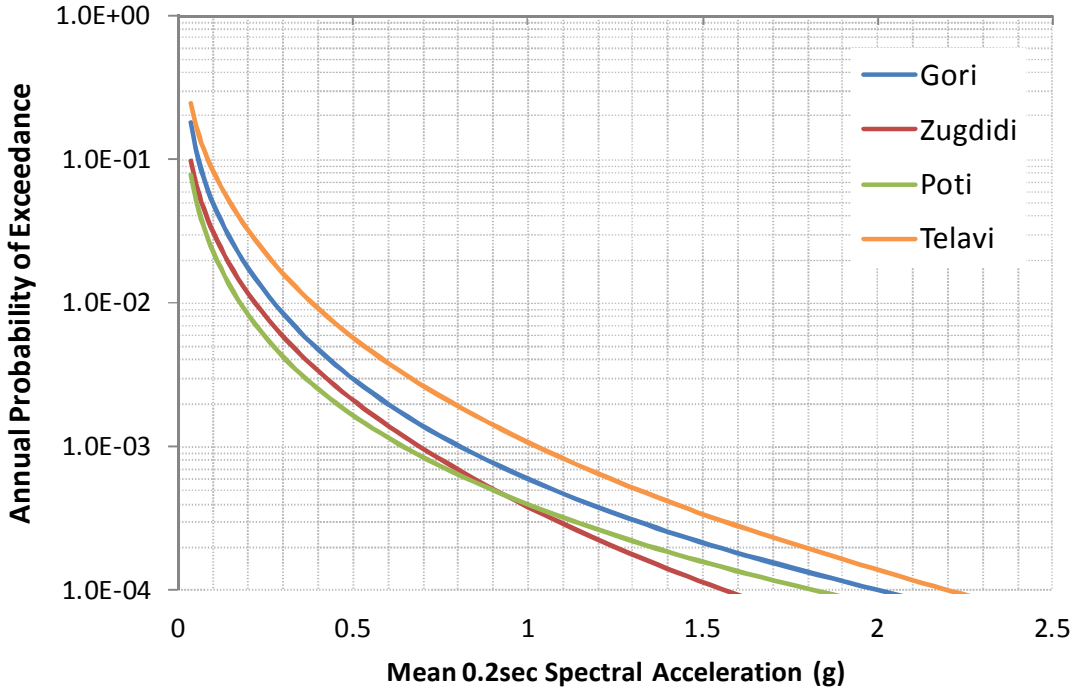


*Figure C2b. Hazard curves for Spectral Acceleration at 0.2sec for Gori, Zugdidi, Poti and Telavi*

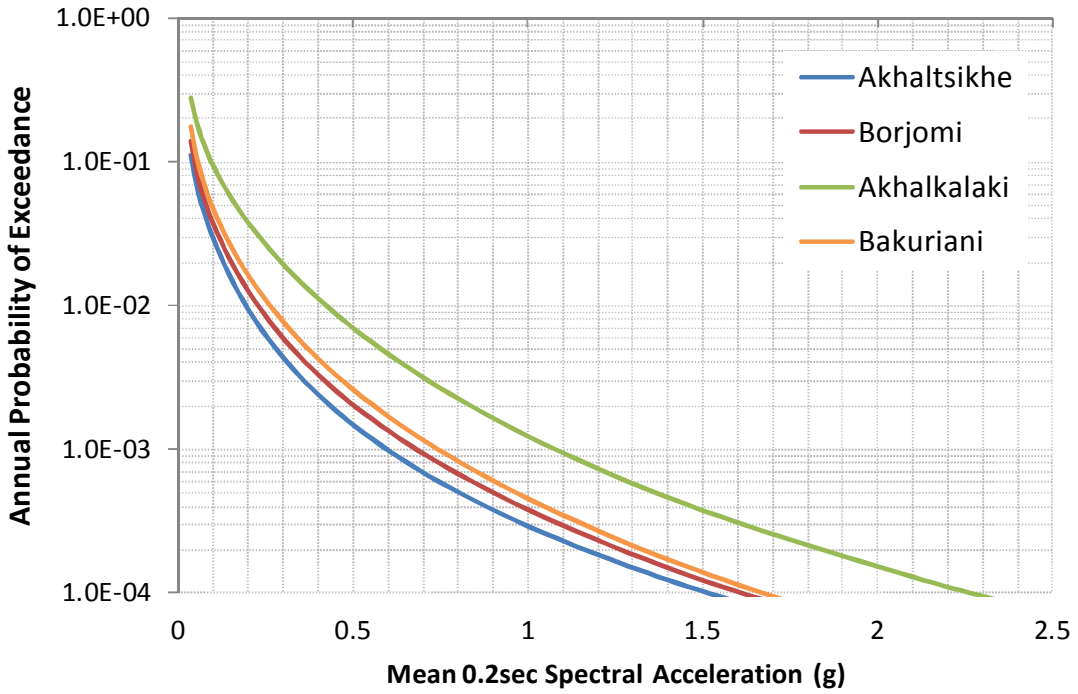


*Figure C2c. Hazard curves for Spectral Acceleration at 0.2sec for Akhaltsikhe, Borjomi, Akhalkalaki and Bakuriani*

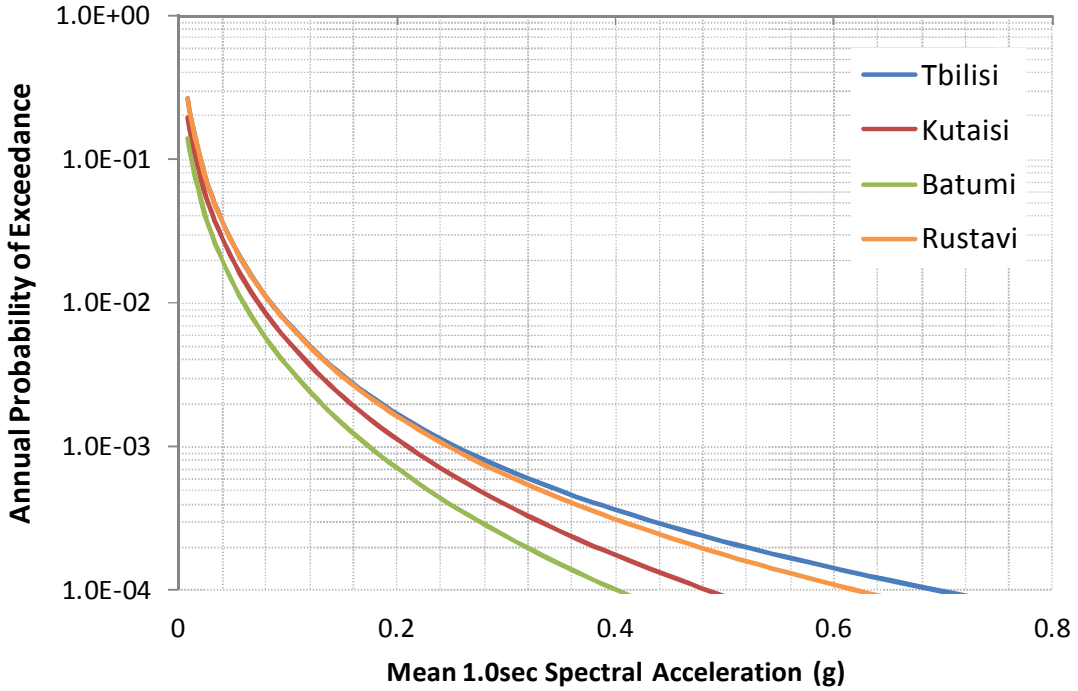


*Figure C3a. Hazard curves for Spectral Acceleration at 1.0sec for Tbilisi, Kutaisi, Batumi and Rustavi*

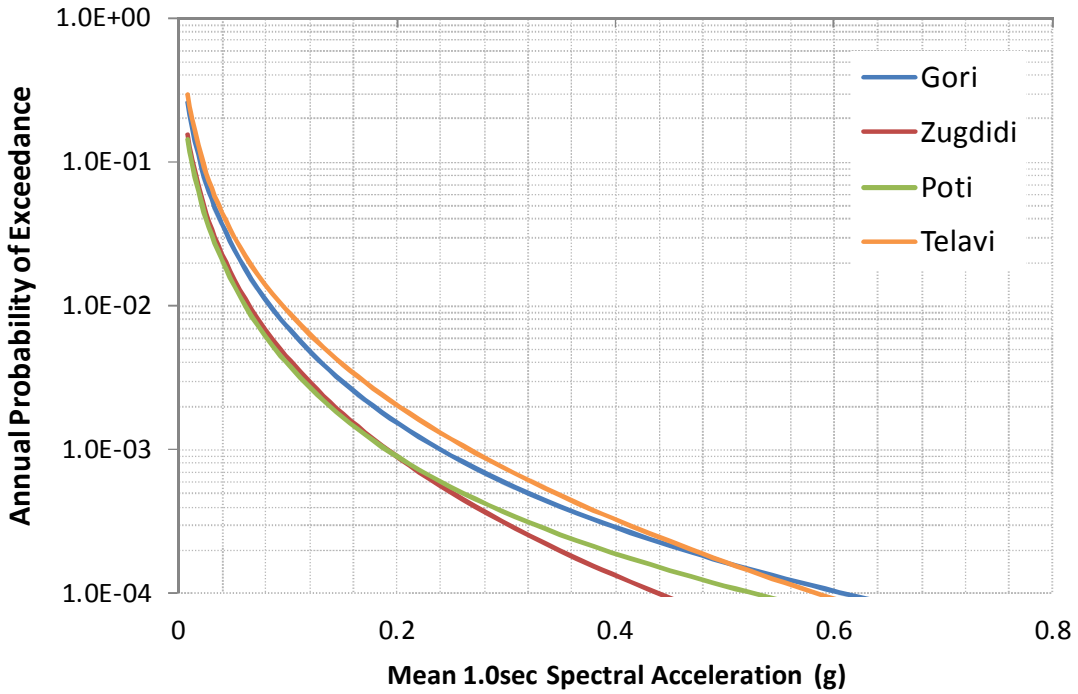


*Figure C3b. Hazard curves for Spectral Acceleration at 1.0sec for Gori, Zugdidi, Poti and Telavi*

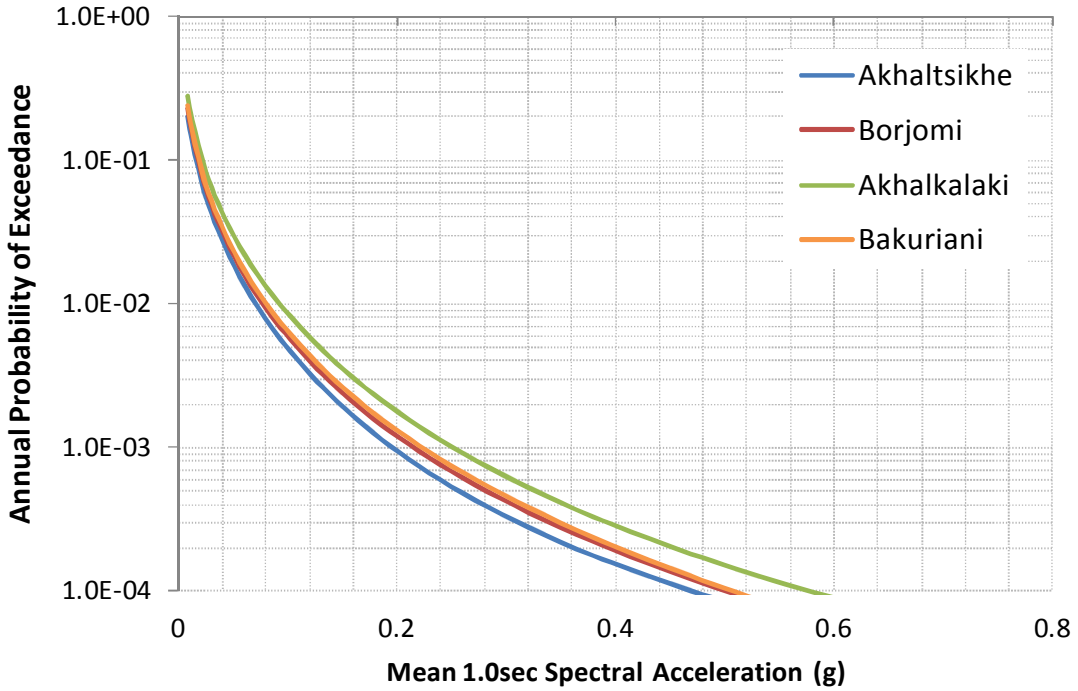


*Figure C3c. Hazard curves for Spectral Acceleration at 1.0sec for Akhaltsikhe, Borjomi, Akhalkalaki and Bakuriani*

## APPENDIX D

Hazard deaggregations for Tbilisi, Kutaisi and Batumi for PGA, Sa(0.2sec) and Sa(1.0sec) are presented below at 10% and 2% probabilities of exceedance in 50 years.

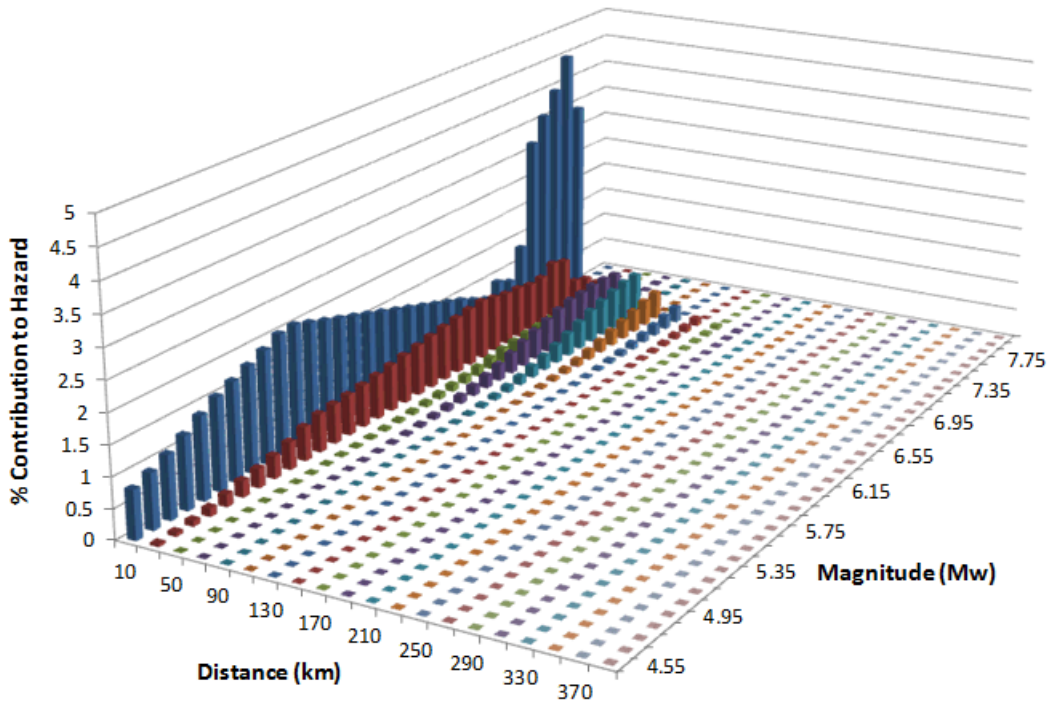


*Figure D1. Hazard deaggregation for 10%-in-50-year PGA for Tbilisi (mean magnitude: 6.55, mean distance: 30km, mode magnitude: 7.65, mode distance: 10km)*

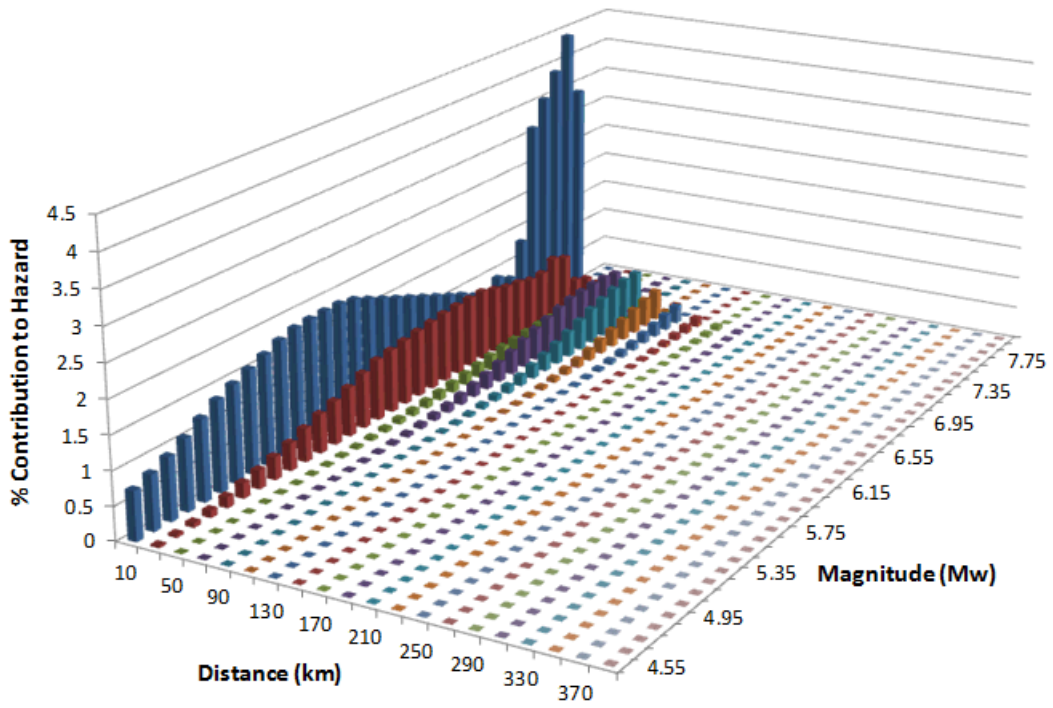


*Figure D2. Hazard deaggregation for 10%-in-50-year Spectral Acceleration at 0.2sec for Tbilisi (mean magnitude: 6.57, mean distance: 31km, mode magnitude: 7.65, mode distance: 10km)*

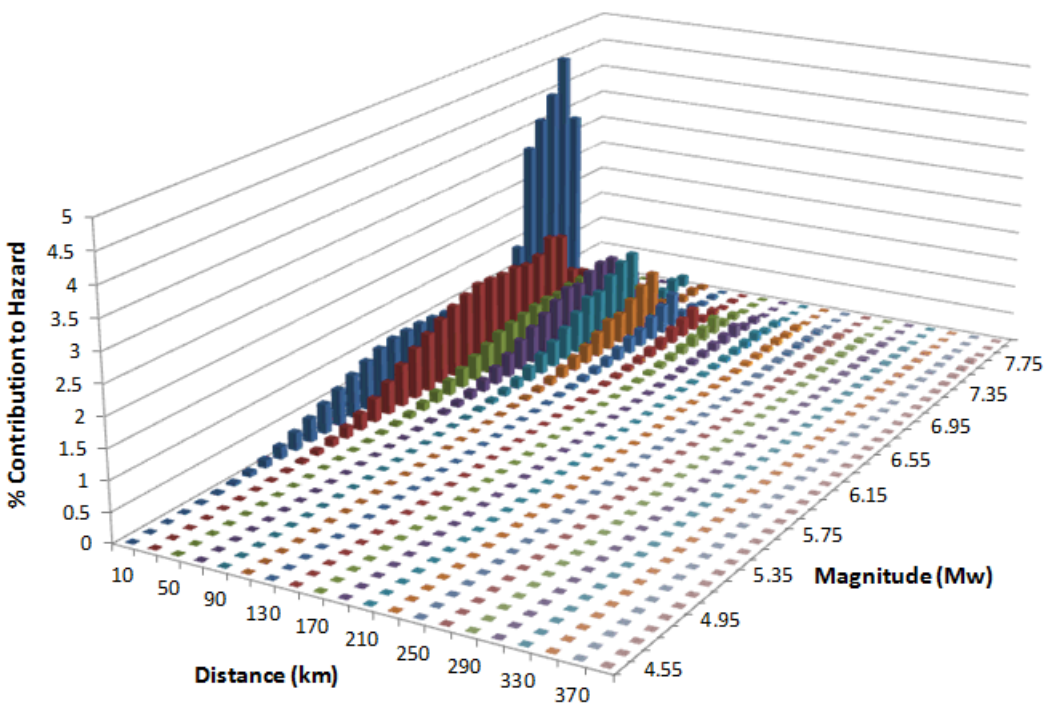


*Figure D3. Hazard deaggregation for 10%-in-50-year Spectral Acceleration at 1.0sec for Tbilisi (mean magnitude: 7.10, mean distance: 56km, mode magnitude: 7.65, mode distance: 10km)*

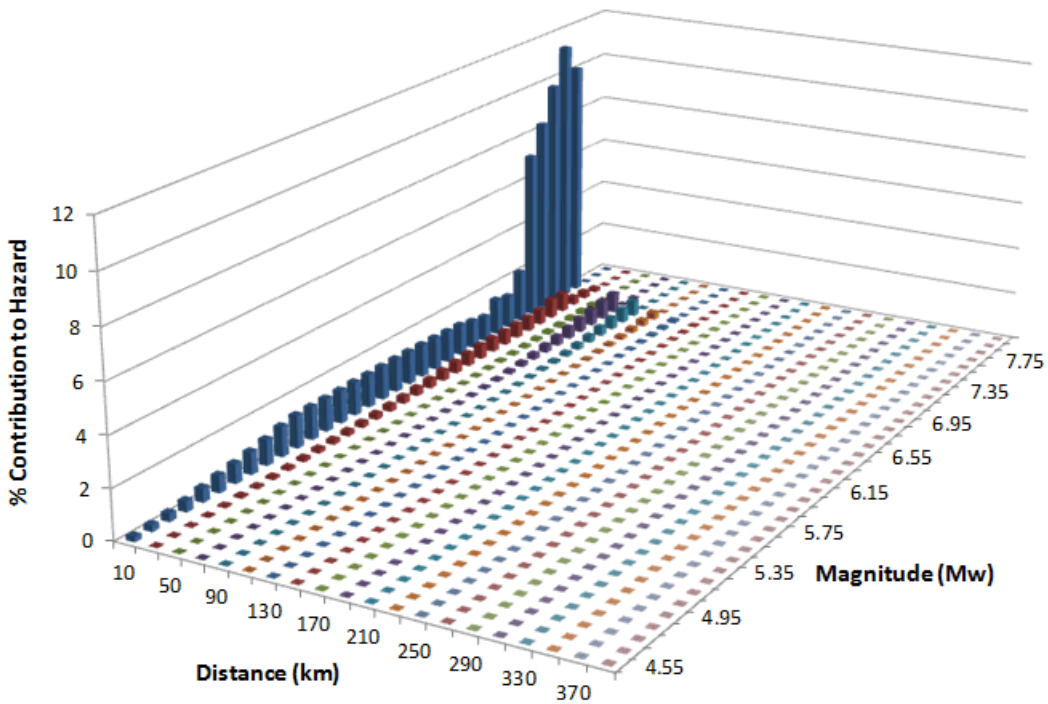


*Figure D4. Hazard deaggregation for 2%-in-50-year PGA for Tbilisi (mean magnitude: 7.00, mean distance: 20km, mode magnitude: 7.65, mode distance: 10km)*

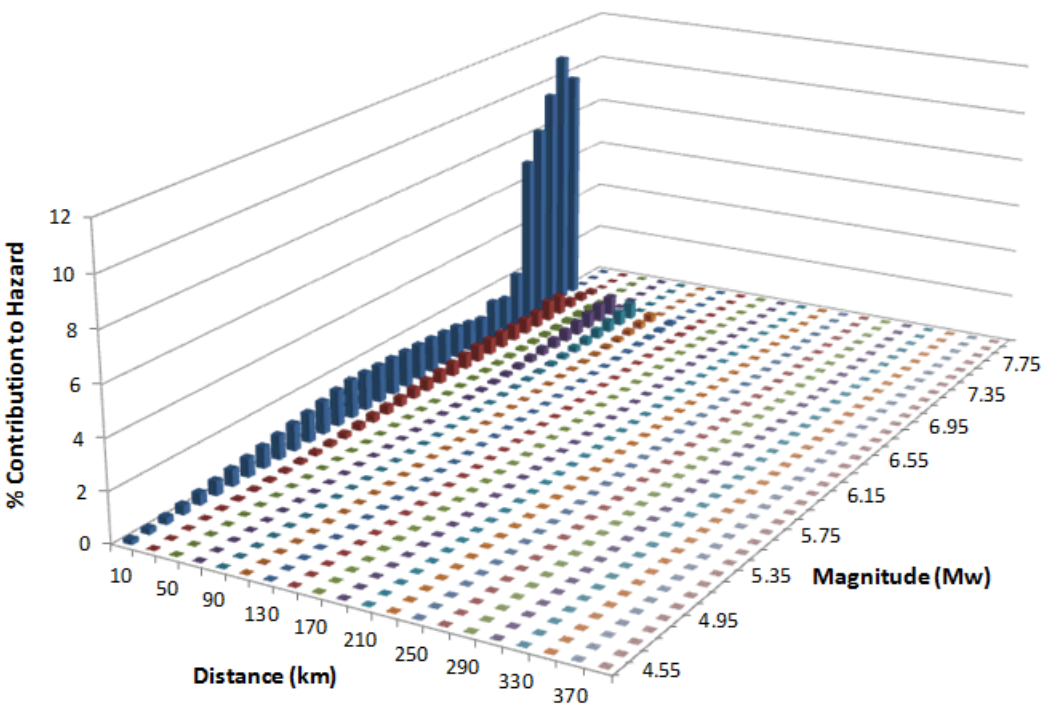


*Figure D5. Hazard deaggregation for 2%-in-50-year Spectral Acceleration at 0.2sec for Tbilisi (mean magnitude: 7.00, mean distance: 21km, mode magnitude: 7.65, mode distance: 10km)*

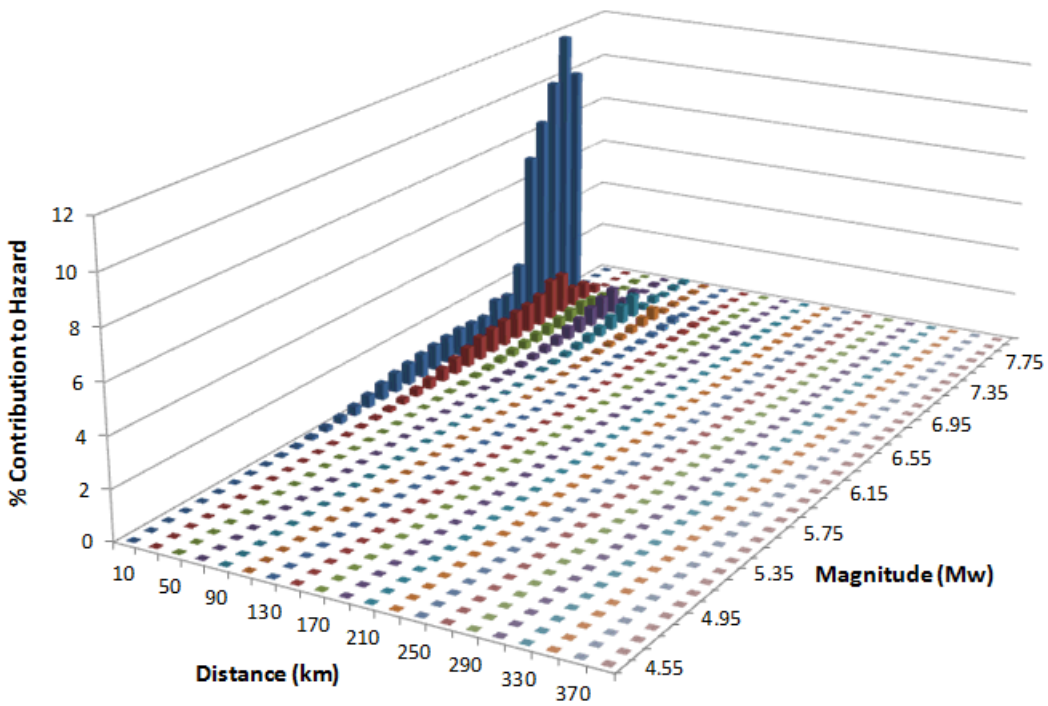


*Figure D6. Hazard deaggregation for 2%-in-50-year Spectral Acceleration at 1.0sec for Tbilisi (mean magnitude: 7.31, mean distance: 31km, mode magnitude: 7.65, mode distance: 10km)*

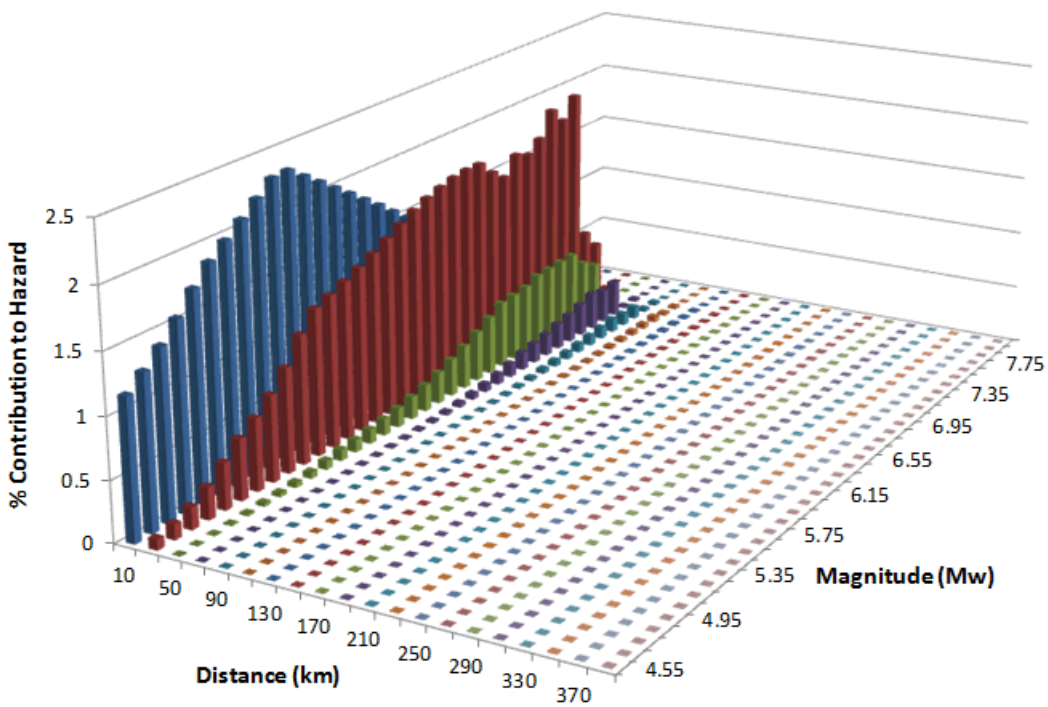


*Figure D7. Hazard deaggregation for 10%-in-50-year PGA for Kutaisi (mean magnitude: 6.24, mean distance: 25km, mode magnitude: 5.55, mode distance: 10km)*

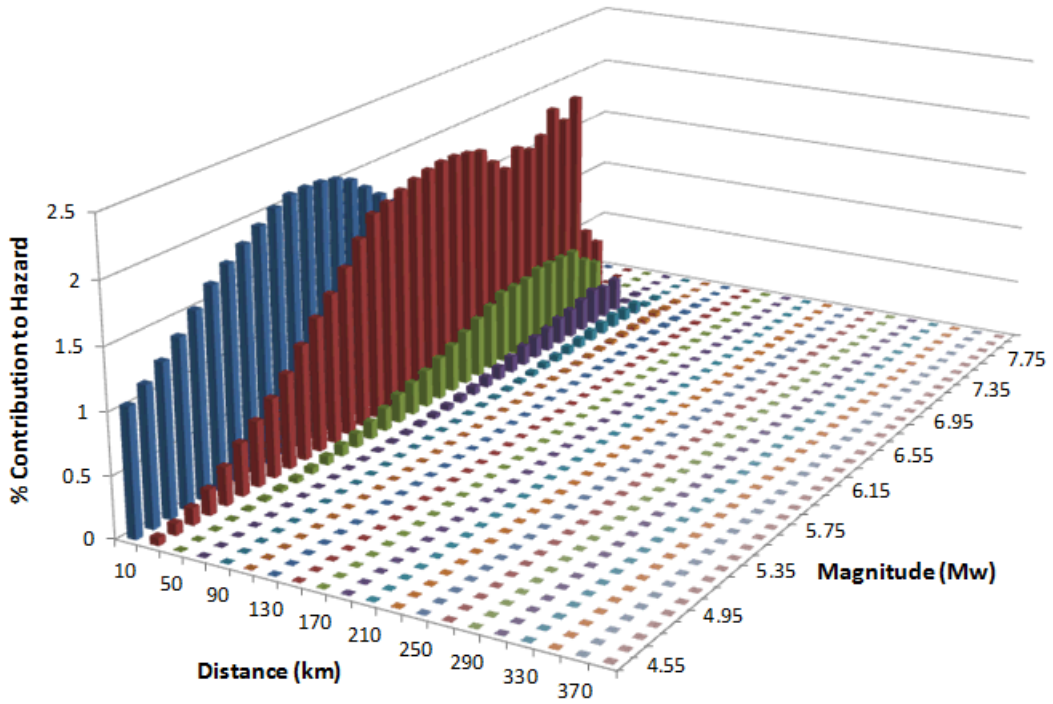


*Figure D8. Hazard deaggregation for 10%-in-50-year Spectral Acceleration at 0.2sec for Kutaisi (mean magnitude: 6.27, mean distance: 25km, mode magnitude: 5.65, mode distance: 10km)*

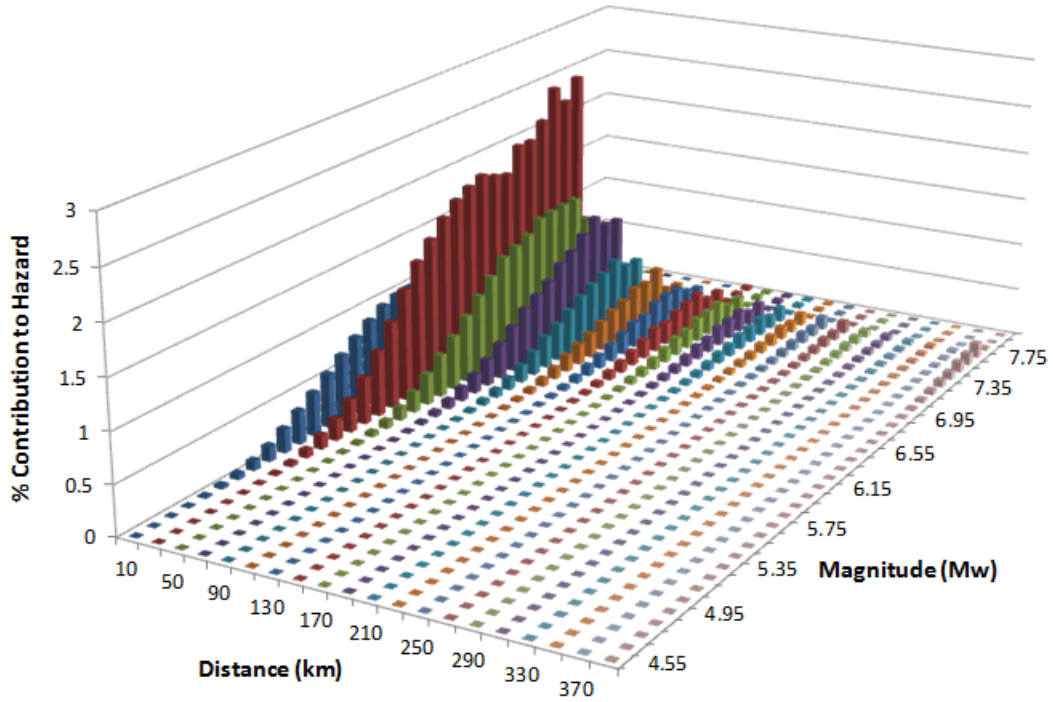


*Figure D9. Hazard deaggregation for 10%-in-50-year Spectral Acceleration at 1.0sec for Kutaisi (mean magnitude: 6.95, mean distance: 65km, mode magnitude: 7.55, mode distance: 30km)*

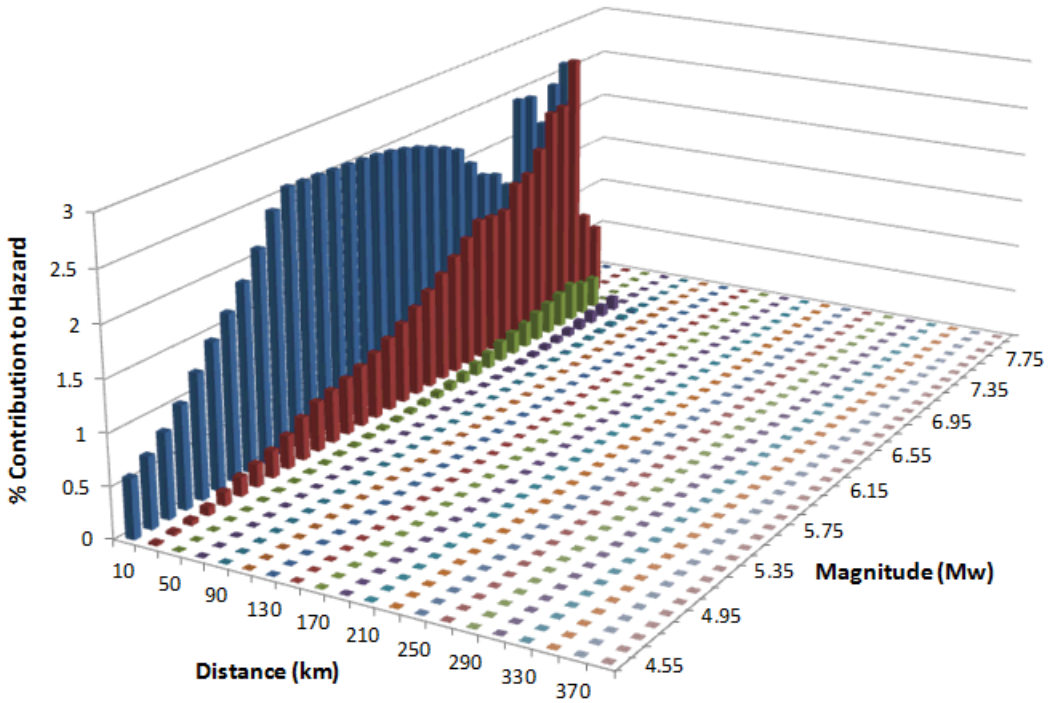


*Figure D10. Hazard deaggregation for 2%-in-50-year PGA for Kutaisi (mean magnitude: 6.45, mean distance: 18km, mode magnitude: 7.55, mode distance: 30km)*

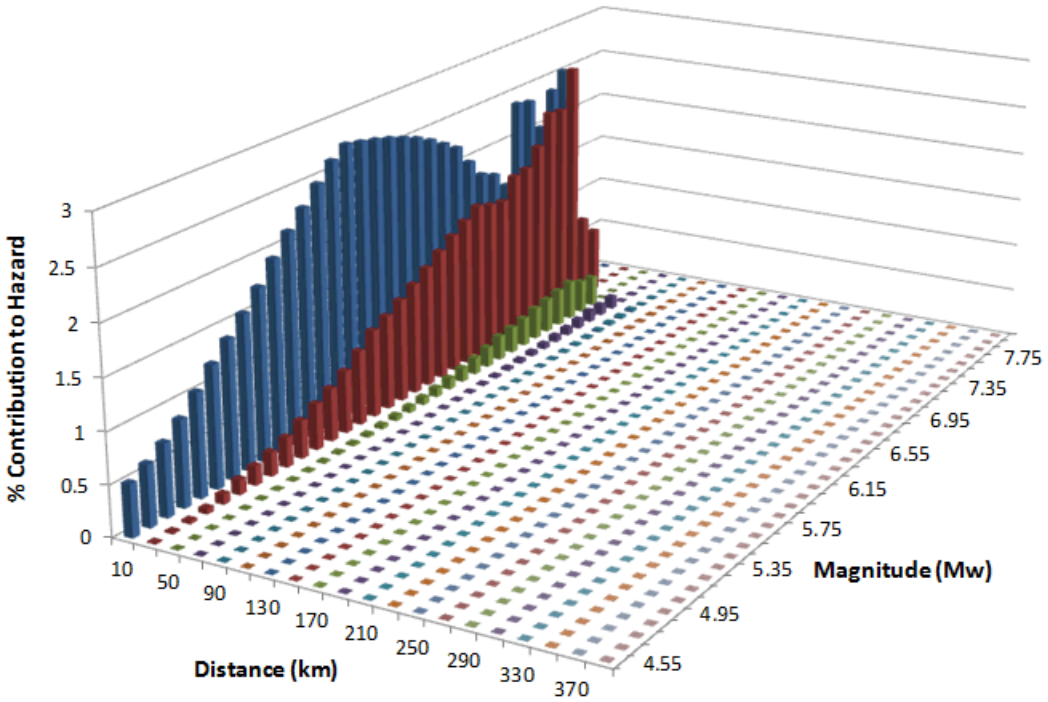


*Figure D11. Hazard deaggregation for 2%-in-50-year Spectral Acceleration at 0.2sec for Kutaisi (mean magnitude: 6.48, mean distance: 19km, mode magnitude: 5.95, mode distance: 10km)*

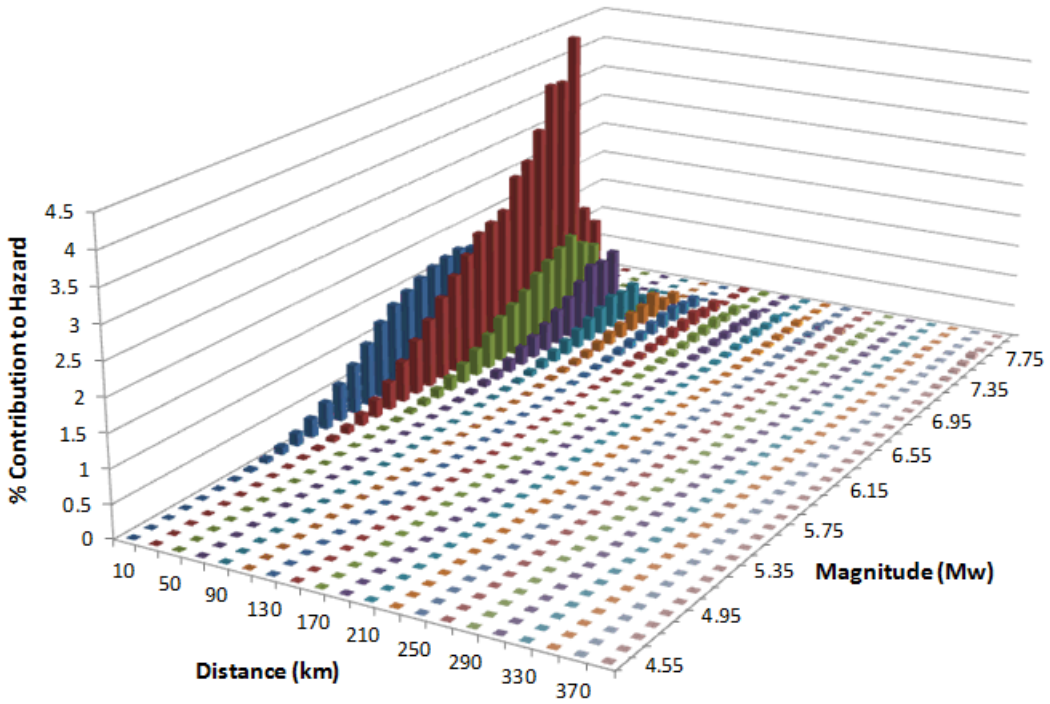


*Figure D12. Hazard deaggregation for 2%-in-50-year Spectral Acceleration at 1.0sec for Kutaisi (mean magnitude: 7.06, mean distance: 44km, mode magnitude: 7.55, mode distance: 30km)*

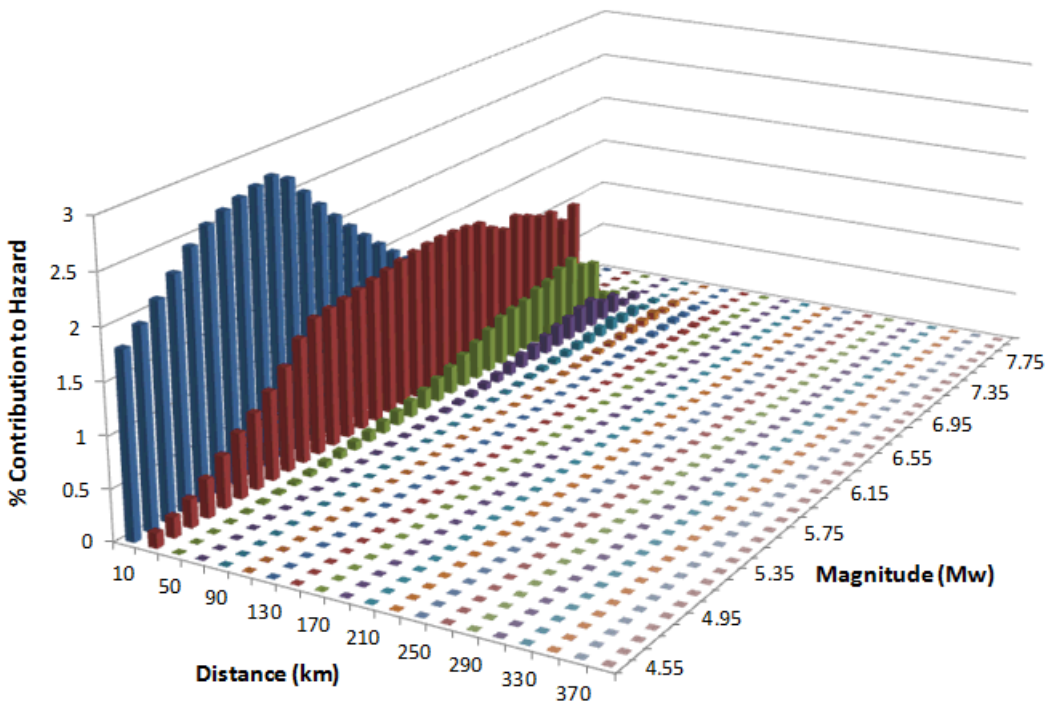


*Figure D13. Hazard deaggregation for 10%-in-50-year PGA for Batumi (mean magnitude: 6.07, mean distance: 24km, mode magnitude: 5.45, mode distance: 10km)*

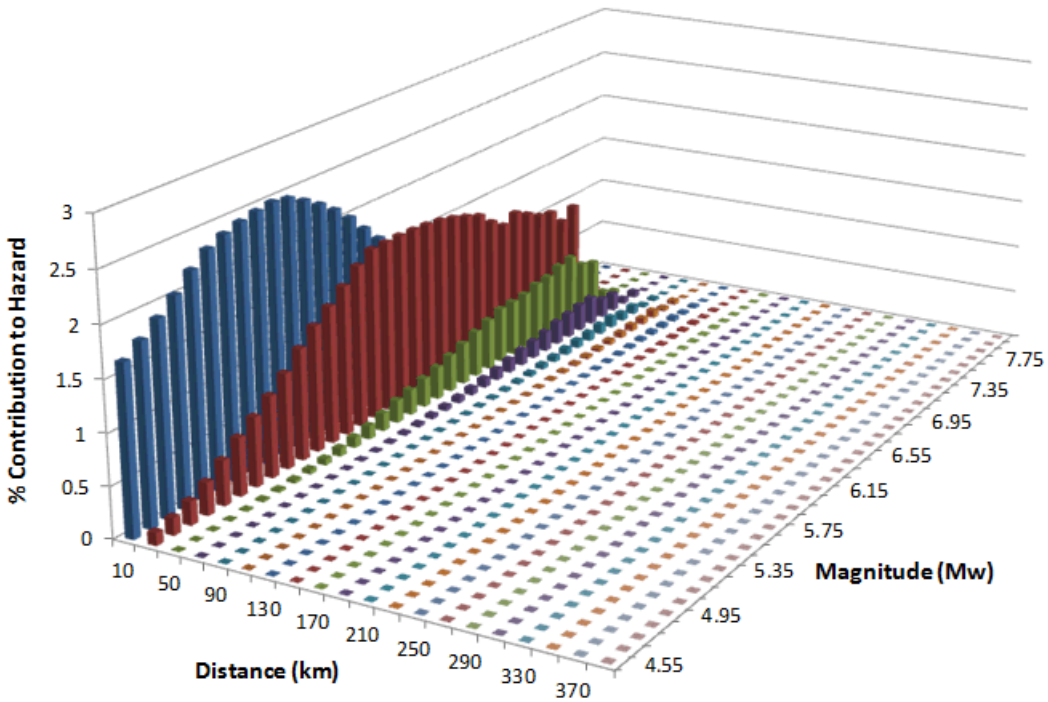


*Figure D14. Hazard deaggregation for 10%-in-50-year Spectral Acceleration at 0.2sec for Batumi (mean magnitude: 6.10, mean distance: 25km, mode magnitude: 5.45, mode distance: 10km)*

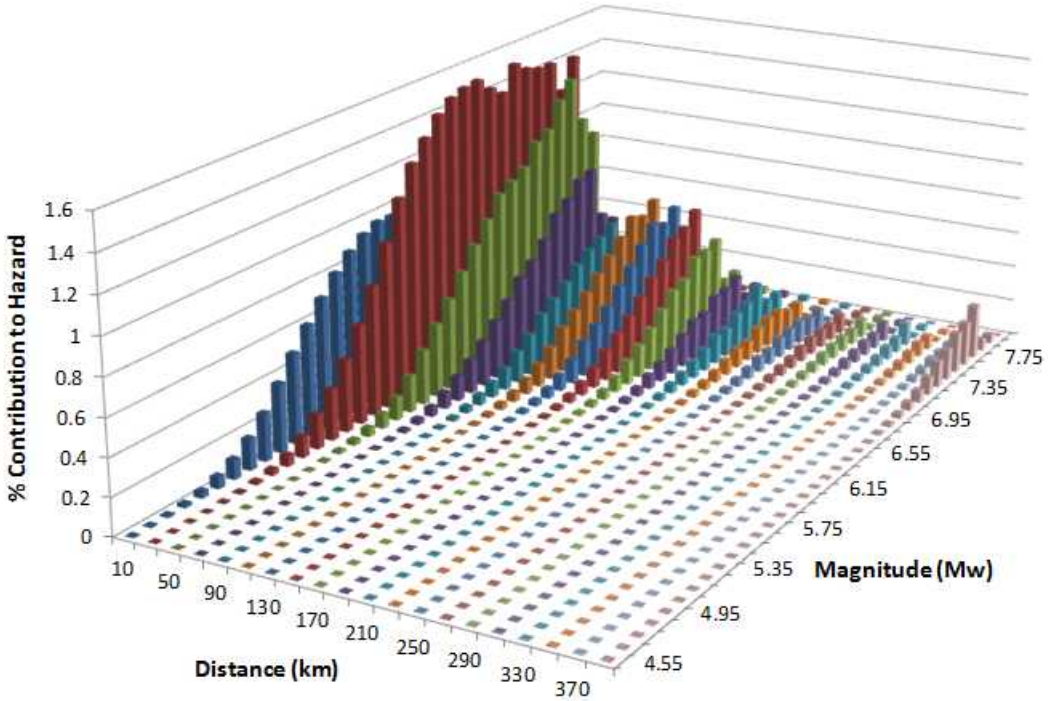


*Figure D15. Hazard deaggregation for 10%-in-50-year Spectral Acceleration at 1.0sec for Batumi (mean magnitude: 6.95, mean distance: 82km, mode magnitude: 7.05, mode distance: 30km)*

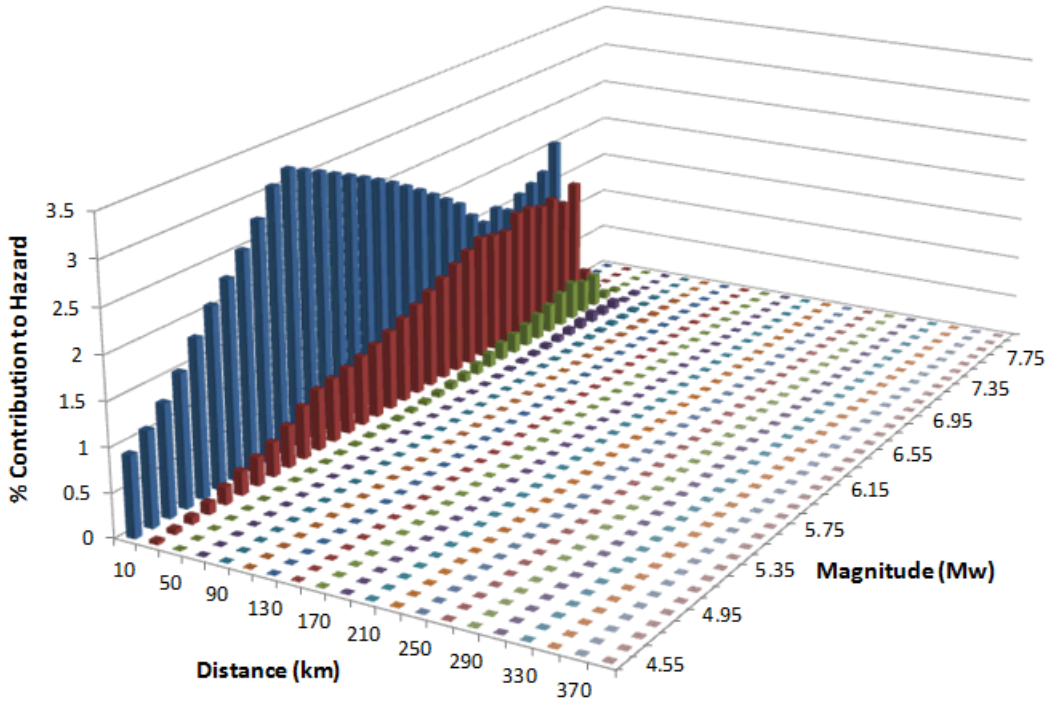


*Figure D16. Hazard deaggregation for 2%-in-50-year PGA for Batumi (mean magnitude: 6.24, mean distance: 18km, mode magnitude: 5.55, mode distance: 10km)*

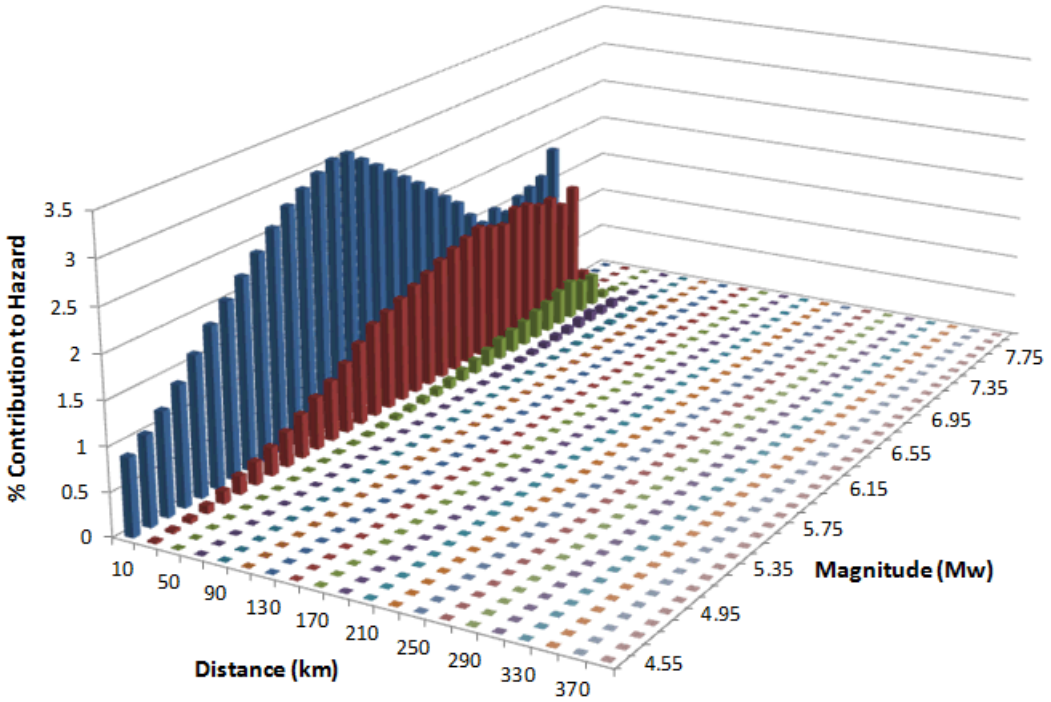


*Figure D17. Hazard deaggregation for 2%-in-50-year Spectral Acceleration at 0.2sec for Batumi (mean magnitude: 6.27, mean distance: 19km, mode magnitude: 5.95, mode distance: 10km)*

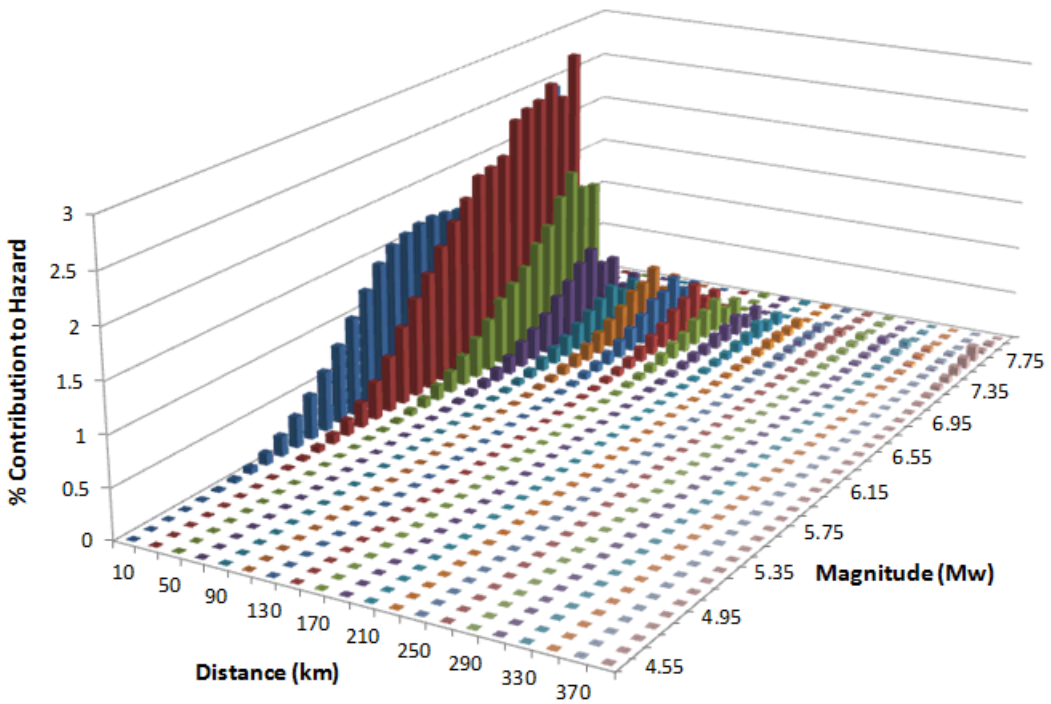


*Figure D18. Hazard deaggregation for 2%-in-50-year Spectral Acceleration at 1.0sec for Batumi (mean magnitude: 7.00, mean distance: 55km, mode magnitude: 7.55, mode distance: 30km)*